UNIVERSITY OF COPENHAGEN
FACULTY OF SCIENCE

X^3		φ^6 and $\varphi^4 D^2$		$\psi^2\varphi^3$	
Q_G	$f^{ABC}G^{A\nu}_{\mu}G^{B\rho}_{\nu}G^{C\mu}_{\rho}$	Q_{φ}	$(\varphi^\dagger\varphi)^3$	$Q_{e\varphi}$	$(\varphi^\dagger\varphi)(\bar{l}_p e_r\varphi)$
$Q_{\widetilde{G}}$	$f^{ABC}\widetilde{G}^{A\nu}_{\mu}G^{B\rho}_{\nu}G^{C\mu}_{\rho}$	$Q_{\varphi\Box}$	$(\varphi^\dagger\varphi)\Box(\varphi^\dagger\varphi)$	$Q_{u\varphi}$	$(\varphi^\dagger\varphi)(\bar{q}_p u_r\widetilde{\varphi})$
Q_W	$\varepsilon^{IJK}W^{I\nu}_{\mu}W^{J\rho}_{\nu}W^{K\mu}_{\rho}$	$Q_{\varphi D}$	$\left(\varphi^\dagger D^\mu\varphi\right)^\star\left(\varphi^\dagger D_\mu\varphi\right)$	$Q_{d\varphi}$	$(\varphi^\dagger\varphi)(\bar{q}_p d_r\varphi)$
$Q_{\widetilde{W}}$	$\varepsilon^{IJK}\widetilde{W}^{I\nu}_{\mu}W^{J\rho}_{\nu}W^{K\mu}_{\rho}$				
$X^2\varphi^2$		$\psi^2 X\varphi$		$\psi^2\varphi^2 D$	
$Q_{\varphi G}$	$\varphi^\dagger\varphi\, G^A_{\mu\nu}G^{A\mu\nu}$	Q_{eW}	$(\bar{l}_p\sigma^{\mu\nu}e_r)\tau^I\varphi W^I_{\mu\nu}$	$Q^{(1)}_{\varphi l}$	$(\varphi^\dagger i\overleftrightarrow{D}_\mu\varphi)(\bar{l}_p\gamma^\mu l_r)$
$Q_{\varphi\widetilde{G}}$	$\varphi^\dagger\varphi\,\widetilde{G}^A_{\mu\nu}G^{A\mu\nu}$	Q_{eB}	$(\bar{l}_p\sigma^{\mu\nu}e_r)\varphi B_{\mu\nu}$	$Q^{(3)}_{\varphi l}$	$(\varphi^\dagger i\overleftrightarrow{D}^I_\mu\varphi)(\bar{l}_p\tau^I\gamma^\mu l_r)$
$Q_{\varphi W}$	$\varphi^\dagger\varphi\, W^I_{\mu\nu}W^{I\mu\nu}$	Q_{uG}	$(\bar{q}_p\sigma^{\mu\nu}T^A u_r)\widetilde{\varphi}\,G^A_{\mu\nu}$	$Q_{\varphi e}$	$(\varphi^\dagger i\overleftrightarrow{D}_\mu\varphi)(\bar{e}_p\gamma^\mu e_r)$
$Q_{\varphi\widetilde{W}}$	$\varphi^\dagger\varphi\,\widetilde{W}^I_{\mu\nu}W^{I\mu\nu}$	Q_{uW}	$(\bar{q}_p\sigma^{\mu\nu}u_r)\tau^I\widetilde{\varphi}\,W^I_{\mu\nu}$	$Q^{(1)}_{\varphi q}$	$(\varphi^\dagger i\overleftrightarrow{D}_\mu\varphi)(\bar{q}_p\gamma^\mu q_r)$
$Q_{\varphi B}$	$\varphi^\dagger\varphi\, B_{\mu\nu}B^{\mu\nu}$	Q_{uB}	$(\bar{q}_p\sigma^{\mu\nu}u_r)\widetilde{\varphi}\,B_{\mu\nu}$	$Q^{(3)}_{\varphi q}$	$(\varphi^\dagger i\overleftrightarrow{D}^I_\mu\varphi)(\bar{q}_p\tau^I\gamma^\mu q_r)$
$Q_{\varphi\widetilde{B}}$	$\varphi^\dagger\varphi\,\widetilde{B}_{\mu\nu}B^{\mu\nu}$	Q_{dG}	$(\bar{q}_p\sigma^{\mu\nu}T^A d_r)\varphi\, G^A_{\mu\nu}$	$Q_{\varphi u}$	$(\varphi^\dagger i\overleftrightarrow{D}_\mu\varphi)(\bar{u}_p\gamma^\mu u_r)$
$Q_{\varphi WB}$	$\varphi^\dagger\tau^I\varphi\, W^I_{\mu\nu}B^{\mu\nu}$	Q_{dW}	$(\bar{q}_p\sigma^{\mu\nu}d_r)\tau^I\varphi\, W^I_{\mu\nu}$	$Q_{\varphi d}$	$(\varphi^\dagger i\overleftrightarrow{D}_\mu\varphi)(\bar{d}_p\gamma^\mu d_r)$
$Q_{\varphi\widetilde{W}B}$	$\varphi^\dagger\tau^I\varphi\,\widetilde{W}^I_{\mu\nu}B^{\mu\nu}$	Q_{dB}	$(\bar{q}_p\sigma^{\mu\nu}d_r)\varphi\, B_{\mu\nu}$	$Q_{\varphi ud}$	$i(\widetilde{\varphi}^\dagger D_\mu\varphi)(\bar{u}_p\gamma^\mu d_r)$

$(\bar{L}L)(\bar{L}L)$		$(\bar{R}R)(\bar{R}R)$		$(\bar{L}L)(\bar{R}R)$	
Q_{ll}	$(\bar{l}_p\gamma_\mu l_r)(\bar{l}_s\gamma^\mu l_t)$	Q_{ee}	$(\bar{e}_p\gamma_\mu e_r)(\bar{e}_s\gamma^\mu e_t)$	Q_{le}	$(\bar{l}_p\gamma_\mu l_r)(\bar{e}_s\gamma^\mu e_t)$
$Q^{(1)}_{qq}$	$(\bar{q}_p\gamma_\mu q_r)(\bar{q}_s\gamma^\mu q_t)$	Q_{uu}	$(\bar{u}_p\gamma_\mu u_r)(\bar{u}_s\gamma^\mu u_t)$	Q_{lu}	$(\bar{l}_p\gamma_\mu l_r)(\bar{u}_s\gamma^\mu u_t)$
$Q^{(3)}_{qq}$	$(\bar{q}_p\gamma_\mu\tau^I q_r)(\bar{q}_s\gamma^\mu\tau^I q_t)$	Q_{dd}	$(\bar{d}_p\gamma_\mu d_r)(\bar{d}_s\gamma^\mu d_t)$	Q_{ld}	$(\bar{l}_p\gamma_\mu l_r)(\bar{d}_s\gamma^\mu d_t)$
$Q^{(1)}_{lq}$	$(\bar{l}_p\gamma_\mu l_r)(\bar{q}_s\gamma^\mu q_t)$	Q_{eu}	$(\bar{e}_p\gamma_\mu e_r)(\bar{u}_s\gamma^\mu u_t)$	Q_{qe}	$(\bar{q}_p\gamma_\mu q_r)(\bar{e}_s\gamma^\mu e_t)$
$Q^{(3)}_{lq}$	$(\bar{l}_p\gamma_\mu\tau^I l_r)(\bar{q}_s\gamma^\mu\tau^I q_t)$	Q_{ed}	$(\bar{e}_p\gamma_\mu e_r)(\bar{d}_s\gamma^\mu d_t)$	$Q^{(1)}_{qu}$	$(\bar{q}_p\gamma_\mu q_r)(\bar{u}_s\gamma^\mu u_t)$
		$Q^{(1)}_{ud}$	$(\bar{u}_p\gamma_\mu u_r)(\bar{d}_s\gamma^\mu d_t)$	$Q^{(8)}_{qu}$	$(\bar{q}_p\gamma_\mu T^A q_r)(\bar{u}_s\gamma^\mu T^A u_t)$
		$Q^{(8)}_{ud}$	$(\bar{u}_p\gamma_\mu T^A u_r)(\bar{d}_s\gamma^\mu T^A d_t)$	$Q^{(1)}_{qd}$	$(\bar{q}_p\gamma_\mu q_r)(\bar{d}_s\gamma^\mu d_t)$
				$Q^{(8)}_{qd}$	$(\bar{q}_p\gamma_\mu T^A q_r)(\bar{d}_s\gamma^\mu T^A d_t)$

$(\bar{L}R)(\bar{R}L)$ and $(\bar{L}R)(\bar{L}R)$		B-violating	
Q_{ledq}	$(\bar{l}^j_p e_r)(\bar{d}_s q^j_t)$	Q_{duq}	$\varepsilon^{\alpha\beta\gamma}\varepsilon_{jk}\left[(d^\alpha_p)^T C u^\beta_r\right]\left[(q^{\gamma j}_s)^T C l^k_t\right]$
$Q^{(1)}_{quqd}$	$(\bar{q}^j_p u_r)\varepsilon_{jk}(\bar{q}^k_s d_t)$	Q_{qqu}	$\varepsilon^{\alpha\beta\gamma}\varepsilon_{jk}\left[(q^{\alpha j}_p)^T C q^{\beta k}_r\right]\left[(u^\gamma_s)^T C e_t\right]$
$Q^{(8)}_{quqd}$	$(\bar{q}^j_p T^A u_r)\varepsilon_{jk}(\bar{q}^k_s T^A d_t)$	Q_{qqq}	$\varepsilon^{\alpha\beta\gamma}\varepsilon_{jn}\varepsilon_{km}\left[(q^{\alpha j}_p)^T C q^{\beta k}_r\right]\left[(q^{\gamma m}_s)^T C l^n_t\right]$
$Q^{(1)}_{lequ}$	$(\bar{l}^j_p e_r)\varepsilon_{jk}(\bar{q}^k_s u_t)$	Q_{duu}	$\varepsilon^{\alpha\beta\gamma}\left[(d^\alpha_p)^T C u^\beta_r\right]\left[(u^\gamma_s)^T C e_t\right]$
$Q^{(3)}_{lequ}$	$(\bar{l}^j_p\sigma_{\mu\nu}e_r)\varepsilon_{jk}(\bar{q}^k_s\sigma^{\mu\nu}u_t)$		

A thesis presented to the Faculty of Science in partial fulfillment of the requirements for the degree

Doctor of Philosophy in Physics

Effective Field Theories of Particle Physics and Gravity

Anagha Vasudevan

Supervisors: Prof. Dr. Michael Trott and Prof. Dr. Peter Hansen

Submitted: January 2022

This thesis has been submitted to the PhD School of The Faculty of Science, University of Copenhagen

Contents

Abstract

This thesis examines effective field theories. We briefly provide an overview of the properties underlying such theories and then look at concrete examples. For one, we will discuss the effective field theoretic expansion of the Standard Model of particle physics and some novel theoretical results important to understanding New Physics at the Large Hadron Collider. The second part of this thesis will address effective theories of gravity and current results in this field in the context of fundamental quantities such as the black hole metric which are relevant to the experiment LIGO.

Resumé

Denne afhandling er tilegnet effektive feltteorier. Vi danner os et overblik over sådanne teorier og undersøger konkrete eksempler. Først diskuterer vi den effektive feltteori-udvidelse af standardmodellen indenfor partikelfysik og nye teoretiske resultater til at fremme forståelsen af Ny Fysik ved LHC. Den anden del af denne afhandling undersøger effektive feltteorier i forbindelse med tyngdekraft og aktuelle resultater i dette felt i sammenhæng med fundamentale kvantiteter såsom sort hul-metrikken, der er væsentlige i LIGO-eksperimentet.

Three quarks for Muster Mark
Sure he hasn't got much of a bark
And sure any he has it's all beside the mark.

James Joyce

Acknowledgments

This PhD has been one of the most challenging periods of my life. I would not have been able to complete it without the support of many people.

Firstly, I would like to thank my supervisors Michael Trott and Peter Hansen. They have both been extremely supportive throughout my time at the Niels Bohr Institute and I have been very glad to get to know them and work with them. Mike and I have had many enjoyable discussions, whether it be about conflicts within the EFT community or minus signs and factors of 2. I would also like to thank Jan Thomsen, head of the Niels Bohr Institute, for his invaluable kindness and support in the last few months of my time here. I appreciate N.E.J. Bjerrum-Bohr for introducing me to the exciting world of modern calculations in gravitational physics. None of this would have been possible if it hadn't been for Sune Olander Rasmussen. I would also like to thank my colleagues over the years for both their friendship as well as fruitful discussions- Abdurahhman Barzinji, Kays Haddad, Meera Machado, Andreas Helset, Charlotte Rosenstrøm, Laurie Walk, Andrea Cristofoli, Anna Suliga, Matthew Von Hippel, M. Rameez, and Subodh Patil. I would also like to express my sincere gratitude to Manfred Kraus for his input to my thesis and support both as my friend as well as colleague.

I am extremely grateful to my family and friends for all they've done for me over the last few years. Firstly, I would like to thank my parents Anitha and Rajiv, my brother Nachiket, my grandmother Ammini, and my grandfather P. Damodaran, for the love and understanding that they've shown me particularly over the last few years. My best friend Rakesh has been a huge source of encouragement and positivity, believing in my Nobel Prize-winning capabilities sometimes far more than my mother. In no particular order, I would like to thank the various friends who have been part of this journey, without whom this would not have been possible: Trisha Chandran, Satender Singh Vijayran, Malavika Vidyarthi, Shruthi Venkat, Erik Gunnarsson, Subodh Pareek, Christian K. Miller, Aishwarya Mohan, Neel Tamhane, and Ramachandran Cheeniyil.

Lastly, I am indebted to my dearest Jeppe Jacobsen for believing in me so much, and for his immeasurable kindness and support.

Chapter 1

Introduction

This thesis examines different aspects of effective theories, one of the most exciting theoretical tools for those of us who work on quantum field theories today. Effective theories have a wide range of application in physics, since we can consider all the theories we have today to be an effective field theory (EFT). Essentially, we consider an EFT to be a physical theory that is well-defined in terms of the scales -usually energy scales- under which it is valid. It is possible to ad-hoc construct an EFT for the energy scales one wants to study, based on the principles discussed in this thesis.

Two different branches of effective field theory will be considered here. After discussing the basic ideas behind constructing an EFT in Section 2, the first application will be discussed: the Standard Model Effective Field Theory (SMEFT). The Standard Model (SM) of particle physics has been extremely successful in describing electroweak and strong interactions. In 2012, a boson of mass $125 Gev$ was discovered, consistent with a Higgs boson, whose existence has been postulated since the 1960s. This completed the Standard Model. However, it hasn't been able to explain all observed phenomena. For one, the 2015 Nobel Prize in physics was shared by Takaaki Kajita and Arthur McDonald for their discovery that neutrinos, which are massless in the SM, oscillate between different mass and flavour eigenstates [1]. Incorporating massive neutrinos into the SM is not simple, and requires perhaps an extension. In addition, there are unsolved problems in cosmology, namely those of dark matter and dark energy. E.g., one current approach to solving the dark matter problem involves searching for a potential dark matter candidate at a collider. A standard example of a dark matter candidate is the right-handed neutrino, a particle not in the SM since it does not interact under electroweak or strong interactions. The second run of the LHC hopes to discover a sign of New Physics, i.e., physics beyond the SM. We will discuss in Section 3 how SMEFT is constructed and its different properties that make it uniquely suited to tackling the search for New Physics. In 2017, I published with my supervisor Michael Trott and Abdurrahman Barzinji, a paper where we studied important subleading corrections in the SMEFT and discuss applications of this in Ref. [2]. A detailed version of these novel results will be discussed in Section 4.

The second application we will study is that of effective field theories in gravity. The discovery of gravitational waves in 2015 by the LIGO collaboration has had a big impact on the field of gravity [3]. There is now a pressing need for precise theoretical predictions of scatterings and mergers of objects like black holes and neutron stars. A few years ago, one may have thought that it was impossible to study gravity as a quantum field theory due to the fact that the gravitational coupling has a dimension. However, this issue is completely circumvented by considering general relativity (GR) to be an EFT. A detailed account of the problem under consideration is given in Sec. 5. We will discuss in detail the recharacterisation of gravity as an EFT, and the procedure of constructing a Lagrangian and thereafter

Feynman rules in Section 5.3. Then, applications of this theory will be discussed in Section 6, where important one-loop post-Newtonian corrections to the metric are obtained using the Feynman rules that were earlier established. Finally, ongoing work on simplifying the prior calculation using residue theorem are considered in Section 6.2. We will briefly touch upon the future of such calculations, using unitarity-based approaches in Sec. 6.3. A conclusion and outlook summarise this thesis and succinctly establishes the optimism held for the future of these fields.

Chapter 2

Effective Field Theories

Effective field theories are based on a very simple but powerful idea: the fact that scales in physics are separated. This is encapsulated in the Appelquist-Carrazone theorem which will be discussed shortly. The evolution of physics has seen that over the last centuries we have developed more and more intricate theories that are capable of probing progressively smaller distances, or equivalently, higher and higher energies. Quarks and leptons, elementary particles invisible to the eye, are some of the smallest scales we know of. At the same time, the world consists of a variety of length scales of interest, ranging from these minuscule ones to nuclear and atomic scales, cells and organisms, geophysical scales, astrophysical scales of planets and galaxies, and finally cosmological scales ranging up to the size of the visible universe. This evolution has been possible because we can independently study ranges of scales without being affected by the physics outside of that range- up to a finite, calculable error. To understand this concept better, we will consider the idea of a diagrammatic large mass expansion in greater depth.

2.1 Decoupling and the Appelquist-Carrazone Theorem

Sensible calculations are possible in EFT because of the idea of decoupling, which allows us to consider a specific range of energy scales without making any reference to physics at shorter distance scales, e.g., calculations in atomic physics which make no reference to the deeper structure of the particles within the atom. This decoupling is non-trivial when one considers a quantum theory, because of loops. E.g., one can neglect the heaviest quark, the top quark, in several calculations. This is however, a contradiction because top quarks can still appear within loops at higher order in perturbation theory. Thus, such particles can appear virtually and consequently contribute to cross sections. The decoupling theorem, however, says that heavy masses *decouple* from the theory, appearing only in corrections proportional to $(m^2)^{-1}$ where m is the heavy mass scale. Alternatively, we can say that any processes containing a propagator of the heavy mass scale but with external momenta being relatively small are actually suppressed by this mass scale. This is a generalised statement, applying to any renormalisable theory. This idea was encapsulated in the Appelquist-Carrazone theorem [4]:

"*For any 1PI Feynman graph with external vector mesons only but containing internal fermions, when all external momenta (i.e. p^2) are small relative to m^2 , then apart from coupling constant and field strength renormalization the graph will be suppressed by some power of m relative to a graph with the same number of external vector mesons but no internal fermions.*",

here expressed in the modified wording from Ref. [5].

As a result for n-point Green's functions G^n_{full} of an arbitrary field theory, the theorem can be expressed as

$$\Pi_i^N Z_i G^n_{full}(p_1, p_2, \cdots, p_n; \mu) = \Pi_i^M Z_i G^n_{EFT}(p_1, p_2, \cdots, p_n; \mu) + \frac{1}{m^2}\Pi_i^k Z_i G'^{\,n}_{EFT}(p_1, p_2, \cdots, p_n; \mu) + \cdots . \tag{2.1}$$

The right-hand side in the above contains an effective description of the full theory, with $d \leq 4$ terms contributing to G^n_{EFT} and higher dimensional terms in $G'^{\,n}_{EFT}$. $Z_{1,\ldots,n}$ is the full set of renormalisation constants required to renormalise the full theory, while $Z_{1,\ldots,M}$ would renormalise the $d \leq 4$ terms of the EFT. Finally, the higher-dimensional terms are renormalised using $Z_{1,\ldots,N,\ldots,k}$. Here, in addition to the renormalisation of the lower dimensional terms, we also have those which make the higher dimensional terms, which are suppressed by powers of the heavy mass, finite. This captures what was stated in the Appelquist-Carrazone theorem, i.e., that the heavy mass only appears in the renormalisation of fields or coupling constants. There is the caveat that the heavy mass should not go on-shell in the diagrams that are calculated, since this theorem relies on using the on-shell scheme to avoid any further constants coming in from renormalisation. The on-shell theorem kills terms (as expected) where $p^2 \sim m^2$, $\not{k} = m$ or similar expressions for the momentum and mass under consideration. To conclude, we have stated that where the heavy intermediate mass doesn't go on shell, its contribution to the full theory is solely through new higher-dimensional interactions between light fields that are suppressed by the mass scale, or renormalisation constants.

There are exceptions to the decoupling theorem, most notably in the case of weak interactions. At energies of a few GeV, i.e., far below the mass of the W and Z bosons, weak interactions would not be expected to play a significant role. A low energy effective theory would then consist of strong and electromagnetic interactions only. However, certain weak decays can still be observed. This is due to the fact that these decays are forbidden by discrete symmetries such as parity and charge conjugation, if the weak interaction is neglected. We will briefly discuss low energy EFTs for weak interactions in Section 2, but the main feature of this is that we obtain a non-renormalisable theory containing local contact operators consisting of four fermions with a dimensionful constant called the Fermi constant. This is a typical outcome for exceptions to the decoupling theorem. The existence of cases where the decoupling theorem does not apply does not mean that EFTs break down or are invalid. Rather, one must carefully consider the conditions of the decoupling theorem. In general, there are two classes of examples of non-decoupling as detailed in Ref. [6]:

- Theories with spontaneous symmetry breaking have the property that the mass is related to a dimensionless coupling. In the case of the Higgs field, the mass parameter is directly connected to the coupling λ that appears in the Lagrangian. The decoupling theorem assumes that the mass parameter is increased by going to higher order in dimensional parameters [7, 8].
- Some dimensionless couplings needed by power-counting violate the renormalisability of the low energy theoery [9].

Renormalisability is intimately connected to the idea of large mass expansion. In practice, one can test Eq. 2.1 by taking the large mass limit of Feynman diagrams. Such an illustration

reveals some of the deeper properties of EFTs. In the following section, we will discuss one such illustration. To keep it simple, all quantities will be worked with at the level of the bare (non-renormalised) Lagrangian.

2.2 Large Mass Expansion

In this section, we will investigate scale separations in physics further, in the context of a generic quantum field theory of scalars. The following example has been taken from Ref. [6]. To begin with, we consider a bare-bone example of the procedure of integrating out heavy modes.

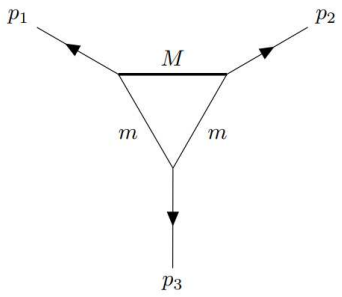

Figure 2.1: Feynman diagram consisting of two scalar fields with mass m and M

Here, we consider Feynman diagrams containing just two scalar fields for simplicity, and take the limit of one mass (represented by the thick line) going to infinity, or $m \ll M$. Our aim is to look into the triangle integral and its different limits to potentially decouple the two scales in the problem. Essentially, we consider the procedure of converting a Lagrangian of a UV theory

$$\mathcal{L}_{UV} = \mathcal{L}_\ell + \mathcal{L}_h, \tag{2.2}$$

where $\mathcal{L}_{UV}$ is the full theory consisting of the interactions between the heavy and light fields and their mass terms, into two parts. Here, we require that $\mathcal{L}_\ell$ contains only the lighter field, while $\mathcal{L}_h$ can contain both heavy and light fields. Ultimately, we want to obtain a consistent Wilsonian Operator Product Expansion (OPE) and subsequently an effective Lagrangian of the form

$$\mathcal{L}_{EFT} = \mathcal{L}_\ell + \sum_{n=1}^{\infty} \frac{1}{M^n} C_{ni} Q_{ni}. \tag{2.3}$$

Here, $\mathcal{L}_\ell$ has the same dimensions of the original theory, while the series contains higher order operator combinations of light fields. In the above, we see an OPE based on an expansion in the heavy scale M. It additionally contains complex numbers C_{ni}, representing

Wilson coefficients and Q_{ni}, representing various operator combinations at higher dimensions. We look now at the triangle integral which corresponds to Fig. 6.3:

$$I = \int \frac{d^4k}{(2\pi)^4} \frac{1}{[k^2 - M^2][(k+p_1)^2 - m^2][(k-p_2)^2 - m^2]}. \tag{2.4}$$

Simple power counting shows us that this integral is both UV and IR finite in four dimensions (See Sec. 2.7). We will look at the case where $p_i \sim m$ for the external momenta and consequently consider two limits of the above integral separately, namely $m \gg p_i$ and $m \sim p_i$.

In the first case, the first term in the Taylor series, where we simply set p_i to zero is

$$I \approx \int \frac{d^4k}{(2\pi)^4} \frac{1}{[k^2 - M^2][k^2 - m^2]^2}. \tag{2.5}$$

This integral is clearly finite. Subsequent terms in this expansion will have $2 + 2(n+2)$ powers of k in the denominator and $2n$ powers of k in the case of even terms, while odd terms are zero. Thus, we can conclude that for this case, we can simply Taylor expand the integral without additional considerations. However, in the case of the other limit where $p_i \sim m$, we run into some complications. Naively expanding in the small parameters yields

$$I \approx \int \frac{d^4k}{(2\pi)^4} \frac{1}{[k^2 - M^2]k^4}. \tag{2.6}$$

We can see that this is an IR divergent integral and thus cannot be the correct limit of the original integral. We can solve this differently by introducing a subtraction as follows:

$$\begin{aligned} I &= \int \frac{d^4k}{(2\pi)^4} \frac{1}{[k^2 - M^2][(k+p_1)^2 - m^2][(k-p_2)^2 - m^2]} \\ &= \int \frac{d^4k}{(2\pi)^4} \left(\frac{1}{k^2 - M^2} - \frac{1}{-M^2} \right) \frac{1}{[(k+p_1)^2 - m^2][(k-p_2)^2 - m^2]} \\ &+ \int \frac{d^4k}{(2\pi)^4} \left(\frac{1}{-M^2} \right) \frac{1}{[(k+p_1)^2 - m^2][(k-p_2)^2 - m^2]}. \end{aligned} \tag{2.7}$$

The above steps are allowed by the properties of integrals in dimensional regularisation. In the first term, if we look at the $k \to 0$ limit, we obtain a zero, which is unaffected if we subsequently take $p_i, m \to 0$. The second term is firstly UV divergent, but also does not yield a regular expression under similar considerations. So, we now expand only on the first term

$$I \approx \int \frac{d^4k}{(2\pi)^4} \left(\frac{1}{k^2 - M^2} - \frac{1}{-M^2} \right) \frac{1}{k^4} + \int \frac{d^4k}{(2\pi)^4} \frac{1}{-M^2} \frac{1}{[(k+p_1)^2 - m^2][(k+p_2)^2 - m^2]}. \tag{2.8}$$

This can now be split into three integrals as

$$I \approx \int \frac{d^4k}{(2\pi)^4} \left(\frac{1}{k^2 - M^2} \right) \frac{1}{k^4} + \left(\frac{1}{M^2} \right) \int \frac{d^4k}{(2\pi)^4} \frac{1}{k^4} - \frac{1}{M^2} \int \frac{d^4k}{(2\pi)^4} \frac{1}{[(k+p_1)^2 - m^2][(k+p_2)^2 - m^2]}. \tag{2.9}$$

Now, consider the divergence properties of the above integrals. The first one is IR divergent. The second one is scaleless, and such an integral can be discarded in dimensional regularisation. The third one continues to be UV divergent. Thus, we are left with one IR divergent integral and one UV divergent one. Since we expect that the above expression should capture the results of the original integral in Eq. (2.4), we should have the two divergences cancel against each other. This is in fact a feature of effective field theories. Since we already have Renormalisation Group (RG) methods, we can replace IR divergent theories with UV divergent ones. We also see some of the properties mentioned in the decoupling theorem. For one, the above example illustrates how the large mass expansion results in the integral splitting into several integrals where the UV physics, represented by the heavy mass M, decouples from the rest of the theory. The decoupling theorem offers an advantage when it comes to practically calculating scattering processes. By separating the scales, we have obtained multiple integrals that are significantly easier to evaluate than the complicated triangle integral that we had started off with.

The results of the large mass expansion can be expressed in terms of diagrams, by looking at the integrals we obtained:

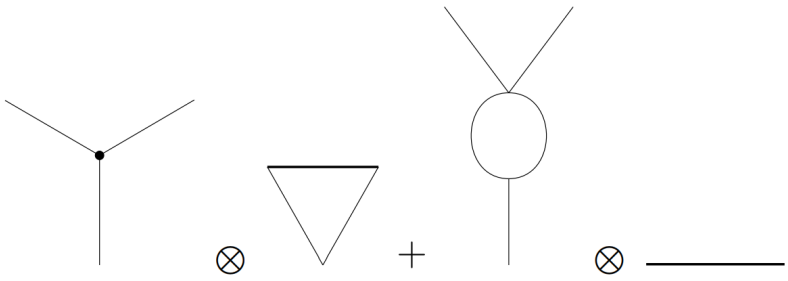

Figure 2.2: A diagrammatic representation of large mass expansion

Fig. 2.2 shows us how one can use different types of operators in order to discuss a particular result. Thus, complicated loop diagrams can be re-expressed in terms of point operators that potentially disobey the rules of dimensionality, where terms in Lagrangians are usually expected to have a mass dimension of four. In addition, this diagram shows us that large masses are decoupled from lower scales since the bold lines exist only in one type of diagram, whereas the light masses can appear abundantly in the other terms.

Our study of the procedure of diagrammatic large mass expansions has shown that by replacing a full theory's Lagrangian and corresponding Feynman rules with an effective Lagrangian and effective vertices, it is possible to obtain the same result as in the full theory. In addition, the issue of renormalisability is much easier to treat in an EFT, since we can make connections between the UV and IR divergences, where for the former we have RG

methods. However, we will now discuss how to construct this effective Lagrangian and obtain Feynman rules. As we know, the effective Lagrangian has heavy modes integrated out, and thus only consists of higher-dimensional combinations of light fields that obey the same symmetries as the light theory. E.g., if we were to construct an EFT of the Standard Model (SM) itself, we would write out higher-dimensional combinations of the same fields present in the SM, but still obeying the $SU(3) \times SU(2) \times U(1)$ symmetry of the SM. We will soon see the full list of such operators, but here are two examples of such an operator consisting only of Higgs doublets:

$$Q_H = (H^\dagger H)^6, \quad Q_{H\Box} = (H^\dagger H)\Box(H^\dagger H). \tag{2.10}$$

In general, we express an effective Lagrangian as follows

$$\mathcal{L}^0_{eff} = \mathcal{L}^0_\ell + \sum_{n=1}^{\infty} \frac{1}{\Lambda^n} \sum_i \mathcal{C}^0_{ni} \mathcal{O}^0_{ni}. \tag{2.11}$$

Λ above denotes the scale of the heavy state. We will not consider a multiscale problem here, so only one such expansion exists in Λ. In addition, the superscripts denote that we are working on the level of the bare, non-renormalised parameters. Of course, we expect that the full theory is finite, which is a reasonable expectation to have: we expect that our effective theory will also produce finite Green's functions since it is representative of a finite UV theory. Firstly, we have to think about renormalisability in general terms. We expect that the new operators will produce UV divergences. For any theory to be renormalisable, we need to have a finite number of divergences that are canceled out by renormalising a finite number of fields and coefficients. Thus, we consider the theory order-by-order in the given expansion above. At any given order, due to the dimensional constraints and fields having positive dimension, we will have a finite number of operators, and consequently a finite number of complex Wilson coefficients. We expect that by using RGEs to renormalise these Wilson coefficients, we can systematically deal with each UV divergent graph. In EFTs, unlike in the case of the SM, we have an additional complication due to potential operator mixing, which will be discussed in Sec. 3.5. This is in fact, one of the huge difficulties in having an automated program to calculate EFT S-matrix elements and decay rates. Thus, the key point of this discussion is that by working order by order in the EFT expansion in Eq. (2.11), i.e., looking at the terms for each n separately, we will only have a finite number of divergent terms that can be dealt with using appropriate RGE methods.

2.3 Examples of EFTs

The classical example of an EFT is what is called Heavy Quark Effective Field Theory (HQET), which is also known as the Fermi theory of weak interactions. Here, the W and Z boson masses are neglected and we instead consider tetra-quark interactions and expand in the masses of quarks. This is an example of a bottom-up approach, now that we are aware of the full Standard Model. HQET was extremely important in the discovery of the Higgs Boson, completing the SM particles. This is an example of a low-energy EFT where the power counting parameter is p/M_Q where M_Q is the mass of the heavy bottom and charm quarks m_b and m_c. In the example of the muon decay, p, the momentum, is of the order of

the muon mass. However, in other kinds of decays, such as in hadronic weak decays, the momentum that describes the scale of the problem can be in the range of hadron or quark masses. Historically, this theory has been used when the W and Z boson masses had not yet been measured. This has been found to be the optimal method to test the unitarity of the Cabibbo-Kobayashi-Maskawa (CKM) matrix which contains a parameter that determines the level of CP violation in the SM. In addition, non-perturbative QCD is a limit that this theory can be used for. A concise summary of HQET can be found in Ref. [10].

A similar theory, called Low-Energy Effective Theory (LEFT) describes a low-energy limit of the SM that does not include the W and Z bosons, the Higgs, or the top quark. The gauge group here is $SU(3) \times U(1)$. A review can be found in Ref. [11].

Chiral perturbation theory is commonly used by nuclear physicists to describe the interactions of pions and nucleons in the low momentum limit. In essence, we are looking at the low energy dynamics of QCD. While the QCD Lagrangian consists of quark and gluon fields, χPT has meson and baryon fields. Pion scatterings were an example of how this theory was used to obtain collider appropriate calculations, but the matching cannot be computed analytically due to the non-perturbative nature of χPT. Nevertheless, this theory can be used to compute parameters suitable to collider experiments.

SCET, or soft-collinear effective field theory, is another interesting example of an EFT. This theory involves using a different frame of reference to study a different type of hard interactions, in the soft and collinear limits. The soft and collinear limits describe some of the classic divergences in QFTs. A soft limit implies that we have a small momentum, where the scale of reference $\Lambda \gg p_{soft}$ where the latter quantity is the momentum of the particle. The collinear limit can best be understood in the context of jets by considering jets being collinear. Collinear DOFs describe particles that are moving in a close to parallel but not exactly the same directions. There is a connection to HQET, where in the case that $p_{soft} \sim \Lambda_{QCD}$, the soft modes are non-perturbative like in HQET for bound B or D mesons. However, this can be generalised to other particles in high-energy physics. In the end, these are all particles within the infrared regime of QCD in its divergences. We can use SCET to describe energetic particles and in essence, all amplitudes in high energy physics to first approximation. However, it is particularly interesting because of its application to deriving factorization theorems and resummation. Soft and collinear limits of high energy physics processes are notoriously difficult to handle due to the presence of Sudakov double logarithms. One example of a process that was calculated using SCET in conjunction with HQET is that of B-meson decays, and in fact, this was a theory first studied for the case of inclusive B-decays. The Drell-Yan process and the connected case of the Higgs were studied to N^3LL, or to the third degree of the leading logarithm by using SCET resummation procedures. Jet observables in their important soft and collinear limits are the most well-known applications of SCET. Another important example is that of Deep Inelastic Scattering. An extensive review of all these applications can be found in Ref. [12]. To summarise, some of the applications are:

- B-decays
- Inclusive hard scattering processes such as $e^- p \to e^- X$, also known as Deep Inelastic scattering, or a classic Drell-Yan process $p\bar{p} \to X l^+ l^-$.
- Jet processes such as $e^+ e^- \to jets$

- Hard scattering processes involving photons such as γ^*

SCET is special as an EFT since it involves non-local operators due to the frame of reference and variables used.

2.4 Scale Separation

In this section, we will discuss scale separation in terms of a more concrete example. EFTs are complex multi-scale problems and one example is that of a hydrogen atom. We have several scales at play here– the masses and momenta of protons and electrons along with a hierarchy of scales relating to the multitude of elementary particles that comprise the quantum world.

An EFT can be built just by having some basic information– we need to identify the degrees of freedom (DOF) and the symmetries that restrict them. In essence, this would require us to know the field content, as well as all interactions that are allowed between these particles, as per the gauge groups under consideration. In addition, we would need to look at the expansion parameters and the power counting involved. These rules are general, applying to a straightforward theory such as SMEFT as well as effective descriptions of gravity.

We can use the following example of the hydrogen atom, taken from Ref. [13]. As we know of course, a most basic description of the hydrogen atom consists of an electron coupled to a proton through the electromagnetic interaction: thus, this interaction is mediated by a photon. However, for the considerations of elementary particle physics, while the electron is a fundamental particle, protons are known to consist of a trio of confined quarks. An important observable that is calculated in the connection of this basic atom, is its binding energy, given by

$$E_0 = \frac{1}{2} m_e \alpha^2 \left[1 + \mathcal{O}\left(\frac{m_e^2}{m_b^2} \right) \right]. \tag{2.12}$$

In the above, m_e represents the electron mass and α, which will be discussed further, is called the fine-structure constant.

We can naively see here the property of scale separation in EFTs. On one hand, we are able to obtain a reasonable approximation for the binding energy of hydrogen using simply $E = 1/2 m_e \alpha^2$, and this was calculated without knowledge of the deeper structure of the proton. However, if we now consider this as an effective description and want to include e.g., the effect of bottom quarks, this would appear as a correction to Eq. (2.12) which is proportionate to the inverse square of the bottom mass $1/m_b^2$. Such a correction would take the form of the following Feynman diagram:

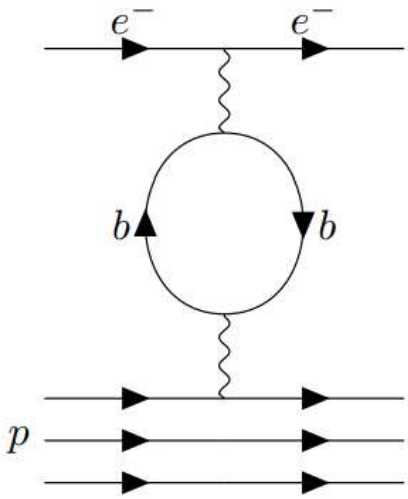

Figure 2.3: Bottom quark corrections to the binding energy of the hydrogen atom

This procedure does not just stop here, because there is an additional subtlety in quantum field theory– that of renormalisation. E.g., the original numerical value of the fine-structure constant was known to be $1/137$. However, this coupling gets renormalised according to the energy scale that we are considering. The running of the constant goes as $\alpha(0) = 1/137$ for energies below the W-boson mass scale to $\alpha(M_W) = 1/127$. For an experiment conducted at atomic scales, we can use the former values and ignore the bottom quark mass. However, at energies where the bottom quark mass comes into play, we would have

$$\mathcal{L}(p, e^-, \gamma, b; \alpha, m_b) = \mathcal{L}(p, e^-, \gamma; \alpha') + \mathcal{O}\left(\frac{1}{m_b^2}\right). \tag{2.13}$$

Here, we firstly look at one Lagrangian which accounts for the interaction between a proton, electron, photon, and bottom quark. We separate this into two parts, the first of which is independent of m_b and the second contains the corrections due to the heavy quark. α and α' describe the running of the fine-structure constant, meaning that we look at the value at the two different scales. This argument can be extended to higher masses. E.g., we have as per Ref. [14]

$$m_t \frac{d}{dm_t}\left(\frac{1}{\alpha}\right) = -\frac{1}{3\pi}, \tag{2.14}$$

for the top quark mass m_t and the proton mass has the following dependence

$$m_p \propto m_t^{2/27}. \tag{2.15}$$

An obvious clarification here is the following. The proton consists of a combination of the lightest quarks, namely the up and down quarks. As seen in Table. 3.1, the up and down quarks have masses in the MeV range, whereas the bottom has a mass in the GeV range. The momentum transfer in hydrogen is $|\mathbf{p}| \sim m_e\alpha$ which is smaller than the proton size of

200 MeV. A crucial conclusion of the above discussion is that we are able to make reasonable conclusions using the above EFT ideas without any consideration for what happens at even higher scales, e.g., if the top quark were to be included. Any possible UV divergences do not invalidate the theory.

The above example was used to sketch a multi-scale problem such as is commonly encountered when one considers EFTs. E.g., SMEFT involves all of the scales in the SM itself, and it is crucial to understand the hierarchy of scales as well as the renormalisation of these.

2.5 The Two Types of EFTs

As seen in the previous section, EFTs usually involve multiple scales. We can use the ideas of EFTs to build two kinds of theories, a top-down or bottom-up one.

- A Top-Down EFT refers to one where we are aware of the UV theory but "integrate out" some heavy scales in order to study low-energy observables. The most well known example of this would be Heavy Quark Effective Theory. It's also often common to consider predictions in the SM after integrating out the heaviest particles, most commonly the top quark. Such theories can greatly simplify calculations since they do not include DOFs that are outside the scales of interest.
- The opposite would be a Bottom-Up EFT. In this case, we may not have knowledge of the UV theory. However, the IR theory can be systematically expanded using the Wilsonian approach and making minimal assumptions on the UV theory. We will be considering an example of this in fair detail, namely the SM and its expansion-SMEFT.

2.6 Representation Independence

When writing out an EFT Lagrangian, one must follow Gell-Mann's Totalitarian Principle, which states

"Among baryons, antibaryons, and mesons, any process which is not forbidden by a conservation law actually does take place with appreciable probability. We have made liberal and tacit use of this assumption, which is related to the state of affairs that is said to prevail in a perfect totalitarian state.",

or in its more concise form that, *everything not forbidden is compulsory*.

This means that given a set of degrees of freedom and their gauge group, one has to write down every possible operator that fulfils those constraints. This leads, as expected, to a large number of operators, but also a great deal of redundancy. In this section, we will be discussing how such redundancies are treated. Later, the discussion of building a complete and coherent operator basis for SMEFT will elucidate how this works for a real-world theory. It is extremely important to identify these redundant operators since they make calculations severely more tedious. As we know, the Lagrangian is not a physical quantity, however, amplitudes are. This mean that we can have repetitions of operators in a Lagrangian which do not contribute to the final amplitude. We use here an example from Ref. [15] to look at representation independence. This tells us that once we have a

non-redundant basis for an EFT, we obtain exactly the same results when computing an amplitude, had we used a different non-redundant basis. The following example is from φ^4 theory, where we work with the Lagrangian

$$\mathcal{L} = \frac{1}{2}(\partial_\mu \varphi)^2 - \frac{1}{2}m^2\varphi^2 - \lambda\varphi^4 + \eta g_1 \varphi^6 + \eta g_2 \varphi^3 \partial^2 \varphi, \tag{2.16}$$

within the limit $\eta \ll 1$. The standard method of eliminating redundant operators is to use equations of motion to eliminate related categories of operators. Alternatively, one can make use of field redefinitions. In this case, we have an extension of the Klein-Gordon equation that is

$$\partial^2 \varphi = -m^2\varphi - 4\lambda\varphi^3. \tag{2.17}$$

The equivalent field redefinition would be

$$\varphi \to -m^2\varphi - 4\lambda\varphi^3. \tag{2.18}$$

This results in the following transformations of the terms from our Lagrangian:

$$\frac{1}{2}(\partial_\mu \varphi^2) \to \frac{1}{2}(\partial_\mu \varphi)^2 - \eta g_2 \varphi^3 \partial^2 \varphi + \mathcal{O}(\eta^2) \tag{2.19}$$

$$m^2\varphi^2 \to m^2\varphi^2 + 2\eta g_2 m^2 \varphi^4 + \mathcal{O}(\eta^2) \tag{2.20}$$

$$\lambda\varphi^4 \to \lambda\varphi^4 + 4\eta g_2 \lambda \varphi^6 + \mathcal{O}(\eta^2). \tag{2.21}$$

This results in the following new Lagrangian:

$$\mathcal{L} = \frac{1}{2}(\partial_\mu \varphi)^2 - \frac{1}{2}m^2\varphi^2 - \lambda'\varphi^4 + \eta g_1' \varphi^6 + \mathcal{O}(\eta^2). \tag{2.22}$$

In the above, we have modified versions of the couplings, where, e.g., η' is a function of the original η and so on. The result of the above Lagrangian is that we have managed to eliminate a term and thus have obtained a Lagrangian with fewer terms, meaning that it is easier to obtain a succinct amplitude without additional terms. In the following sections, we will consider different approaches to eliminating redundancies in EFT Lagrangians in order to obtain theories that offer an easier approach to calculating physical scattering amplitudes.

2.6.1 Total Derivatives

The Warsaw basis of the SMEFT is based on avoiding terms involving derivatives in order to simplify the derivation of Feynman rules. We will here consider how one can eliminate such terms using partial integration and associated methods. Following Ref. [16], we consider the example of a generic low-energy field φ and a total derivative operator appearing in an EFT expansion of it:

$$S_{int} = -g \int d^4x \, \partial_\mu(\varphi^2 \partial^\mu \varphi). \tag{2.23}$$

Here, φ is a generic low-energy field. In a manipulation commonly used in physics, we can use Stokes' theorem to show that the above is equivalent to a boundary term on the surface of the sphere of integration

$$\int_M d^4x \, \partial_\mu(\varphi^2 \partial_\mu \varphi) = \int_{\partial M} d^3x \, n_\mu(\varphi^2 \partial_\mu \varphi). \tag{2.24}$$

It is common to assume for quantum fields that they vanish at the boundaries and so these terms can be dropped. This method can also be used to simplify calculations in another way, since it allows us to move derivatives around the given term to aid calculations. In the above, n_μ refers to the outward-directed unit normal to the boundary under consideration, which is ∂M. We can make a fair assumption here that these integrals vanish at infinity and this allows us to completely drop terms involving total derivatives. Of course, depending on the theory under consideration, the asymptotic behaviour must be carefully examined in order to determine whether the previous statement holds true.

2.6.2 Equations of Motion

The Euler Lagrange equations of motion for the theory

$$0 = \int d^4x \left[\frac{\partial \mathcal{L}}{\partial \mathcal{F}} \delta \mathcal{F} - \partial_\mu \left(\frac{\partial \mathcal{L}}{\partial(\partial_\mu \mathcal{F})} \right) \delta \mathcal{F}) \right], \tag{2.25}$$

can be used to relate different operator structures and thus eliminate redundant operators. While the above may look complex at first glance, it is simply an extension of the Euler-Lagrange equation in classical mechanics. We vary the action,

$$S = \int d^4x \mathcal{L}(\mathcal{F}, \partial_\mu \mathcal{F}), \tag{2.26}$$

where in the above $\mathcal{F}$ represents the various fields in the theory. Equations of motion tell us that operator structures are not independent from each other. This process will be described in detail in the next section, where we study EOM corrections to the SM. Exemplifying this, Ref. [17] uses these methods to eliminate related operator structures.

2.6.3 Field Redefinitions

As mentioned previously, the Lagrangian is not a physical quantity, meaning that one can scale fields as they please. However, these redundancies are eliminated once one calculates the physical quantity in question, which is the scattering amplitude. This is due to the fact that physical quantities have to be independent of the choice of variables. We have another tool to eliminate redundant operators at our disposal, namely, field redefinitions. The equivalence principle for the S-matrix states that S-matrix elements are invariant under reparametrisation of fields. Here, we will consider an example from Ref. [16], where we expand the action in a Taylor series in a small parameter, ε.

$$S[\varphi] = S_0[\varphi] + \varepsilon S_1[\varphi] + \varepsilon^2 S_2[\varphi] + \cdots . \tag{2.27}$$

In general, this procedure is quite similar to that of using the Euler-Lagrange equations, where we say that the action is invariant under small transformations. We look at this from a different perspective, where we perform an infinitesimal field redefinition in the field in question, the scalar field φ. This looks like

$$\delta\varphi = \varepsilon f_1[\varphi] + \varepsilon^2 f_2[\varphi] + \cdots . \tag{2.28}$$

In the above, we expand our scalar field infinitesimally in the same small parameter, ε, where the functions f_i are arbitrary functions of the fields and their derivatives, giving us $f_i(\varphi, \partial\varphi. \cdots)$. These changes manifest in the action as follows

$$\delta S = \int d^4x \left\{ \frac{\delta S}{\delta\varphi(x)} + \varepsilon \frac{\delta S_1}{\delta\varphi(x)} + \varepsilon^2 \frac{\delta S_2}{\delta\varphi(x)} + \cdots \right\} \delta\varphi. \tag{2.29}$$

Looking at the definition of $\delta\varphi$, the above can be rewritten as

$$\int d^4x \left\{ \varepsilon \left[\frac{\delta S_0}{\delta\varphi} f_1 \right] + \varepsilon^2 \left[\frac{\delta S_0}{\delta\varphi(x)} f_2 + \frac{\delta S_1}{\delta\varphi(x)} f_1 \right] + \cdots \right\}. \tag{2.30}$$

The function f_1 can be used here to erase the interaction term proportional to S_1 by making choices in the non-physical terms in the Lagrangian. As per the review, we consider a local function $B[\varphi]$ in the following consideration for a term S_i

$$S_i \subset \int d^4x \frac{\delta S_0}{\delta\varphi(x)} B[\varphi], \tag{2.31}$$

we can use the choice $f_i = -B$ to successfully deal with the above functions. In this manner, we see how field redefinitions can be used to eliminate Lagrangian redundancies.

2.7 Power Counting and Renormalisation

There exists a naive method to determine the renormalisability of a theory, based on the units of the coupling constant. Essentially, one can use power counting to determine which of the following four categories a quantum theory falls into,

- Non-renormalisable theory
- Renormalisable theory
- Super-renormalisable theory
- Finite theory

By definition, the action is a quantity that is dimensionless (or equivalently, to $\hbar$), so using the definition

$$S = \int d^4x \, \mathcal{L}, \tag{2.32}$$

we establish that any term in the Lagrangian should have a dimension of 4. One can examine the degree of divergence of any graph by looking at the terms in the Lagrangian that go into it. The dimension of a field can be determined using the aforementioned method or by looking at how the propagator behaves in the large momentum limit. Using this knowledge, one can establish the following dimensions, in d-dimensions for the scalar and fermion fields respectively:

$$[\varphi] = \frac{d-2}{2} \tag{2.33}$$

$$[\psi] = \frac{d-1}{2}, \tag{2.34}$$

equaling 1 for scalar fields and 3/2 for spin-1/2 fields in four dimensions. Non-renormalisable theories generally have a negative power in the coupling constant. Other examples include:

- Gravity, whose coupling constant we describe as $\kappa^2 = 32\pi G$ where G is the known Newtonian gravitational constant, has a negative dimension. This means that using the traditional action for gravity, commonly known as the Einstein-Hilbert action, will yield a non-renormalisable theory with spurious infinities.
- Supergravity, a supersymmetric theory of a gravity, is through similar arguments non-renormalisable.
- The previously discussed heavy quark EFT is a common example of a non-renormalisable theory which has a dimensionful constant proportional to the inverse of a quark mass. However, this has been one of the first examples of how an effective field theory approach can be used to circumvent infinities and get usable calculations. As we also noted, SMEFT itself contains four fermion terms as part of its Lagrangian.

There are of course more examples. On the other hand, renormalisable theories comprise a very small number of the theories particle physicists work with. Such theories have exclusively dimensionless coupling constants. The most important example from this category is of course, the Standard Model itself, which was proved to be fully renormalisable by t'Hooft and Veltman in Ref. [18]. Other examples of renormalisable theories are φ^4 theory, which is a classic toy model. Another familiar example is the theory of QED which has no dimensionful coupling constants. In addition, as a subcategory of SM-like theories, massless non-Abelian gauge theories as well as spontaneously broken non-Abelian gauge theories are in general renormalisable. Even though massive non-Abelian gauge theories tend to be non-renormalisable, in the case of spontaneous breaking of the gauge symmetry, renormalisability is retained.

Super renormalisable theories are a category of theories which converge, so the number of divergent graphs is very limited. As we go to higher and higher orders in the theory, or equivalently add more loops, the degree of divergence gets limited. Unlike non-renormalisable theories, such theories have dimensionful constants, with positive dimension however. The most simple example of such a theory is φ^3 theory, which needs to come with a positive coupling constant in order to achieve the required dimension of 4 for terms in a Lagrangian. However, φ^4 theory is also super-renormalisable, albeit in three dimensions.

It must be noted that the renormalisability of a theory depends on its dimensionality. Thus, there are theories that are renormalisable in $d \neq 4$ dimensions, e.g., φ^3 theory is renormalisable in six dimensions despite not being renormalisable in four dimensions. As per Ref. [19] the following is a complete set of interactions for spin 0, $\frac{1}{2}$, and 1 fields that are potentially renormalisable in four dimensions

$$\varphi^4, \ , \bar{\psi}\psi\varphi, \ (A^2)^2, \ \bar{\psi}\not{A}\psi, \ \varphi^\dagger\partial_\mu\varphi A^\mu, \ \varphi^\dagger\varphi A^2. \tag{2.35}$$

To put this all into the context of effective field theories, a theory is renormalisable when one has a finite number of parameters and consequently, a finite number of graphs to be used in order to eliminate the infinities in these parameters. EFTs are known to have an infinite number of terms and thus can appear to be non-renormalisable at first glance. However,

this issue is solved by working order by order when building the tower of operators. Thus, at a given dimension, an EFT only has a finite number of operators and therefore this is not a problem. In addition, the discussion on large mass expansions shows how by using an effective approach, one can convert infinities to obtain finite results up to a calculable error. At higher loop orders, one can examine the *superficial degree of divergence* of a diagram. This is a standard procedure where one compares the powers of the loop momentum in the numerator and denominator. Following the discussion in Ref. [20], we consider an arbitrary QED graph, whose corresponding Feynman integral can be represented as follows

$$= \frac{d^d k_1 \cdots d^d k_L}{(\not{k}_i - m) \cdots (k_j^2) \cdots (k_n^2)}. \tag{2.36}$$

Thus, in d-dimensions given an L-loop diagram, we obtain 4 powers of the loop momentum k in the numerator. However, this is compensated by one power of k in the denominator for every fermion propagator containing the loop momentum, and two powers of k for photon propagators. Note that the QED Feynman rules do not have momentum factors in the numerator so we ignore the algebraic structures that can appear in the numerator for this discussion. The superficial degree of divergence D is given by subtracting the number of powers in the numerator from that in the denominator:

$$D = dL - P_e - 2P_\gamma, \tag{2.37}$$

where d is the dimension of the theory, L refers to the number of loops, and P_e and P_γ are respectively the number of electron and photon propagators. $D = 0$ corresponds to a logarithmic divergence, while $D > 0$ leads to a UV divergence that could potentially be treated by putting a momentum cutoff. $D < 0$ is the ideal case of not having divergences, although in other theories with massless particles there could be issues of IR divergence. This quantity D is called only the superficial degree of divergence because it is a naive estimate that can be affected by factors such as Ward identities that lead to cancellations that can alleviate the divergence. The above relation also fails for the trivial case of a diagram with no propagators or loops, since $D = 0$ implies it would be divergence. Some of these exceptions are shown in Ref. [20]. Nevertheless, in the traditional approach to renormalisation, D can be manipulated using graph theoretical ideas that allow one to immediately test diagrams and check their divergence properties quickly. Manipulating the above expression leads us to the following expression for D in d-dimensional QED:

$$D = d + \left(\frac{d-4}{2}\right) V - \left(\frac{d-2}{2}\right) N_\gamma - \left(\frac{d-1}{2}\right) N_e, \tag{2.38}$$

where V is the number of vertices and N_γ and N_e are respectively the number of external photons and electrons. Note that since the above expression explicitly contains the number of vertices at $d \neq 4$ dimensions, it also includes that many powers of the coupling constant. In this sense, we see how the renormalisability of the theory can be understood in terms of the coupling constant of the theory. Fortunately, QED has a dimensionless coupling. The above expression can be evaluated for different dimensions. E.g., as d increases, the positive contribution from the vertices means that amplitudes will gradually become more divergent. Thus, we can expand on our previous ideas of super-renormalisable, renormalisable and non-renormalisable theories as follows. A super-renormalisable theory will only

contain a finite number of divergent Feynman graphs. Renormalisable theories such as the SM will have divergences to all orders in perturbation theory, although these will be a finite number at each order. Non-renormalisable theories tend to have an increasing number of divergent graphs as we go to higher orders in the perturbative series.

However, as seen in our discussion on diagrammatic large mass expansion in Section 2.2, effective field theories essentially help us avoid this problem, due to the cancellation of UV and IR divergences. As we discussed in Section 3, Fermi theory was an early non-renormalisable theory that supported the idea that one can still obtain plausible results from a non-renormalisable theory. Besides this problem of practicalities, we need to consider carefully the limit we take when we go from a classical theory to a quantum one, namely that Planck's constant $\hbar$ goes to 1, compared to classic theories where we generally set $\hbar \to 0$. In particle physics, one generally uses "God-given units" where we set $c = \hbar = 1$. Thus, these factors are absent and we are unable to see them clearly. In general, loop corrections in particle physics are considered to be an expansion not only in the coupling constant but also in $\hbar$. In gravity, we encounter both classical and quantum corrections and thus $\hbar$ is crucial to distinguish between the two. Thus, we will consider how to restore powers of $\hbar$ into our amplitudes. Firstly, we should note that a general n-point amplitude has a mass dimension of $4 - n$. If we continue to keep $c = 1$, we can see that the dimensions of masses and momenta remain unchanged, according to

$$E = p(c) \tag{2.39}$$

$$E = m(c^2). \tag{2.40}$$

However, what does get affected is the dimensions of the coupling constants, which are affected by a factor of $1/\sqrt{\hbar}$. (add more here) Another thing we need to note is the scales of the problem. An effective field theory treatment of GR is thought to lose validity at the Planck scale ($\sim 10^{19} GeV$).

2.8 Why use an EFT?

So far, we have seen a range of properties as well as applications of EFTs. This will allow us to summarise some of the main motivations to use EFTs in physics research. Effective theories are a tool to avoid spurious divergences. However, we have many reasons to use this tool, some of which are mentioned in the following:

- **Every theory is an EFT**. By this we mean that every time we consider a quantum field theory or otherwise, we are always considering a range of scales and therefore, the range of validity of the theory. Thus, the properties of EFTs can be universally applied to any physical theory in order to simplify calculations and have more physical clarity.
- EFTs manifest the property of scale separation. A clear understanding of the DOFs relevant to the scales under consideration will allow us to both quantify and suitably include or neglect DOFs that fall outside of the range that is relevant to a specific problem.
- EFTs also manifest the symmetries of the theory in question. Thus, when we are working with SMEFT, we are using an extension of the SM gauge group which is

$SU(3) \times SU(2) \times U(1)$ and in the case of gravity, we use the Poincaré symmetry to obtain the classes of operators.

- The power counting procedure within EFTs along with using EOM ensures that EFTs only include relevant interactions. This means that we get rid of irrelevant operators and are able to easier obtain physical quantities such as the scattering amplitude.
- As we noted in the example of the large mass expansion, EFTs allow us to deal with divergences better. We can connect UV divergences to IR divergences, which are much more difficult to deal with and thus, get rid of infinities. We go from a theory that is incalculable to a theory that gives us results. To elaborate, UV divergences can be solved using RGE methods and using counterterms and anomalous dimensions, whereas IR divergences are much more difficult to treat. By equating the infinities, using the fact that we need to obtain finite results, we can deal with the IR infinities in an easier fashion. Thus, non-renormalisable theories can be employed to produce finite results using this approach.

Chapter 3

Standard Model Effective Field Theory

3.1 The Standard Model

A discussion of the SMEFT must begin at dimension 4, comprising the SM itself. This section will quickly review the SM fields and how these fields interact under various gauge transformations. This also serves the purpose of setting up the notation that will be used in the following sections. The conventions followed are the same as in Ref. [5] and Ref. [2]. The Lagrangian associated with the SM can be written as

$$\mathcal{L}_{SM} = -\frac{1}{4}G^A_{\mu\nu}G^{A\mu\nu} - \frac{1}{4}W^I_{\mu\nu}W^{I\mu\nu} - \frac{1}{4}B_{\mu\nu}B^{\mu\nu} + \sum_{\psi=q,u,d,\ell,e}\overline{\psi}i\not{D}\psi \tag{3.1}$$
$$(D_\mu H)^\dagger(D^\mu H) - \lambda\left(H^\dagger H - \frac{1}{2}v^2\right)^2 - \left[H^{\dagger j}\overline{d}Y_d q_j + \tilde{H}^{\dagger j}\overline{u}Y_u q_j + H^{\dagger j}\overline{e}Y_e \ell_j + h.c.\right].$$

In the first line above, we have coupling constants for three different gauge bosons, transforming under the $SU_c(3)$, $SU_L(2)$ and $U_Y(1)$ gauge groups respectively. These refer to the strong and electroweak interactions. The corresponding coupling constants g_3, g_2, and, g_1 respectively, accompany these terms. The covariant derivative mentioned above is fixed to be

$$D_\mu = \partial_\mu + ig_3T^A A^A_\mu + ig_2t^I W^I_\mu + ig_1y_iB_\mu. \tag{3.2}$$

Further, we normalise the $SU_c(3)$ generators, i.e., Gell-Mann matrices, as $Tr(T^AT^B) = 2\delta^{AB}$. The $SU_L(2)$ generators are defined as $t^I = \tau^I/2$ where τ^I are the usual Pauli matrices. Finally, we can note that y_i is the $U(1)$ hypercharge generator. We also have the kinetic term for the Dirac spinors. $\tilde{H}_j = \epsilon_{jk}H^{*k}$, often also expressed as $\tilde{H} = -i\tau^2H^{*k}$, is the complex-conjugated Higgs doublet with $\epsilon_{12} = 1$ being the usual anti-symmetric tensor. The second line on the other hand contains the Higgs sector starting with the standard kinetic term for a scalar field followed by its self interaction. While the QCD sector of the SM remains unbroken, the vacuum expectation value (vev) of the Higgs field which breaks the electroweak sector $SU_L(2) \times U_Y(1) \to U_{em}(1)$ is given by $\langle H^\dagger H\rangle = v^2/2$ with $v \sim 246GeV$. The last term given above is related to the mass terms for the fermion fields, with flavour indices having been suppressed. Y_i are the Yukawa couplings, associated with fermions masses as $M_{u,d,e} = Y_{u,d,e}v\sqrt{2}$. The masses in the SM have a wide spectrum, here as shown in the Table 3.1 using data from the Particle Data Group from 2020:

Particle	Mass
γ(photon)	$m < 1 \times 10^{-18} eV$
g(gluon)	$m = 0$
W boson	$m = 80.379 \pm 0.012 GeV$
Z boson	$m = 91.1876 \pm 0.0021 GeV$
Higgs boson	$m = 125.25 \pm 0.17 GeV$
e(electron)	$m = 0.5109989461 \pm 0.0000000031 MeV$
μ(muon)	$m = 105.6583745 \pm 0.000024 MeV$
τ(tau)	$m = 1776.86 \pm 0.012 MeV$
ν_e(electron neutrino)	$m < 460 eV$
ν_μ(muon neutrino)	$m < 0.19 MeV$
ν_τ(tau neutrino)	$m < 18.2 MeV$
u(up quark)	$m = 2.16^{+0.49}_{-0.26} MeV$
d(down quark)	$m = 4.67^{+0.48}_{-.17} MeV$
s(strange quark)	$m = 93^{+11}_{-5} MeV$
c(charm quark)	$m = 1.27 \pm 0.02 GeV$
b(bottom quark	$m = 4.18^{0.03}_{-0.02} GeV$
t(top quark)	$m = 172.76 \pm 0.30 GeV$

Table 3.1: Masses of the SM particles. Source: PDG 2020

In addition, It should be noted that when working in theory, firstly, the neutrino masses in the SM are considered to be zero. However, dimension five terms allow for neutrino masses to be non-zero. The Nobel Prize of 2015 proved that we have a mixing of neutrino states, between mass and flavour eigenstates [21]. This results in the phenomenon called neutrino oscillations, which requires non-zero neutrino masses. It is very non-trivial to include neutrino masses into the SM and we cannot naively use the Higgs process to do so. In addition, the above terms describe experimental data. However, the above parameters are not theoretically predictable within the SM and actually vary depending on the RGE methods used. Thus, they are different, depending on which renormalisation scheme is implemented, the most common examples being the on-shell scheme and the $\overline{MS}$ scheme, or the modified minimal subtraction scheme. In the following, we see explicitly how each of the fields transform under the various gauge groups of the SM:

Field	$SU_c(3)$	$SU_L(2)$	$U_Y(1)$	$SO^+(3,1)$
$q_i = (u_L^i, d_L^i)^T$	**3**	**2**	$1/6$	$(1/2, 0)$
$u_i = \{u_R, c_R, t_R\}$	**3**	**1**	$2/3$	$(0, 1/2)$
$d_i = \{d_R, s_R, b_R\}$	**3**	**1**	$-1/3$	$(0, 1/2)$
$\ell_i = (\nu_L^i, e_L^i)^T$	**1**	**2**	$-1/2$	$(1/2, 0)$
$e_i = \{e_R, \mu_R, \tau_R\}$	**1**	**1**	-1	$(0, 1/2)$
H	**1**	**2**	$1/2$	$(0, 0)$

(3.3)

Table 3.2: Gauge group transformations of SM particles

We expect that if we take the low energy limit of SMEFT, we will land up with simply the SM described above. It must also be noted, that the SM has been shown to be renormalisable in Ref. [18]. Now that our notation is fixed, we can approach the SM as an EFT.

3.2 SMEFT as a Probe of New Physics

The EFT phenomenology program in particle physics has two major motivations, namely

- Improving the precision of the SM parameters, particularly in the context of a Higgs phenomenology program, and
- Facilitating the discovery of new particles not described in the SM, within as general a framework as possible.

In the following, we will explain why EFTs are particularly suited to this task.

The key here is that we are limited in our experiments by their energy scale. While there are hopes of building a $100 TeV$ collider as reviewed in Ref. [22] to compare with $14 TeV$ at the LHC, this is a difficult process since one would have to discuss all the practicalities of building such a collider- financial, political, etc. This can be seen in Fig. 3.2. From a steady increase in centre-of-mass energy in the early years of having colliders, there is a significant dip in the energies achieved. This is of course expected since the technical challenge and costs involved in building such a collider increase dramatically as we try to achieve progressively higher magnitudes of energies.

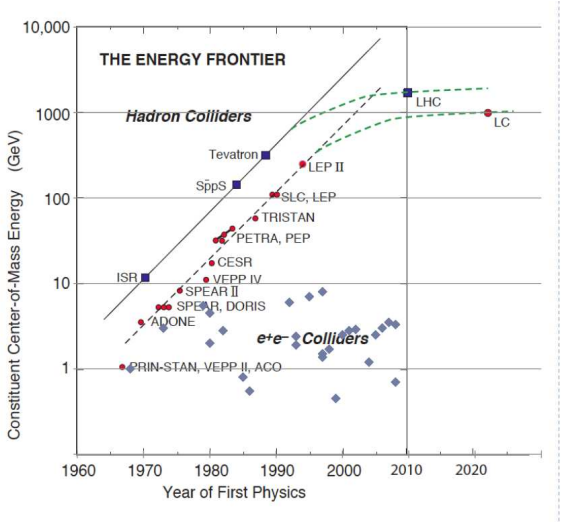

Figure 3.1: Source: http://www.hep.ucl.ac.uk/iop2010/talks/14.pdf

In addition, we can see in Fig. 3.2 some of the many plans that are currently being considered for Future Colliders. At least for the next ten years, even under the most optimistic circumstances, we will be limited to the precise data available from the LHC and prior colliders. Thus, theoretical studies need to make use of the large amount of statistics available from the LHC and LEP.

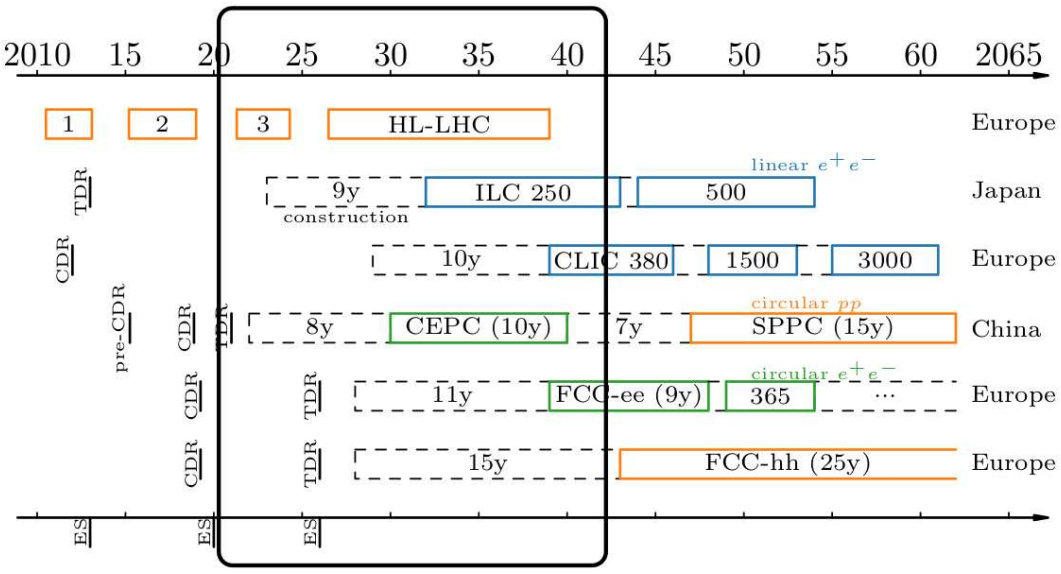

Figure 3.2: Source: G. Durieux, IDT-WG3- Phys Open Meeting, 17 June 2021

The standard approach to New Physics is using what are called "simplified models" [23]. This involves adding a small number of new particles which are weakly coupled to the SM.

The theory of super symmetry has been another big contender. The problem with these approaches is that they are unfalsifiable–i.e., our experimental limits on the energy scales that can be reached implies that when particles that have been predicted are not found, these particles are presumably at a higher energy scale, and thus haven't emerged, since the mass parameters are not predicted in the theory. We can see in Fig. 3.3 examples of such models and their current exclusion limits for predicted particles. One could possibly conclude that going from $\sqrt{s} = 8TeV$ to the full data at $13Tev$ only seems to produce larger and larger exclusion limits.

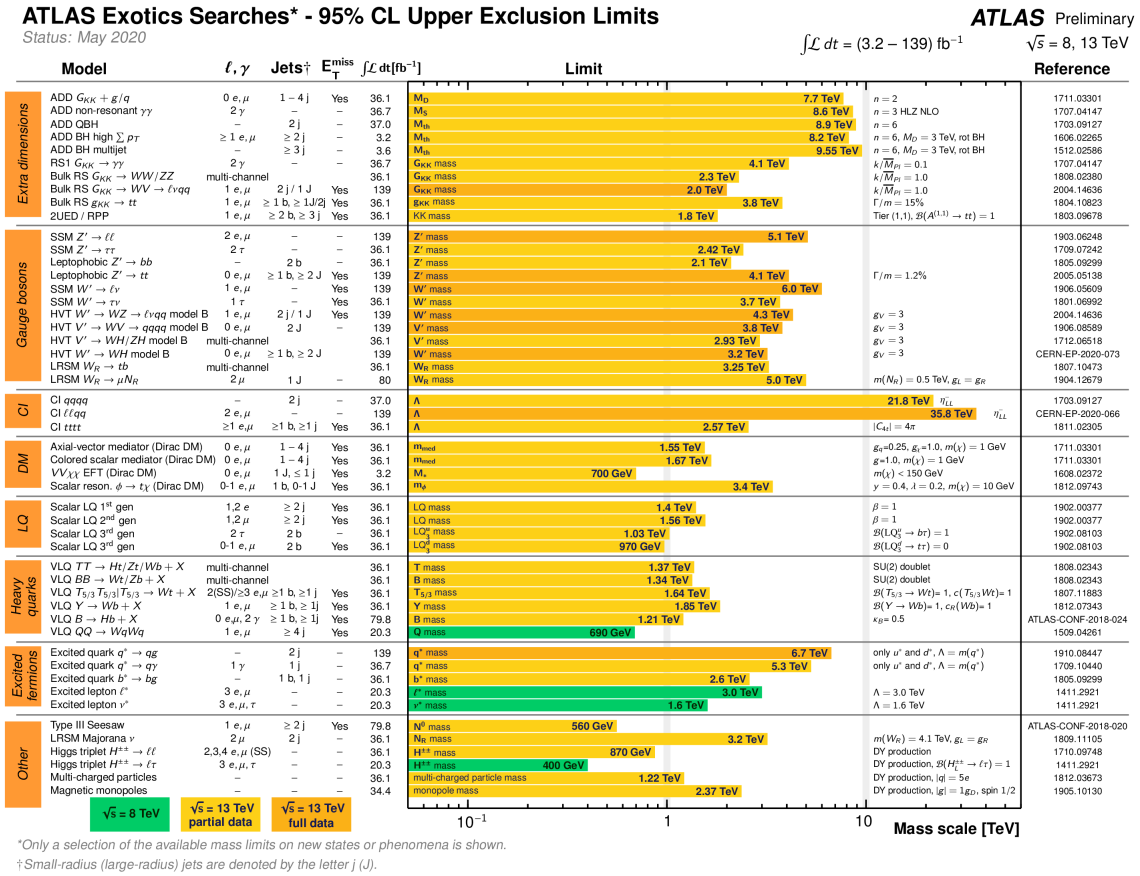

*Only a selection of the available mass limits on new states or phenomena is shown.
†Small-radius (large-radius) jets are denoted by the letter j (J).

Figure 3.3: Source:https://twiki.cern.ch/twiki/bin/view/AtlasPublic/ExoticsPublicResults

On the other hand, what we do have is an immense amount of statistics on SM particles and their interactions. This is where an EFT can make a difference, because it is a minimal and generalised extension on the SM. SMEFT is a simple extension of the SM, containing only the SM fields obeying the constraints of the SM symmetry group, $SU(3) \times SU(2) \times U(1)$. It is built as a tower of operators at higher dimensions, starting with 5 dimensions where there is only one operator (and its Hermitian conjugate), called the Weinberg operator

$$\mathcal{Q}_{mn}^{(5)} = \left(\overline{\ell^{c,m}}\,\tilde{H}^{\star}\right)\left(\tilde{H}^{\dagger}\,\ell^{n}\right), \tag{3.4}$$

and then 6 dimensions, where the number of operators increases quite dramatically to 59

operators in the Warsaw basis [17] and thereon exponentially increasing as you go up in dimension as explicitly calculated in Ref. [24].

Our conviction in the existence of physics beyond the SM also means that we can expect the SM to break down as we probe higher energy scales. SMEFT perfectly fits the role of a theoretical basis that we can use to probe NP at colliders even when the SM has broken down, since it is so general and is a self-consistent theory. Although SMEFT can be more complicated to work with than a simplified model, it offers the opportunity to simultaneously probe a large variety of NP scenarios.

Further evidence of this statement comes from historical studies. EFTs have been key in finding early evidence of new particles. The most common example for a phenomenologist would be that of the use of Fermi theory before the discovery of electroweak bosons such as the W boson. A summary of the discussion in Ref. [5] is given here. The Fermi theory of β decay on the particle level amounts to the process $\mu^- \to e^- + \bar{\nu}_e + \nu_\mu$ described by the "non-renormalisable" Lagrangian

$$\mathcal{L}_{G_F} = -G_F(\bar{\psi}_i\gamma^\mu P_L\psi_j)(\bar{\psi}_k\gamma_\mu P_L\psi_l), \tag{3.5}$$

where we have the Fermi constant G_F and a chiral Lagrangian consisting of various flavours of quarks whose flavour indices are denoted by subscripts. This theory functions up to energies below the masses of the electroweak bosons, so about $100GeV$. Later, as we know, the four-point contact operator between four fermions was replaced by a tree diagram where an electroweak boson would participate in the exchange. In fact, EFT studies proved to be crucial in discovering the weak bosons. A crucial point to note here is that these parameters are modified in the SMEFT. E.g., in Ref. [25], a detailed study of the effect of SMEFT on W mass measurements was done. Additionally, one of the motivations of the SMEFT programme and New Physics, was to understand neutrino masses. The Weinberg operator given in Eq. (3.4) is a candidate for explaining Majorana neutrino masses within the well-known seesaw model for neutrino oscillations. A matching of coefficients for neutrinos up to dimension 7 in SMEFT was done in Ref. [26]. SMEFT provides a general approach to this problem, not limiting itself to the seesaw model and offers a way to interpret neutrino data through these operators. Thus, an EFT can be very useful in phenomenological studies, even when the UV completion is unknown.

3.3 Higgs Precision Phenomenology

There are many reasons to believe that the current parametrisation of the Higgs field, which we see in the SM Lagrangian may only be an effective description. The Higgs sector of the SM looks like

$$\mathcal{L}_{HIGGS} = (D_\mu\varphi)^2 + \mu^2\varphi^\dagger\varphi - \lambda(\varphi^\dagger\varphi)^2. \tag{3.6}$$

The above takes the shape of a Mexican hat potential, as seen in Fig. 3.4 with a VEV at $\langle H^\dagger H\rangle = \frac{1}{2}v^2$. The Goldstone bosons coming from the spontaneous breaking of symmetry result in the EW bosons acquiring masses. However, one problem we have here is that the Higgs mechanism has no fundamental origin in the SM. Using EFT methods is motivated by wanting to find a more fundamental description.

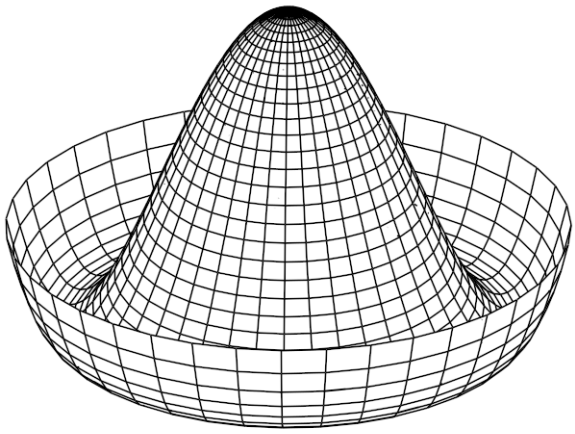

Figure 3.4: The Mexican hat potential

This is further corroborated by the well-known connections between the parametrisation of the Higgs in the SM and the Ginzburg-Landau model for super conductors.

The Ginzburg-Landau model is an example of Abelian Higgs model being described near the critical temperature T_c:

$$\mathcal{L}_{LG} = \int dx^3 \left[\frac{1}{2}|(d - 2ieA)s|^2 + \frac{\gamma}{2}(|s|^2 - a^2) \right]. \tag{3.7}$$

While in the case of the non-Abelian Higgs mechanism as seen in the SM the $F_{\mu\nu}$s describe a non-Abelian field, and φ describes a Higgs field; here $F_{\mu\nu}$ is an Abelian vector field, the photon and φ is the order parameter. In addition, $m^2 \sim T - T_c$ and D_μ is the Abelian covariant derivative.
Clearly, the temperature going lower than the critical temperature sends $m^2 < 0$ and causes the spontaneous breaking of symmetry.

Consider the effect of SMEFT corrections due to dimension 6 operators. In the SM, we have

$$V(H^\dagger H) = \lambda \left(H^\dagger H - \frac{1}{2}v^2 \right). \tag{3.8}$$

Now, adding the first corrections from SMEFT gives us

$$V(H^\dagger H) = \lambda \left(H^\dagger H - \frac{1}{2}v^2 \right) - \mathcal{C}_H (H^\dagger H)^3, \tag{3.9}$$

which modifies the vacuum expectation value from just $v^2/2$ to the above, which includes higher dimensional contributions. One interesting example to consider is that the Higgs may be a composite particle. Such a model says that the Higgs comprises of more elementary particles, in the same way as a nucleon. Such ideas were inspired by several simplified models such as the Little Higgs constructions, extra dimensional models, and holographic composite Higgs models, as explained in Ref. [5]. A discussion of SMEFT is not complete without including its counterpart, Higgs Effective Field Theory, or HEFT. This EFT can be used to describe composite Higgs models and other processes and nevertheless, reproduces

the SM at lower energies. As per Ref. [5], the Callan-Coleman-Wess-Zumino (CCWZ) formalism allows us to parameterise the scalar sector of the SM with minimal IR assumptions. HEFT is the ideal theoretical tool to describe scenarios such as the composite Higgs. A review of some of the motivations behind HEFT can be found in Ref. [27].

3.4 Operator Bases in the SMEFT

The Warsaw basis given in Ref. [17] is the first example of a non-redundant basis for the SMEFT. This has made it a calculable theory and potentially one where we can look at higher order corrections numerically, as is expanded upon in Sec. 4. It is most appropriate that we appreciate the superhuman effort in transforming approximately 2500 redundant and non-redundant operators to a concise basis of 59 operators, as seen in Table 3.4. SMEFT consists of an expansion over the SM Lagrangian

$$\mathcal{L}_{SMEFT} = \mathcal{L}_{SM} + \mathcal{L}^{(5)} + \mathcal{L}^{(6)} + \mathcal{L}^{(7)} + \cdots, \tag{3.10}$$

where Gell-Mann's totalitarian principle applies- as is true for all EFTs. Thus, we require that:

- the SM gauge group $SU(3)_c \times SU(2)_L \times U(1)_Y$ should be a subgroup of the gauge group of this theory
- all SM degrees of freedom should be included in the form of either fundamental or composite fields
- the low energy limit of this theory should reproduce the SM, with the caveat that this may change if weakly coupled light particles such as right-handed neutrinos or axions are proven to exist.

Now, we return to examine the remaining operators that make up the SMEFT as seen in Eq. 3.10.

$$\mathcal{L}^{(d)} = \sum_{i=1}^{n_d} \frac{C_i^{(d)}}{\Lambda^{d-4}} Q_i^{(d)}. \tag{3.11}$$

As we can see, any operator at d-dimensions is suppressed by $d-4$ powers of Λ, the cut-off scale of the theory. Note that we will often absorb this factor into the Wilson coefficient. Thus, the leading corrections to the SM can be captured by considering $\mathcal{L}^{(5)}$ and $\mathcal{L}^{(6)}$. Of course, making the most of the data-rich era of the LHC has lead to interest in capturing sub-leading effects, which will be the focus of the next chapter. At dimension 5, fortunately, there is only one possible operator. Scalar and vector fields have mass dimension $[1]$ respectively, while spinor fields have dimension $[3/2]$. Dimensional and gauge group constraints can be used to see that this is the only possible operator. This term is a lepton number violating term, that can only arise out of SM after spontaneous breaking of $SU(2) \times U(1)$ symmetry. At higher dimensions, we use equations of motion and field redefinitions to reduce a full overcomplete basis to a non-redundant one. It can be noted that while it is technically possible to work with an overcomplete basis, having an enormous number of operators that ultimately do not contribute to the S-matrix elements can make it impossible to realise these calculations. On the other hand, the full process of reducing the set of

dimension 6 operators to a non-redundant basis was one that took many years. One significant development in this regard was the result by Buchmuller and Wyler [28] from 1986. This basis was ultimately realised to be overcomplete. However the most well-known basis, the Warsaw basis, [17] was published only in 2010. This shows that EFTs as a fundamental theoretical tool to study quantum physics were neglected to a large degree. The compact Warsaw basis only consists of non-redundant operators, often used in EFT calculations, unlike the SILH basis and HISZ basis. As stated in Ref. [5], these do not constitute a minimal non-redundant basis. In further developments, a method has been found by permutation and combination to determine the precise number of operators for a non-redundant theory in any given dimension in SMEFT by the authors of Ref. [29].

$1: X^3$	
Q_G	$f^{ABC} G_\mu^{A\nu} G_\nu^{B\rho} G_\rho^{C\mu}$
$Q_{\widetilde{G}}$	$f^{ABC} \widetilde{G}_\mu^{A\nu} G_\nu^{B\rho} G_\rho^{C\mu}$
Q_W	$\epsilon^{IJK} W_\mu^{I\nu} W_\nu^{J\rho} W_\rho^{K\mu}$
$Q_{\widetilde{W}}$	$\epsilon^{IJK} \widetilde{W}_\mu^{I\nu} W_\nu^{J\rho} W_\rho^{K\mu}$

$2: H^6$	
Q_H	$(H^\dagger H)^3$

$3: H^4 D^2$	
$Q_{H\Box}$	$(H^\dagger H)\Box(H^\dagger H)$
Q_{HD}	$\left(H^\dagger D_\mu H\right)^* \left(H^\dagger D_\mu H\right)$

$5: \psi^2 H^3 + \text{h.c.}$	
Q_{eH}	$(H^\dagger H)(\bar{l}_p e_r H)$
Q_{uH}	$(H^\dagger H)(\bar{q}_p u_r \widetilde{H})$
Q_{dH}	$(H^\dagger H)(\bar{q}_p d_r H)$

$4: X^2 H^2$	
Q_{HG}	$H^\dagger H\, G_{\mu\nu}^A G^{A\mu\nu}$
$Q_{H\widetilde{G}}$	$H^\dagger H\, \widetilde{G}_{\mu\nu}^A G^{A\mu\nu}$
Q_{HW}	$H^\dagger H\, W_{\mu\nu}^I W^{I\mu\nu}$
$Q_{H\widetilde{W}}$	$H^\dagger H\, \widetilde{W}_{\mu\nu}^I W^{I\mu\nu}$
Q_{HB}	$H^\dagger H\, B_{\mu\nu} B^{\mu\nu}$
$Q_{H\widetilde{B}}$	$H^\dagger H\, \widetilde{B}_{\mu\nu} B^{\mu\nu}$
Q_{HWB}	$H^\dagger \tau^I H\, W_{\mu\nu}^I B^{\mu\nu}$
$Q_{H\widetilde{W}B}$	$H^\dagger \tau^I H\, \widetilde{W}_{\mu\nu}^I B^{\mu\nu}$

$6: \psi^2 X H + \text{h.c.}$	
Q_{eW}	$(\bar{l}_p \sigma^{\mu\nu} e_r) \tau^I H W_{\mu\nu}^I$
Q_{eB}	$(\bar{l}_p \sigma^{\mu\nu} e_r) H B_{\mu\nu}$
Q_{uG}	$(\bar{q}_p \sigma^{\mu\nu} T^A u_r) \widetilde{H} G_{\mu\nu}^A$
Q_{uW}	$(\bar{q}_p \sigma^{\mu\nu} u_r) \tau^I \widetilde{H} W_{\mu\nu}^I$
Q_{uB}	$(\bar{q}_p \sigma^{\mu\nu} u_r) \widetilde{H} B_{\mu\nu}$
Q_{dG}	$(\bar{q}_p \sigma^{\mu\nu} T^A d_r) H G_{\mu\nu}^A$
Q_{dW}	$(\bar{q}_p \sigma^{\mu\nu} d_r) \tau^I H W_{\mu\nu}^I$
Q_{dB}	$(\bar{q}_p \sigma^{\mu\nu} d_r) H B_{\mu\nu}$

$7: \psi^2 H^2 D$	
$Q_{Hl}^{(1)}$	$(H^\dagger i \overleftrightarrow{D}_\mu H)(\bar{l}_p \gamma^\mu l_r)$
$Q_{Hl}^{(3)}$	$(H^\dagger i \overleftrightarrow{D}_\mu^I H)(\bar{l}_p \tau^I \gamma^\mu l_r)$
Q_{He}	$(H^\dagger i \overleftrightarrow{D}_\mu H)(\bar{e}_p \gamma^\mu e_r)$
$Q_{Hq}^{(1)}$	$(H^\dagger i \overleftrightarrow{D}_\mu H)(\bar{q}_p \gamma^\mu q_r)$
$Q_{Hq}^{(3)}$	$(H^\dagger i \overleftrightarrow{D}_\mu^I H)(\bar{q}_p \tau^I \gamma^\mu q_r)$
Q_{Hu}	$(H^\dagger i \overleftrightarrow{D}_\mu H)(\bar{u}_p \gamma^\mu u_r)$
Q_{Hd}	$(H^\dagger i \overleftrightarrow{D}_\mu H)(\bar{d}_p \gamma^\mu d_r)$
$Q_{Hud} + \text{h.c.}$	$i(\widetilde{H}^\dagger D_\mu H)(\bar{u}_p \gamma^\mu d_r)$

$8: (\bar{L}L)(\bar{L}L)$	
$Q_{\ell\ell}$	$(\bar{l}_p \gamma_\mu l_r)(\bar{l}_s \gamma^\mu l_t)$
$Q_{qq}^{(1)}$	$(\bar{q}_p \gamma_\mu q_r)(\bar{q}_s \gamma^\mu q_t)$
$Q_{qq}^{(3)}$	$(\bar{q}_p \gamma_\mu \tau^I q_r)(\bar{q}_s \gamma^\mu \tau^I q_t)$
$Q_{\ell q}^{(1)}$	$(\bar{l}_p \gamma_\mu l_r)(\bar{q}_s \gamma^\mu q_t)$
$Q_{\ell q}^{(3)}$	$(\bar{l}_p \gamma_\mu \tau^I l_r)(\bar{q}_s \gamma^\mu \tau^I q_t)$

$8: (\bar{R}R)(\bar{R}R)$	
Q_{ee}	$(\bar{e}_p \gamma_\mu e_r)(\bar{e}_s \gamma^\mu e_t)$
Q_{uu}	$(\bar{u}_p \gamma_\mu u_r)(\bar{u}_s \gamma^\mu u_t)$
Q_{dd}	$(\bar{d}_p \gamma_\mu d_r)(\bar{d}_s \gamma^\mu d_t)$
Q_{eu}	$(\bar{e}_p \gamma_\mu e_r)(\bar{u}_s \gamma^\mu u_t)$
Q_{ed}	$(\bar{e}_p \gamma_\mu e_r)(\bar{d}_s \gamma^\mu d_t)$
$Q_{ud}^{(1)}$	$(\bar{u}_p \gamma_\mu u_r)(\bar{d}_s \gamma^\mu d_t)$
$Q_{ud}^{(8)}$	$(\bar{u}_p \gamma_\mu T^A u_r)(\bar{d}_s \gamma^\mu T^A d_t)$

$8: (\bar{L}L)(\bar{R}R)$	
Q_{le}	$(\bar{l}_p \gamma_\mu l_r)(\bar{e}_s \gamma^\mu e_t)$
Q_{lu}	$(\bar{l}_p \gamma_\mu l_r)(\bar{u}_s \gamma^\mu u_t)$
Q_{ld}	$(\bar{l}_p \gamma_\mu l_r)(\bar{d}_s \gamma^\mu d_t)$
Q_{qe}	$(\bar{q}_p \gamma_\mu q_r)(\bar{e}_s \gamma^\mu e_t)$
$Q_{qu}^{(1)}$	$(\bar{q}_p \gamma_\mu q_r)(\bar{u}_s \gamma^\mu u_t)$
$Q_{qu}^{(8)}$	$(\bar{q}_p \gamma_\mu T^A q_r)(\bar{u}_s \gamma^\mu T^A u_t)$
$Q_{qd}^{(1)}$	$(\bar{q}_p \gamma_\mu q_r)(\bar{d}_s \gamma^\mu d_t)$
$Q_{qd}^{(8)}$	$(\bar{q}_p \gamma_\mu T^A q_r)(\bar{d}_s \gamma^\mu T^A d_t)$

$8: (\bar{L}R)(\bar{R}L) + \text{h.c.}$	
Q_{ledq}	$(\bar{l}_p^j e_r)(\bar{d}_s q_{tj})$

$8: (\bar{L}R)(\bar{L}R) + \text{h.c.}$	
$Q_{quqd}^{(1)}$	$(\bar{q}_p^j u_r)\epsilon_{jk}(\bar{q}_s^k d_t)$
$Q_{quqd}^{(8)}$	$(\bar{q}_p^j T^A u_r)\epsilon_{jk}(\bar{q}_s^k T^A d_t)$

$8: (\bar{L}R)(\bar{L}R) + \text{h.c.}$	
$Q_{lequ}^{(1)}$	$(\bar{l}_p^j e_r)\epsilon_{jk}(\bar{q}_s^k u_t)$
$Q_{lequ}^{(3)}$	$(\bar{l}_p^j \sigma_{\mu\nu} e_r)\epsilon_{jk}(\bar{q}_s^k \sigma^{\mu\nu} u_t)$

Table 3.3: The Warsaw basis Source: Ref. [5]

3.5 Operator Mixing

The anomalous dimension matrix is a crucial test of consistency of a given operator basis. In the case of six-dimensional operators in SMEFT, studying the counter term structure is important. Luckily, we can determine this without looking at the modified VEV of the Higgs boson. However, it must be grossly emphasised that, a full parameterisation of the DOFs is essential. The renormalisability of the SM was proved, as already mentioned; nevertheless, a pertinent challenge in SMEFT is now to prove its renormalisability at six dimensions. A major development in this regard can be found in Refs. [30–32], where a complete study of the Renormalisation Group Equations (RGE) for the SMEFT at six-dimensional operators in the Warsaw basis was laid out. A simple example of operators mixing and their connection to EOM and field redefinitions has been briefly reproduced from Ref. [30]. We consider the example of $s \to d$ transition between quarks. Initially, this is described through a tetra-quark operator such as

$$o_q = \bar{u}\gamma^\mu P_L s \bar{d}\gamma_\mu P_L u, \tag{3.12}$$

where we have the up quark in addition to the s and d quarks. In addition, we have P_L the left projection operator given by $P_L = (1 - \gamma_5)/2$.

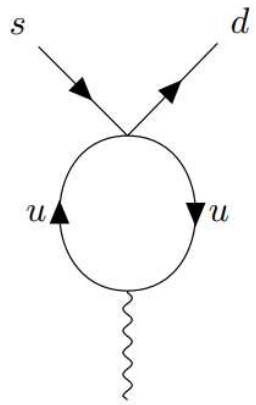

Figure 3.5: Penguin diagram for $s \to d$ transitions

At one-loop order, it becomes necessary to include operators containing other gauge fields. In this case, the divergent penguin diagram considered in Fig. 3.5 needs to be renormalised using an operator proportional to

$$O_P = \bar{d}T^A\gamma^\mu P_L s g_3 [D^\nu, G_{\nu\mu}], \tag{3.13}$$

where, in addition to the terms from the tetra-quark operator, we now also have the $SU(3)$ gauge coupling g_3 and the colour matrix T^A, as well as covariant derivatives on the gluon field-strength tensor. The gauge field EOM, written in detail in Eq. (4.16), is of the form seen above and can be used to replace the gluon tensor in order to obtain terms only containing quarks:

$$O_P \to \bar{d}T^A\gamma^\mu P_L s \sum_q g_3^2 \left[\bar{q}T^A\gamma_\mu P_L q + \bar{q}T^A\gamma_\mu P_R q\right]. \tag{3.14}$$

The above now has a summation in quark flavours. We can include such an operator in an extension of the Warsaw basis as part of a set of operators that appear due to field redefinitions. We call this E_i, with the condition that the SMEOM make these zero. This extension can be written as:

$$\mathcal{L}^{(6)} = \sum_{i=1}^{59} C_i Q_i + \sum_r D_R E_R. \tag{3.15}$$

The first term in the above has the full set of operators from the Warsaw basis, now with additional redundant operators that should not contribute, since we have established that operators that can be related through field redefinitions to our non-redundant basis can be systematically eliminated. In general, the RGE for such a Lagrangian would have the form

$$\mu \frac{\mathrm{d}}{\mathrm{d}\mu} \begin{bmatrix} Q_i \\ E_r \end{bmatrix} = \begin{bmatrix} -\gamma_{ji} & -a_{si} \\ 0 & -b_{sr} \end{bmatrix} \begin{bmatrix} Q_j \\ E_s \end{bmatrix}. \tag{3.16}$$

The 2×2 matrix on the RHS is called the anomalous dimension matrix, or often as γ_{mn}. A subset of this, here called γ_{ji} expresses the mixing between the Warsaw basis operators themselves. We have also defined two subsets of the matrix, a_{si} and b_{sr}, which contain the mixing between the redundant operators E_r and E_s with the Q_i and Q_j operators from the Warsaw basis. The operators E_r and E_s themselves do not mix because the EOM operators are renormalised independently within themselves. The full anomalous dimension matrix should be a 59×59 matrix, referring to all the independent parameters in the Warsaw basis for $\mathcal{L}_6$. If one is to incorporate the full set of flavour indices to this, it would make it even larger. We can write out a similar expression for the Wilson coefficients C_i and D_r. Ultimately, the usage of operators that do not contribute to the amplitude result in an expression that has eliminated any trace of the additional terms we added to the Lagrangian in Eq. (3.15) to obtain

$$\mu \frac{d}{d\mu} C_i = \gamma_{ij} C_j. \tag{3.17}$$

There are a few conclusions one can make from the above calculation:

- The anomalous dimension matrix is basis-dependent. Since we have different operator structures in different non-redundant bases, the resulting γ_{mn} will be modified.
- Redundant operators do not contribute to the RGE evolution. However, they can still appear in the calculation of counterterms at higher orders in an EFT. This also means that there is dependence on our choice of gauge and renormalisation schemes in such calculations.
- It is important to eliminate all redundant operators. If we used both the tetra-quark operators as well as the counterterm operator containing the EOM for the gluon field tensor, it would result in an anomalous dimension matrix that is not uniquely determined; the results can be compared to what is obtained in Sec. 4.

3.5.1 The Anomalous Dimension Matrix for SMEFT

The anomalous dimension matrix for the six-dimensional SMEFT has been reproduced here from Ref. [30] for NLO. The rows and columns are the various classes of operators that appear in the Warsaw basis. Refs. [31, 32] further elaborate on this discussion.

		g^3X^3	H^6	H^4D^2	$g^2X^2H^2$	$y\psi^2H^3$	$gy\psi^2XH$	ψ^2H^2D	ψ^4
		1	2	3	4	5	6	7	8
g^3X^3	1	0	0	0	1	0	0	0	0
H^6	2	$g^6\lambda$	0	$g^2\lambda, \lambda^2$	λg^4	λy^2	0	$\lambda g^2, \lambda y^2$	0
H^4D^2	3	g^6	0	g^2	g^4	0	g^2y^2	g^2	0
$g^2X^2H^2$	4	g^4	0	0	0	0	0	0	0
$y\psi^2H^3$	5	g^6	0	g^2, λ, y^2	g^4	y^2	$g^2\lambda, g^2y^2$	g^2, λ, y^2	λ, y^2
$gy\psi^2XH$	6	g^4	0	0	0	0	g^2, y^2	1	1
ψ^2H^2D	7	g^6	0	g^2	g^4	0	g^2y^2	g^2, y^2	g^2, y^2
ψ^4	8	g^6	0	0	0	0	g^2y^2	g^2, y^2	g^2, y^2

		g^3X^3	H^6	H^4D^2	$g^2X^2H^2$	$y\psi^2H^3$	$gy\psi^2XH$	ψ^2H^2D	ψ^4
		1	2	3	4	5	6	7	8
g^3X^3	1	g^2	0	0	1	0	0	0	0
H^6	2	0	λ, g^2	$g^4, g^2\lambda, \lambda^2$	$g^6, g^4\lambda$	y^4	0	y^4	0
H^4D^2	3	0	0	g^2, λ	g^4	y^2	0	y^2	0
$g^2X^2H^2$	4	g^4	0	1	g^2, λ	0	y^2	1	0
$y\psi^2H^3$	5	0	0	g^2, y^2	g^4	g^2, λ, y^2	$g^2\lambda, g^4, g^2y^2$	g^2, λ, y^2	y^2
$gy\psi^2XH$	6	g^4	0	0	g^2	1	g^2, y^2	1	1
ψ^2H^2D	7	0	0	y^2	g^4	y^2	g^2y^2	g^2, λ, y^2	y^2
ψ^4	8	0	0	0	0	0	g^2y^2	y^2	g^2, y^2

Table 3.4: The Anomalous Dimension Matrix for SMEFT operators Source: Ref. [30]

The Table 3.4 depicts the mixing between various operators, and the entries refer to the order in perturbation theory at which the operators mix. We look at the classes of operators following the notation from Table 3.4. Clearly, there are a large number of non-zero entries and this offers a challenge to NLO calculations in SMEFT. An analysis of this matrix will not be made here and the full details can be found in Refs. [30–32].

3.6 Collider Studies and Current Developments

SMEFT has been gaining traction as an important probe of New Physics (NP) in the last years, with a working group having been set up at the LHC to study experimental data through an effective approach (See for example Ref. [33]). A huge advantage of SMEFT over simplified models is that it is the most general probe of physics that is beyond the energy constraints of the collider, since it captures the IR effects of such physics. We know now that the SMEFT is well-defined order-by-order in perturbation theory. The RG flow equations are known and have been listed in Refs. [30–32] and thus, the radiative corrections can be systematically calculated. SMEFT harnesses the power of the large amount of statistics we currently have due to the LHC, without requiring us to obtain data at higher energy. Thus, there are many reasons to consider SMEFT to be the premier probe of New Physics. There are two major directions of interest within collider studies in SMEFT:

- The precision experiments at the LHC as well as LEP data demand a comparable level of precision theoretical results. Hence, collider studies aim to compute cross sections at higher orders in perturbation theory. It is important to have both analytic and numerical results and there have been developments in both these directions. In addition, a main challenge is to have an automated program at NLO in SMEFT. A part of such studies is also to make a comparison to SM results and find possible conflicts, which could point at hints of NP.
- The large number of free parameters in SMEFT need to be systematically matched. Thus, other major challenge within the SMEFT program is to universally match the $\mathcal{L}^{(6)}$ Wilson coefficients to the SM parameters.

Let us first discuss some of the current progress in higher order precision studies. We can use the following master equation as the starting point in such analyses:

$$\Delta Obs = Obs^{EXP} - Obs^{SM} = \frac{1}{\Lambda^2}\sum_i a_i^{(6)}(\mu) C_i^{(6)}(\mu) + \mathcal{O}\left(\frac{1}{\Lambda^4}\right) + \cdots . \tag{3.18}$$

In the above equation, we simply relate the discrepancy between experimental data and SM predictions (including higher-order corrections) to predictions in the EFT. The EFT predictions are separated by orders in Λ, the scale of NP. At each order, we include the most precise predictions available. This is complicated by the fact that observables at a given order in Λ mix operators of different dimensionalities at the Lagrangian level, as seen in Sec. 3.5. Besides the challenges of working with operator mixing and a much larger parameter space than in the SM or a simplified model, SMEFT contains a lot of subtleties, which have been explained thoroughly in Ref. [5]. The next section is dedicated to looking at some interesting subleading corrections relevant to NLO predictions.

Some important examples of analytic NLO computations for Z and Higgs decays can be found in Refs. [34, 35]. There are several new computations available in both the top quark sector as well as for Higgs production. A very incomplete set of these are found in Refs. [36–40]. On the side of Monte Carlo calculations, a recent development in the automation process is the program SMEFTSim, reviewed in Ref. [41]. This program is a SMEFT extension to the `FeynRules` package and incorporates the full set of Feynman rules. Another example is `SMEFT@NLO`, which can be found in Ref. [42]. Both these programs use the Warsaw basis. There are several programs for NLO calculations in the SM such as `Sherpa` [43] and `POWHEG Box` [44], and there is hope that these can perhaps be extended to incorporate SMEFT corrections in the coming years.

On the other hand, some novel results for universal coefficient matching are given below. We see the predicted values of various Wilson coefficients suppressed by the scale Λ where the dashed line indicates the expected value from the SM. Clearly, we are seeing a consistent trend towards non-zero Wilson coefficients in the sectors that have been studied. These results were obtained by the `SMEFiT` Collaboration.

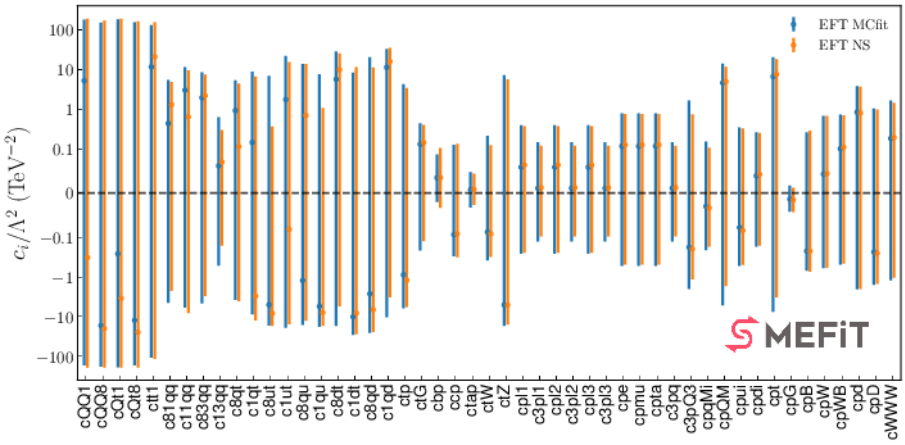

Figure 3.6: Matching results obtained in Ref. [45]

These results will likely soon be extended to all of the parameter space of SMEFT. We have not reviewed the notation but a detailed explanation of the status of the work can be found in Ref. [45].

Finally, there is a growing interest in using on-shell unitary-based approaches to compute problems in SMEFT. A short review of such methods and their applications to gravity is given in Sec. 6.3. These methods have become increasingly popular for SM precision computations; in the last few years the reproduction of SMEFT results using on-shell unitarity-based schemes has become more popular. E.g., in Sec. 3.5, the anomalous dimension matrix was shown. The anomalous dimension matrix may seem fairly random, and this has led to attempts at better understanding the deeper nature of physical structures in SMEFT and finding new patterns that could help explain them better. In Ref. [46], the results from Refs. [30–32] were verified and the value of on-shell methods in extending these to higher loops was discussed.

Chapter 4

Equations of Motion for the Standard Model Effective Field Theory

Theoretical particle physics is a field that requires high precision predictions, particularly in the age of the Large Hadron Collider (LHC). It is necessary to go to higher orders in the perturbative expansion of the SM in order to match the remarkable degree of precision, and statistics that have been attained by the LHC. Using the SM, higher-order corrections to collider observables can be systematically computed in perturbation theory. The state-of-the-art computations comprise of $NNLO$ for 2 to 3 processes [47] and N^3LO predictions for 2 to 1 scattering processes such as Higgs production [48] in gluon fusion or Drell-Yan [49, 50]. SMEFT, as an extension to the SM, aims to achieve the same level of precision. However, SMEFT is a far more complicated quantum field theory, that is yet to be fully understood. Power counting is one of several reasons for precision studies in SMEFT being more complicated when compared with the SM. A next-to-leading order computation at the level of the six-dimensional Lagrangian $\mathcal{L}^{(6)}$ requires consideration of mixing with $\mathcal{L}^{(8)}$, as can be seen by looking at the powers of Λ.

The following sections discuss theoretical advancements in SMEFT, specifically discussing important sub-leading corrections that are relevant to precision calculations in this theory. The Lagrangian of SMEFT contains many operator structures that are reduced and related to each other by equations of motion. Here, novel results are discussed where these EOM produce non-trivial and non-intuitive effects when one matches the theory, i.e., when a Feynman diagram in the UV theory is reduced to a simpler diagram with the contact operators seen in the SMEFT Lagrangian. Firstly, we will discuss what we mean by EOM, and why they are so important in a theory such as SMEFT.

4.1 The Role of EOM in an EFT

EOM are a concept first encountered in the study of classical mechanics. Following the seminal discussion of this presented in Ref. [51], we will set up the basis of Lagrangian mechanics. Firstly, we note that we are discussing the variables associated with point particles, i.e., we are not working with an extended body. A particle is described using two sets of variables associated with its position and velocity. Further, it can be noted that the velocity is the derivative of the position, $\mathbf{v} = d\mathbf{r}/dt = \dot{r}$. Thus, we are working with position coordinates and their derivatives. Empirically, we know that knowledge of the aforementioned variables means that we have complete knowledge of the system at hand. We are familiar with the derivative of the velocity itself, called the acceleration. The statement we made can be simplified and expressed as: if a system is given by known position coordinates q and known velocity coordinates $\dot{q}$ at a given instant, $\ddot{q}$, the acceleration is also specified

uniquely. We define the EOM preliminary as the relations between q, $\dot{q}$, and $\ddot{q}$ that allow us to uniquely define the acceleration $\ddot{q}$ given knowledge of q and $\dot{q}$.
In the mid 18th century, Euler and Lagrange working in conjunction developed the Euler-Lagrange EOM. The basis of this is the *principle of least action*. $\mathcal{L}(q, \dot{q}, t)$ is defined as a function containing the variables we use to describe the system. Classical mechanics is based on the condition that the integral

$$S = \int_{t_1}^{t_2} \mathcal{L}(q, \dot{q}, t) dt, \tag{4.1}$$

acquires a minimal value[1]. This condition reiterates the previous claim that knowledge of q and $\dot{q}$ is sufficient to uniquely determine all higher derivatives of q, beginning with $\ddot{q}$. Here, S and $\mathcal{L}$ are familiar functions- the action and the Lagrangian respectively.

Now, we will do a small exercise in variational calculus to obtain the Euler-Lagrange equations in their classical mechanics avatar. Let $q(t)$ be the function that minimises the action S. Any variation in this function will naturally cause S to increase. We will effect an infinitesimal variation to this function as follows, replacing $q(t)$ with

$$q(t) + \delta q(t). \tag{4.2}$$

Our condition that S should be minimised tells us that at the limits of the integral, i.e., t_1 and t_2,

$$\delta q(t_1) = \delta q(t_2) = 0. \tag{4.3}$$

We express the principle of least action as

$$\delta S = \delta \int_{t_1}^{t_2} \mathcal{L}(q, \dot{q}, t) = 0. \tag{4.4}$$

Essentially, any infinitesimal variation in the function $q(t)$ should bring S away from its extremum. The right hand side of the above equation can be expanded out as follows

$$\int_{t_1}^{t_2} \left(\frac{\partial \mathcal{L}}{\partial q} \delta q + \frac{\partial \mathcal{L}}{\partial \dot{q}} \delta \dot{q} \right) dt = 0. \tag{4.5}$$

We can rewrite the second term as follows

$$\int_{t_1}^{t_2} \left(\frac{\partial \mathcal{L}}{\partial q} \delta q - \frac{d}{dt} \frac{\partial \mathcal{L}}{\partial \dot{q}} \delta q + \frac{d}{dt} \left(\frac{\partial \mathcal{L}}{\partial \dot{q}} \delta q \right) \right) dt = 0. \tag{4.6}$$

The last term is essentially a surface term and it vanishes under the conditions given in Eq. (4.3). We obtain the same results if we integrate the second term by parts. We are left with

$$\delta S = \int_{t_1}^{t_2} \left(\frac{\partial \mathcal{L}}{\partial q} - \frac{d}{dt} \frac{\partial \mathcal{L}}{\partial \dot{q}} \right) \delta q \, dt = 0. \tag{4.7}$$

We have an integral that has to be identically zero for all values of the variation δq. This requires that the integrand is zero, leading us to the Euler-Lagrange equations in classical mechanics

$$\frac{\partial \mathcal{L}}{\partial q} - \frac{d}{dt} \left(\frac{\partial \mathcal{L}}{\partial \dot{q}} \right) = 0. \tag{4.8}$$

[1] Technically, an extremum. Usually a minimum.

If we have further degrees of freedom, the process must be iterated for each of them. In this case, we would write the above as

$$\frac{\partial \mathcal{L}}{\partial q_i} - \frac{d}{dt}\left(\frac{\partial \mathcal{L}}{\partial \dot{q}_i}\right) = 0. \tag{4.9}$$

This would give us an EOM for each degree of freedom.

The above derivation can be analogously repeated for a Lagrangian that is a function of fields and their derivatives, to obtain a quantum field theoretical version of Eq. (4.9)

$$\frac{\partial \mathcal{L}}{\partial \varphi_i} - \partial_\mu\left(\frac{\partial \mathcal{L}}{\partial(\partial_\mu \varphi_i)}\right) = 0. \tag{4.10}$$

Here, $\mathcal{L}$ is a function of the fields φ_i and $\partial_\mu \varphi_i$. The index i points to the fact that the Lagrangian can be a function of different fields. We will see shortly that in the case of the SM and SMEFT, which have the same field content, there will be an EOM for each field. In the derivation of the classical Euler-Lagrange equations, we encountered a surface term. It should be noted that in the case of SMEFT, we can only claim that the surface term disappears to a certain degree of accuracy since the fields themselves are only defined up to order(d) depending on the power counting.

EOM are important in a field theory. One classical example is the use of EOM in order to obtain an expression for the two-point function of a field by solving for the Green's function. This is traditionally done in the context of obtaining a free-field propagator. In the absence of interactions, even and odd spin fields have the Klein-Gordon and Dirac equations respectively as their equations of motion. In the Klein-Gordon case, we solve

$$(\partial^2 + m^2) D_R(x-y) = i\delta(x-y), \tag{4.11}$$

under the condition $x^0 < y^0$ to obtain the retarded Green's function. This is solved by Fourier transforming the above equation

$$(-p^2 + m^2)\tilde{D}_R(p) = -i, \tag{4.12}$$

such that the momentum space Green's function is given by

$$\tilde{D}_R(p) = \frac{i}{p^2 - m^2}. \tag{4.13}$$

In the SMEFT, EOM play a very crucial role. As we know, EFTs can contain redundant operators. Ref. [52] reported a full list of the baryon-number-conserving operators one can write at dimension 6 in the SMEFT. These redundancies make EFT computations extremely cumbersome. However, the authors of Ref. [17] systematically removed these redundancies by relating different operator forms. This brought down the number of baryon-number-conserving operators to a manageable 59, with an additional 4 baryon-number-violating ones. E.g., in the Higgs case the EOM is given by

$$D^2 H^j = \lambda v^2 H^j - 2\lambda (H^\dagger H) H^j - \overline{q}^n_k \, [Y_u]^\star_{mn} \, u^m \epsilon^{kj}, -\overline{d}^n [Y_d]_{nm} q^j_m - \overline{e}^n [Y_e]_{nm} \ell^{m,j}. \tag{4.14}$$

If we consider in general the six-dimensional operators that could be constructed using the Higgs and other SM fields, one possibility is an operator with four derivatives and two

Higgs fields, H^2D^4. Since the Lagrangian is defined under an integral, we have the freedom to use integration by parts to move the covariant derivatives as we please. It becomes convenient to consider examples containing $D_\mu D^\mu H$ so that we can use the EOM. Then, we can obtain forms such as H^4D^2 and ψ^2HD^2. In fact, the Warsaw basis was designed to minimise derivatives since they are relatively difficult to work with.

We can see from the above example how EOM allow us to relate different operator forms and eliminate redundant operators in order to arrive at a non-redundant basis. Since different bases are possible, EOM allow the building of bases with operator forms of the basis builder's choice. Naturally, EOM also act as a bridge between these bases and allow us to translate between them.

We saw in Sec. 3.5, the role that EOM play when using RGEs in the SMEFT.

Finally, EOM also have an important role to play when we are matching Wilson coefficients to a UV theory. Matching entails "integrating out" heavy fields and replacing propagators with local contact operators. However, at subleading order in the matching, there are additional terms that appear due to the equations of motion, as we will see shortly. It turns out that matching at higher dimensions, say that of $\mathcal{L}^{(n)}$, is impacted by the basis choice for $\mathcal{L}^{(m<n)}$. In Section 4.5, we will investigate these effects in detail with examples of matching to generic UV theories.

4.2 The Standard Model Case

Firstly, to set up the notation, we will look into the case of the Standard Model. We express the SM Lagrangian as follows:

$$\begin{aligned}\mathcal{L}_{\text{SM}} = &-\frac{1}{4}G^A_{\mu\nu}G^{A\mu\nu} - \frac{1}{4}W^I_{\mu\nu}W^{I\mu\nu} - \frac{1}{4}B_{\mu\nu}B^{\mu\nu} \\ &+ \sum_\psi \overline{\psi}\, i\not{D}\, \psi + (D_\mu H)^\dagger (D^\mu H) - \lambda\left(H^\dagger H - \frac{1}{2}v^2\right)^2 \\ &- \left[H^{\dagger j}\overline{d}\, Y_d\, q_j + \widetilde{H}^{\dagger j}\overline{u}\, Y_u\, q_j + H^{\dagger j}\overline{e}\, Y_e\, \ell_j + \text{h.c.}\right].\end{aligned} \tag{4.15}$$

The field content involves three gauge boson fields, one scalar $SU(2)$ doublet, and the fermion fields $\psi = \{q, u, d, \ell, e\}$. The equations of motion can be calculated for each of these fields in a straightforward manner by using the Euler-Lagrange equations presented in Eq. (4.10). The gauge fields have the following equations of motion in the SM.

$$\begin{aligned}\left[D^\mu, G_{\mu\nu}\right]^A &= g_3\, j^A_\nu + g_3 \sum_{\text{d}=5}^{\infty} \frac{\Delta^{A,(\text{d})}_{G,\nu}}{\Lambda^{\text{d}-4}}, \\ \left[D^\mu, W_{\mu\nu}\right]^I &= g_2 j^I_\nu + g_2 \sum_{\text{d}=5}^{\infty} \frac{\Delta^{I,(\text{d})}_{W,\nu}}{\Lambda^{\text{d}-4}}, \\ D^\mu B_{\mu\nu} &= g_1 j_\nu + g_1 \sum_{\text{d}=5}^{\infty} \frac{\Delta^{(\text{d})}_{B,\nu}}{\Lambda^{\text{d}-4}}.\end{aligned} \tag{4.16}$$

Note that the $\Delta^{(d)}$ in the above case contains all corrections due to dimension d operators in SMEFT, with a coupling pulled out. We also need to define the covariant derivatives and currents that appear in the above equations:

$$[D^\mu, \mathcal{Q}]^I = \partial^\mu \mathcal{Q}^I - g_2\, \epsilon^{JKI}\, W_J^\mu\, \mathcal{Q}_K, \tag{4.17}$$

$$[D^\mu, \mathcal{Q}]^A = \partial^\mu \mathcal{Q}^A - g_3\, f^{BCA}\, A_B^\mu \mathcal{Q}_C. \tag{4.18}$$

The currents, which we will use again when we incorporate SMEFT corrections into the above, are defined as

$$j_\mu^A = \sum_{\psi=q,u,d} \overline{\psi}\, T^A \gamma_\mu \psi\,, \tag{4.19}$$

$$j_\mu^I = \frac{1}{2}\overline{q}\,\tau^I \gamma_\mu q + \frac{1}{2}\overline{\ell}\,\tau^I \gamma_\mu \ell + \frac{1}{2} H^\dagger\, i \overleftrightarrow{D}^I_\mu H, \tag{4.20}$$

$$j_\mu = \sum_{\psi=u,d,q,\ell.e} \overline{\psi}\, \mathrm{y}_i \gamma_\mu \psi + \frac{1}{2} H^\dagger\, i \overleftrightarrow{D}_\mu H. \tag{4.21}$$

Next we have the SM EOM for the fermion fields

$$\begin{aligned}
i\not{D}\, q_m^j &= u^n\, [Y_u]^\star_{nm}\, \widetilde{H}^j + d^n\, [Y_d]^\star_{nm}\, H^j + \sum_{\mathrm{d}=5}^{\infty} \frac{\Delta^{j,(\mathrm{d})}_{q,m}}{\Lambda^{\mathrm{d}-4}}, \\
i\not{D}\, \ell_m^j &= [Y_e]^\star_{nm}\, e^n H^j + \sum_{\mathrm{d}=5}^{\infty} \frac{\Delta^{j,(\mathrm{d})}_{\ell,m}}{\Lambda^{\mathrm{d}-4}}, \\
i\not{D}\, d_m &= [Y_d]_{mn}\, q_n^j\, H_j^\dagger + \sum_{\mathrm{d}=5}^{\infty} \frac{\Delta^{(\mathrm{d})}_{d,m}}{\Lambda^{\mathrm{d}-4}}, \\
i\not{D}\, u_m &= [Y_u]_{mn}\, q_j^n\, \widetilde{H}^{\dagger\, j} + \sum_{\mathrm{d}=5}^{\infty} \frac{\Delta^{(\mathrm{d})}_{u,m}}{\Lambda^{\mathrm{d}-4}}, \\
i\not{D}\, e_m &= [Y_e]_{mn}\, \ell_j^n H^{\dagger\, j} + \sum_{\mathrm{d}=5}^{\infty} \frac{\Delta^{(\mathrm{d})}_{e,\kappa}}{\Lambda^{\mathrm{d}-4}}.
\end{aligned} \tag{4.22}$$

Finally, we have the EOM for the Higgs scalar field

$$D^2 H^j = \lambda v^2 H^j - 2\lambda (H^\dagger H) H^j - \overline{q}_k^n\, [Y_u]^\star_{mn}\, u^m \epsilon^{kj}, -\overline{d}^n [Y_d]_{nm} q_m^j - \overline{e}^n [Y_e]_{nm} \ell^{m,j} \sum_{\mathrm{d}=5}^{\infty} \frac{\Delta^{j,(\mathrm{d})}_H}{\Lambda^{\mathrm{d}-4}}. \tag{4.23}$$

This allows us to now go beyond the SM to examine corrections due to the SMEFT.

4.3 The 5th Dimension

There is only one operator that needs to be considered at the fifth dimension, and it is commonly called the Weinberg operator [53, 54]

$$\mathcal{Q}^{(5)}_{mn} = \left(\overline{\ell^{c,m}}\, \tilde{H}^\star\right) \left(\tilde{H}^\dagger\, \ell^n\right). \tag{4.24}$$

The above is fairly complex in terms of taking derivatives due to the charge conjugation operators. While most of the fields in the Warsaw basis (excluding the B-number violating ones) consist of fields and their Hermitian conjugates, the charge conjugation operation results in a simple complex conjugation of the field. These operators are defined as $\psi^c = C\bar{\psi}^T$, where we define $C = -i\gamma_2\gamma_0$. Using dimensional and gauge constraints, it is clear that the above operator is the only possible one. E.g., one operator consisting of $(G^2)^2 H$, which fulfils the dimensional constraints, is clearly not gauge invariant. The corrections to the EM from the Weinberg operator in Eq. (4.24) are

$$\Delta^{j,(5)}_{\ell,m} = -\,2\,C^{(5)\star}_{nm}\,\tilde{H}^j\,\left(\tilde{H}^T\ell^c_n\right), \tag{4.25}$$

$$\Delta^{j,(5)}_{H} = -\,C^{(5)\star}_{nm}\,\epsilon^{jk}\,\left[\overline{\ell^m_k}\,(\tilde{H}^T\,\ell^c_n) + (\overline{\ell^m}\tilde{H})\,\ell^{c,k}_n\right]. \tag{4.26}$$

As expected, we obtain one equation each for the leptonic and Higgs fields that appear in Eq. (4.24). We can easily obtain the results for the conjugated fields by conjugating Eqs. (4.25) and (4.26).

4.4 Dimension Six Corrections to the Standard Model EOM

In this section, the results of using the Euler-Lagrange equations, Eq. (4.10), for each SM field on the higher dimensional operators which comprise the Warsaw basis is presented. The results have been reproduced exactly from Ref. [2]. The following currents must be defined:

$$J^{\psi\,\mu}_{pr} = \overline{\psi}_p\gamma^\mu\psi_r, \quad J^{\psi,I,\mu}_{pr} = \overline{\psi}_p\gamma^\mu\,\tau^I\,\psi_r, \quad J^{\psi,A,\mu}_{pr} = \overline{\psi}_p\gamma^\mu\,T^A\,\psi_r \tag{4.27}$$

$$\mathcal{C}^{\mu\nu}_{\substack{\psi_1\psi_2F\\pr,\mathbf{g}}} = C_{\substack{\psi_1F\\pr}}\,\overline{\psi_{2,p}}\sigma_{\mu\nu}\mathbf{G}\,\psi_{1,r}H + \text{h.c.}, \tag{4.28}$$

$$\tilde{\mathcal{C}}^{\mu\nu}_{\substack{\psi_1\psi_2F\\pr,\mathbf{g}}} = C_{\substack{\psi_1F\\pr}}\,\overline{\psi_{2,p}}\sigma_{\mu\nu}\mathbf{G}\psi_{1,r}\tilde{H} + \text{h.c.}. \tag{4.29}$$

For the three SM gauge fields, the dimension 6 corrections to the EOM are:

$$\begin{aligned}
\Delta^{(6)}_{B,\mu} &= 2\mathrm{y}_H (H^\dagger H)\left[\sum_{\psi=\ell,q} \underset{pr}{C^{(1)}_{H\psi}} J^{\psi\,\mu}_{pr} + \sum_{\psi=e,u,d} \underset{pr}{C_{H\psi}} J^{\psi\,\mu}_{pr} + \frac{C_{HD}}{2} H^\dagger i \overleftrightarrow{D}_\mu H\right] + 2\mathrm{y}_H (H^\dagger \tau_I H) \sum_{\psi=\ell,q} \underset{pr}{C^{(3)}_{H\psi}} J^{\psi\,I\,\mu}_{pr},\\
&+ \frac{4\,C_{HB}}{g_1}\partial^\nu (H^\dagger H) B_{\nu\,\mu} + \frac{2\,C_{HWB}}{g_1}[D^\nu, H^\dagger \tau H]_I W^I_{\nu\,\mu} + 4\,C_{HB}\, H^\dagger H\, j_\mu + \frac{2\,g_2}{g_1}\, C_{HWB}\,(H^\dagger \tau_I H) J^I_\mu,\\
&+ \frac{4\,C_{H\tilde{B}}}{g_1}\partial^\nu \left(H^\dagger H \tilde{B}_{\nu\,\mu}\right) + \frac{2\,C_{H\tilde{W}B}}{g_1}[D^\nu, H^\dagger \tau H]_I \tilde{W}^I_{\nu\,\mu} + \frac{2\,C_{H\tilde{W}B}}{g_1}[D^\nu, \tilde{W}_{\nu\,\mu}]_I\, H^\dagger \tau^I H,\\
&+ \frac{2}{g_1}\left(\partial_\nu \underset{pr}{\mathcal{C}^{\nu\mu}_{e\ell B}} + \partial_\nu \underset{pr}{\tilde{\mathcal{C}}^{\nu\mu}_{uqB}} + \partial_\nu \underset{pr}{\mathcal{C}^{\nu\mu}_{dqB}}\right), \qquad (4.30)
\end{aligned}$$

$$\begin{aligned}
\Delta^{I,(6)}_{W,\mu} &= 2(H^\dagger \tau^I H)\left[\sum_{\psi=\ell,q} \underset{pr}{C^{(1)}_{H\psi}} J^{\psi\,\mu}_{pr} + \sum_{\psi=e,u,d} \underset{pr}{C_{H\psi}} J^{\psi\,\mu}_{pr} + \frac{C_{HD}}{2} H^\dagger i \overleftrightarrow{D}_\mu H\right] + 2\,i\,\epsilon^{IJK}\,(H^\dagger \tau_J H) \sum_{\psi=\ell,q} \underset{pr}{C^{(3)}_{H\psi}} J^{\psi\,\mu}_{pr\,K},\\
&+ \underset{pr}{C_{Hud}}(\tilde{H}^\dagger \tau^I H)(\overline{u_p}\,\gamma_\mu d_r) + \underset{pr}{C^\star_{Hud}}(H^\dagger \tau^I \tilde{H})(\overline{d_r}\,\gamma_\mu u_p) + \frac{4}{g_2}\,\partial^\nu (H^\dagger H)(C_{HW} W^I_{\nu\mu} + C_{H\tilde{W}} \tilde{W}^I_{\nu\mu}),\\
&+ 4\,C_{HW}\, H^\dagger H\, j^I_\mu + \frac{4\,C_{H\tilde{W}}}{g_2}\, H^\dagger H\, \left[D^\nu, \tilde{W}_{\nu\mu}\right]^I + \frac{2}{g_2}\partial^\nu \left[(H^\dagger \tau^I H)\, B_{\nu\mu}\, C_{HWB} + (H^\dagger \tau^I H)\, \tilde{B}_{\nu\mu}\, C_{H\tilde{W}B}\right],\\
&+ \frac{2}{g_2}\left[D^\nu, \underset{pr,I}{\mathcal{C}^{\nu\mu}_{e\ell W}}\right]^I + \frac{2}{g_2}\left[D^\nu, \underset{pr,I}{\mathcal{C}^{\nu\mu}_{dqW}}\right]^I + \frac{2}{g_2}\left[D^\nu, \underset{pr,I}{\tilde{\mathcal{C}}^{\nu\mu}_{uqW}}\right]^I + 2(H^\dagger \tau_J H)\epsilon^{IJK} W_{\nu\,K}\,(C_{HWB} B_{\nu\mu} + C_{H\tilde{W}B}\tilde{B}_{\nu\mu}),\\
&+ \frac{6\,C_W}{g_2}\,\epsilon^{IJK}(\partial^\gamma (W^{\mu\nu}_J\, W^{\nu\gamma}_K) + g_2 \epsilon_{RSK} W^R_{\gamma\nu}\, W^S_{\nu\mu}\, W^\gamma_J) + \frac{2\,C_{\tilde{W}}}{g_2}\,\epsilon^{IJK}(\partial^\gamma (\tilde{W}^{\nu\gamma}_J\, W^{\mu\nu}_K) + g_2 \epsilon_{RSJ} \tilde{W}^R_{\nu\gamma}\, W^S_{\mu\nu}\, W^\gamma_K),\\
&+ \frac{2\,C_{\tilde{W}}}{g_2}\,\epsilon^{IJK}(\partial^\gamma (\tilde{W}^{\mu\nu}_J\, W^{\gamma\nu}_K) + g_2 \epsilon_{RSJ} \tilde{W}^S_{\mu\nu}\, W^R_{\nu\gamma}\, W^\gamma_K) + \frac{C_{\tilde{W}}}{g_2}\,\epsilon^{IJK}\epsilon_{\rho\phi}{}^{\gamma\mu}(\partial^\gamma (\tilde{W}^{\rho\nu}_J\, W^{\nu\phi}_K) + g_2 \epsilon_{RSJ} \tilde{W}^S_{\nu\gamma}\, W^R_{\rho\nu}\, W^\phi_K), \qquad (4.31)
\end{aligned}$$

$$\begin{aligned}
\Delta^{A,(6)}_{G,\mu} &= \frac{4}{g_3}\,\partial^\nu (H^\dagger H)(C_{HG} G^A_{\nu\mu} + C_{H\tilde{G}} \tilde{G}^A_{\nu\mu}) + \frac{4}{g_3}\, H^\dagger H\, \left(C_{HG}\, g_3\, j^A_\mu + C_{H\tilde{G}}\, \left[D^\nu, \tilde{G}_{\nu\mu}\right]^A\right),\\
&+ \frac{2}{g_3}\left[D^\nu, \underset{pr,A}{\mathcal{C}^{\nu\mu}_{dqG}}\right]^A + \frac{2}{g_3}\left[D^\nu, \underset{pr,A}{\tilde{\mathcal{C}}^{\nu\mu}_{uqG}}\right]^A + \frac{6\,C_G}{g_3}\, f^{ABC}(\partial^\gamma (G^{\mu\nu}_B\, G^{\nu\gamma}_C) + g_3 f_{DEC} G^D_{\gamma\nu}\, G^E_{\nu\mu}\, A^\gamma_B),\\
&+ \frac{2\,C_{\tilde{G}}}{g_3}\, f^{ABC}(\partial^\gamma (\tilde{G}^{\nu\gamma}_B\, G^{\mu\nu}_C) + g_3 f_{DEB} \tilde{G}^D_{\nu\gamma}\, G^E_{\mu\nu}\, A^\gamma_C) + \frac{2\,C_{\tilde{G}}}{g_3}\, f^{ABC}(\partial^\gamma (\tilde{G}^{\mu\nu}_B\, G^{\gamma\nu}_C) + g_3 f_{DEB} \tilde{G}^E_{\mu\nu}\, G^D_{\nu\gamma}\, A^\gamma_C),\\
&+ \frac{C_{\tilde{G}}}{g_3}\, f^{ABC}\epsilon_{\rho\phi}{}^{\gamma\mu}(\partial^\gamma (\tilde{G}^{\rho\nu}_B\, G^{\nu\phi}_C) + g_3 f_{DEB} \tilde{G}^E_{\nu\gamma}\, G^D_{\rho\nu}\, A^\phi_C). \qquad (4.32)
\end{aligned}$$

The corrections to the fermion EOM due to the B number conserving $\mathcal{L}^{(6)}$ operators are

$$\begin{aligned}
\Delta_{e,m}^{(6,B)} &= -C^{\star}_{\substack{eH\\pm}} (H^\dagger H) H^\dagger \ell_p - C_{\substack{He\\mp}} (H^\dagger i \overleftrightarrow{D}_\mu H) \gamma^\mu e_p - C^{\star}_{\substack{eW\\pm}} \sigma^{\mu\nu} H^\dagger \tau_I \ell_p \, W^I_{\mu\nu} - C^{\star}_{\substack{eB\\pm}} \sigma^{\mu\nu} H^\dagger \ell_p \, B_{\mu\nu}, \\
&\quad - 2\, C_{\substack{ee\\mprs}} \gamma_\mu e_p \, J^{e\,\mu}_{rs} - C_{\substack{eu\\mprs}} \gamma_\mu e_p \, J^{u\,\mu}_{rs} - C_{\substack{ed\\mprs}} \gamma_\mu e_p \, J^{d\,\mu}_{rs} - C_{\substack{\ell e\\prms}} \gamma_\mu e_s \, J^{\ell\,\mu}_{pr} - C_{\substack{qe\\prms}} \gamma_\mu e_s \, J^{q\,\mu}_{pr}, \\
&\quad - C^{\star}_{\substack{\ell edq\\pmst}} (\ell_{p,j}) (\overline{q_t}^j d_s) - C^{(1),\star}_{\substack{\ell equ\\pmst}} (\ell^j_p) \, \epsilon_{jk} \, (\overline{u_t} \, q^k_s) - C^{(3),\star}_{\substack{\ell equ\\pmst}} \sigma_{\mu\nu} \ell^j_p \, \epsilon_{jk} \, (\overline{u_t} \, \sigma^{\mu\nu} q^k_s), \qquad (4.33) \\
\Delta_{d,m}^{(6,B)} &= -C^{\star}_{\substack{dH\\pm}} H^\dagger \, (H^\dagger H) q_p - C_{\substack{Hd\\mp}} (H^\dagger i \overleftrightarrow{D}_\mu H) \gamma^\mu d_p + C^{\star}_{\substack{Hud\\mp}} i \left[(D_\mu H)^\dagger \tilde{H} \right] \gamma^\mu u_p - C^{\star}_{\substack{dW\\pm}} \sigma^{\mu\nu} H^\dagger \tau_I q_p \, W^I_{\mu\nu}, \\
&\quad - C^{\star}_{\substack{dB\\pm}} \sigma^{\mu\nu} H^\dagger \, q_p \, B_{\mu\nu} - C^{\star}_{\substack{dG\\pm}} \sigma^{\mu\nu} H^\dagger \, T_A \, q_p \, G^A_{\mu\nu} - C_{\substack{dd\\mprs}} \gamma_\mu d_p \, J^{d\,\mu}_{rs} - C_{\substack{dd\\rsmp}} \gamma_\mu d_p \, J^{d\,\mu}_{rs} - C_{\substack{ed\\rsmp}} \gamma_\mu d_p \, J^{e\,\mu}_{rs}, \\
&\quad - C^{(1)}_{\substack{ud\\rsmp}} \gamma_\mu d_p \, J^{u\,\mu}_{rs} - C_{\substack{\ell d\\stmp}} \gamma_\mu \, d_p J^{\ell\,\mu}_{st} - C^{(8)}_{\substack{ud\\rsmp}} \gamma_\mu \, T_A \, d_p \, J^{u,A,\,\mu}_{rs} - C^{(1)}_{\substack{qd\\stmp}} \gamma_\mu \, d_p J^{q\,\mu}_{st} - C^{(8)}_{\substack{qd\\stmp}} \gamma_\mu \, T_A \, d_p \, J^{q,A,\,\mu}_{st}, \\
&\quad - C_{\substack{\ell edq\\stmp}} \, q_{p,\,j} \, (\overline{\ell_s}^j \, e_t) - C^{(1),\star}_{\substack{quqd\\stpm}} \, (\overline{u_t} \, q^j_s) \, \epsilon_{jk} \, q^k_p - C^{(8),\star}_{\substack{quqd\\stpm}} \, (\overline{u_t} \, T^A \, q^j_s) \, \epsilon_{jk} \, T_A \, q^k_p, \qquad (4.34)
\end{aligned}$$

$$\begin{aligned}
\Delta^{(6,B)}_{u,m} = & -C^{\star}_{\substack{uH\\pm}} (H^\dagger H)\, \tilde{H}^\dagger\, q_p - C_{\substack{Hu\\mp}} (H^\dagger i\overleftrightarrow{D}_\mu H)\gamma^\mu u_p - C_{\substack{Hud\\mp}}\, i(\tilde{H}^\dagger D_\mu H)\gamma^\mu d_p - C^{\star}_{\substack{uW\\pm}}\, \sigma^{\mu\nu}\tilde{H}^\dagger\, \tau_I q_p\, W^I_{\mu\nu},\\
& - C^{\star}_{\substack{uB\\pm}}\, \sigma^{\mu\nu}\tilde{H}^\dagger\, q_p\, B_{\mu\nu} - C^{\star}_{\substack{uG\\pm}}\, \sigma^{\mu\nu}\tilde{H}^\dagger\, T_A\, q_p\, G^A_{\mu\nu} - C_{\substack{uu\\mprs}}\, \gamma_\mu u_p\, J^{u\,\mu}_{rs} - C_{\substack{uu\\rsmp}}\, \gamma_\mu u_p\, J^{u\,\mu}_{rs} - C_{\substack{eu\\rsmp}}\, \gamma_\mu u_p\, J^{e\,\mu}_{rs},\\
& - C^{(1)}_{\substack{ud\\mprs}}\, \gamma_\mu u_p\, J^{d\,\mu}_{rs} - C_{\substack{\ell u\\stmp}}\, \gamma_\mu\, u_p\, J^{\ell\,\mu}_{st} - C^{(8)}_{\substack{ud\\mprs}}\, \gamma_\mu\, T_A\, u_p\, J^{d,A,\,\mu}_{rs} - C^{(1)}_{\substack{qu\\stmp}}\, \gamma_\mu\, u_p J^{q\,\mu}_{st} - C^{(8)}_{\substack{qu\\stmp}}\, \gamma_\mu\, T_A\, u_p J^{q,A,\,\mu}_{st},\\
& - C^{(1),\star}_{\substack{quqd\\pmst}}\, (\overline{d_t}\, q^k_s)\, \epsilon_{jk}\, q^j_p - C^{(8),\star}_{\substack{quqd\\pmst}}\, (\overline{d_t}\, T_A\, q^k_s)\, \epsilon_{jk}\, T^A\, q^j_p - C^{(1),\star}_{\substack{\ell equ\\stpm}}\, (q^k_p)\, \epsilon_{jk}\, (\overline{e_t}\, \ell^j_s) - C^{(3),\star}_{\substack{\ell equ\\stpm}}\, (\sigma_{\mu\nu}\, q^k_p)\, \epsilon_{jk}\, (\overline{e_t}\, \sigma^{\mu\nu}\, \ell^j_s),
\end{aligned} \tag{4.35}$$

$$\begin{aligned}
\Delta^{(6,B),j}_{\ell,m} = & -C_{\substack{eH\\mp}}\, (H^\dagger H) e_p\, H^j - C_{\substack{eW\\mp}}\, \sigma^{\mu\nu}\, e_p\, \tau_I\, H^j\, W^I_{\mu\nu} - C_{\substack{eB\\mp}}\, \sigma^{\mu\nu}\, e_p\, H^j\, B_{\mu\nu} - C^{(1)}_{\substack{H\ell\\mp}}\, (H^\dagger i\overleftrightarrow{D}_\mu H)\gamma^\mu \ell^j_p,\\
& - C^{(3)}_{\substack{H\ell\\mp}}\, (H^\dagger i\overleftrightarrow{D}^I_\mu H)\gamma^\mu \tau_I\, \ell^j_p - C_{\substack{\ell\ell\\mpst}}\, \gamma_\mu \ell^j_p\, J^{\ell\,\mu}_{st} - C_{\substack{\ell\ell\\stmp}}\, \gamma_\mu \ell^j_p\, J^{\ell\,\mu}_{st} - C^{(1)}_{\substack{\ell q\\mpst}}\, \gamma_\mu \ell^j_p\, J^{q\,\mu}_{st} - C^{(3)}_{\substack{\ell q\\mpst}}\, \gamma_\mu\, \tau_I\, \ell^j_p\, J^{q\,I\,\mu}_{st},\\
& - C_{\substack{\ell e\\mpst}}\, \gamma_\mu \ell^j_p\, J^{e\,\mu}_{st} - C_{\substack{\ell u\\mpst}}\, \gamma_\mu \ell^j_p\, J^{u\,\mu}_{st} - C_{\substack{\ell d\\mpst}}\, \gamma_\mu \ell^j_p\, J^{d\,\mu}_{st} - C_{\substack{\ell edq\\mpst}}\, e_p\, (\overline{d_s}\, q^j_t) - C^{(1)}_{\substack{\ell equ\\mpst}}\, e_p\, \epsilon^{jk}\, (\overline{q_{s,k}}\, u_t),\\
& - C^{(3)}_{\substack{\ell equ\\mpst}}\, e_p \sigma_{\mu\nu}\, \epsilon^{jk}\, (\overline{q_{s,k}}\, \sigma^{\mu\nu} u_t),
\end{aligned} \tag{4.36}$$

$$\begin{aligned}
\Delta^{(6,B),j}_{q,m} = & -C_{\substack{uH\\mp}}\, (H^\dagger H) u_p\, \tilde{H}^j - C_{\substack{dH\\mp}}\, (H^\dagger H) d_p\, H^j - C_{\substack{uW\\mp}}\, \sigma^{\mu\nu}\, u_p\, \tau_I\, \tilde{H}^j\, W^I_{\mu\nu} - C_{\substack{dW\\mp}}\, \sigma^{\mu\nu}\, d_p\, \tau_I\, H^j\, W^I_{\mu\nu},\\
& - C_{\substack{uB\\mp}}\, \sigma^{\mu\nu}\, u_p\, \tilde{H}^j\, B_{\mu\nu} - C_{\substack{dB\\mp}}\, \sigma^{\mu\nu}\, d_p\, H^j\, B_{\mu\nu} - C_{\substack{uG\\pm}}\, \sigma^{\mu\nu} u_p \tilde{H}^j\, T_A\, G^A_{\mu\nu} - C_{\substack{dG\\pm}}\, \sigma^{\mu\nu} d_p\, H^j\, T_A\, G^A_{\mu\nu}\\
& - C^{(1)}_{\substack{Hq\\mp}} (H^\dagger i\overleftrightarrow{D}_\mu H)\gamma^\mu q^j_p - C^{(3)}_{\substack{Hq\\mp}} (H^\dagger i\overleftrightarrow{D}^I_\mu H)\gamma^\mu\, \tau_I\, q^j_p - \left(C^{(1)}_{\substack{qq\\mpst}} + C^{(1)}_{\substack{qq\\stmp}}\right) \gamma_\mu q^j_p J^{q\mu}_{st} - \left(C^{(3)}_{\substack{qq\\stmp}} + C^{(3)}_{\substack{qq\\mpst}}\right) \gamma_\mu \tau_I q^j_p J^{q,I}_{st}\\
& - C^{(1)}_{\substack{\ell q\\stmp}}\, \gamma_\mu q^j_p\, J^{\ell,\mu}_{st} - C^{(3)}_{\substack{\ell q\\stmp}}\, \gamma_\mu \tau_I q^j_p J^{\ell,I,\mu}_{st} - C_{\substack{qe\\mpst}}\, \gamma_\mu q^j_p\, J^{e,\mu}_{st} - C^{(1)}_{\substack{qu\\mpst}}\, \gamma_\mu q^j_p\, J^{u,\mu}_{st} - C^{(8)}_{\substack{qu\\mpst}}\, \gamma_\mu\, T_A\, q^j_p\, J^{u,A,\mu}_{st},\\
& - C^{(1)}_{\substack{qd\\mpst}}\, \gamma_\mu q^j_p\, J^{d,\mu}_{st} - C^{\star}_{\substack{\ell edq\\stpm}} (\overline{e_t} \ell^j_s)\, d_p - C^{(8)}_{\substack{qd\\mpst}}\, \gamma_\mu\, T_A\, q^j_p\, J^{d,A,\mu}_{st} - C^{(1)}_{\substack{quqd\\mpst}}\, u_p\, \epsilon^{jk}\, (\overline{q_{s,k}} d_t) - C^{(1)}_{\substack{quqd\\stmp}}\, (\overline{q_{s,k}} u_t)\, \epsilon^{kj}\, d_p,\\
& - C^{(8)}_{\substack{quqd\\mpst}}\, T^A\, u_p\, \epsilon^{jk} (\overline{q_{s,k}}\, T_A\, d_t) - C^{(8)}_{\substack{quqd\\stmp}}\, (\overline{q_{s,k}}\, T_A\, u_t) \epsilon^{kj}\, T^A\, d_p - C^{(1)}_{\substack{\ell equ\\stmp}}\, (\overline{\ell_{s,k}} e_t) \epsilon^{kj} u_p - C^{(3)}_{\substack{\ell equ\\stmp}}\, (\overline{\ell_{s,k}} \sigma^{\mu\nu} e_t) \epsilon^{kj}\, \sigma_{\mu\nu}\, u_p.
\end{aligned} \tag{4.37}$$

There are additional corrections due to the B number violating operators of $\mathcal{L}^{(6)}$. Defining these operators as

$$\begin{aligned}
\mathcal{Q}_{\substack{duq\\prst}} &= \epsilon^{\alpha\beta\rho} \epsilon^{jk} (\overline{d^{\alpha,c}_p} u^\beta_r)(\overline{q^{\rho,c}_{s,\,j}} \ell_{t,\,k}), & \mathcal{Q}_{\substack{qqu\\prst}} &= \epsilon^{\alpha\beta\rho} \epsilon^{jk} (\overline{q^{\alpha,c}_{p,\,j}} q^\beta_{r,\,k})(\overline{u^{\rho,c}_s} e_t),\\
\mathcal{Q}_{\substack{qqq\\prst}} &= \epsilon^{\alpha\beta\rho} \epsilon^{jo} \epsilon^{kl} (\overline{q^{\alpha,c}_{p,\,j}} q^\beta_{r,\,k})(\overline{q^{\rho,c}_{s,\,l}} \ell_{t,\,o}), & \mathcal{Q}_{\substack{duu\\prst}} &= \epsilon^{\alpha\beta\rho} (\overline{d^{\alpha,c}_p} u^\beta_r)(\overline{u^{\rho,c}_s} e_t),
\end{aligned} \tag{4.38}$$

results in the EOM corrections of the following form

$$\Delta^{(6,\not{B})}_{e,m} = -\epsilon^{\alpha\beta\rho}\left[C^{\star}_{\substack{qqu\\prso}}\,\epsilon^{jk}(\overline{q^{\beta}_{r,k}}q^{\alpha,c}_{p,j})u^{\rho,c}_{s} + C^{\star}_{\substack{duu\\prsm}}(\overline{u^{\beta}_{r}}d^{\alpha,c}_{p})u^{\rho,c}_{s}\right],$$

$$\Delta^{(6,\not{B})}_{u,m\,\rho} = -\epsilon^{\alpha\beta\rho}\left[C^{\star}_{\substack{duq\\pmst}}\,\epsilon_{jk}(\overline{\ell^{j}_{t}}q^{\beta\,k,c}_{s})d^{\alpha,c}_{p} + C^{\star}_{\substack{duu\\prmt}}(\overline{d^{\alpha,c}_{p}}u^{\beta}_{r})^{\star}e^{c}_{t} + C^{\star}_{\substack{qqu\\prmt}}\,\epsilon^{j\,k}(\overline{q^{\alpha,c}_{p,j}}q^{\beta}_{r,k})^{\star}e^{c}_{t} - C^{\star}_{\substack{duu\\pmst}}\,d^{\alpha,c}_{p}(\overline{e_{t}}u^{\beta,c}_{s})\right],$$

$$\Delta^{(6,\not{B})}_{d,m\,\rho} = -\epsilon^{\rho\beta\alpha}\left[C^{\star}_{\substack{duq\\mrst}}\,\epsilon^{j\,k}(\overline{q^{\alpha,c}_{s,j}}\ell_{t,k})^{\star}\,u^{\beta,c}_{r} + C^{\star}_{\substack{duu\\mrst}}(\overline{u^{\alpha,c}_{s}}e_{t})^{\star}\,u^{\beta,c}_{r}\right], \tag{4.39}$$

(here α, β, ρ are $\mathrm{SU}(3)_{\mathrm{c}}$ indices) and for the $\mathrm{SU}(2)_{\mathrm{L}}$ doublet fields

$$\Delta^{(6,\not{B}),j}_{q,m,\rho} = -\epsilon^{\alpha\beta\rho}\left(C^{\star}_{\substack{qqu\\pmst}}\,\epsilon^{jk}(\overline{e_{t}}u^{\beta,c}_{s})q^{\alpha,c}_{p,k} + C^{\star}_{\substack{qqu\\mrst}}\,\epsilon^{jk}(\overline{u^{\beta,c}_{s}}e_{t})^{\star}q^{\alpha,c}_{r,k} + \epsilon^{j}{}_{k}\left[C^{\star}_{\substack{duq\\prmt}}\,\ell^{k,c}_{t}(\overline{d^{\alpha,c}_{p}}u^{\beta}_{r})^{\star}\right.\right.$$
$$\left.\left. - C^{\star}_{\substack{qqq\\prmt}}\,\epsilon^{lo}\ell^{c}_{t,o}(\overline{q^{\alpha,c}_{p,l}}q^{\beta,k}_{r})^{\star}\right]\right), -\epsilon^{\alpha\beta\rho}\epsilon^{jo}\epsilon^{kl}\left[C^{\star}_{\substack{qqq\\mrst}}\,q^{\alpha,c}_{r,k}(\overline{q^{\beta,c}_{s,l}}\ell_{t,o})^{\star} - C^{\star}_{\substack{qqq\\pmst}}\,q^{\alpha,c}_{p,k}(\overline{\ell_{t,l}}q^{\beta,c}_{s,o})\right], \tag{4.40}$$

$$\Delta^{(6,\not{B}),j}_{\ell,m} = -\epsilon^{\alpha\beta\rho}\left(C^{\star}_{\substack{duq\\prsm}}\,\epsilon^{jk}(\overline{u^{\alpha}_{r}}d^{\beta,c}_{p})\,q^{\rho,c}_{s,k} + C^{\star}_{\substack{qqq\\prsm}}\,\epsilon^{jo}\,\epsilon^{kl}(\overline{q^{\alpha}_{r,k}}q^{\beta,c}_{p,o})q^{\rho,c}_{s,l}\right). \tag{4.41}$$

Finally, for the Higgs field, we have

$$
\begin{aligned}
\Delta_H^{j,(6)} &= 3C_H(H^\dagger H)^2 H^j + \sum_{F=\{W,B,G\}} \left(C_{HF}\, H^j F_{\mu\nu} F^{\mu\nu} + C_{H\tilde{F}}\, H^j \tilde{F}_{\mu\nu} F^{\mu\nu} \right) + \sum_{F=\{W,\tilde{W}\}} C_{HFB}\, (\tau_I H)^j F^I_{\mu\nu} B^{\mu\nu}, \\
&+ \left(C_{\substack{uG\\pr}}\, \overline{q}_{p,k} \sigma_{\mu\nu} T^A u_r \epsilon^{kj} + C^\star_{\substack{dG\\pr}}\, \overline{d}_r \sigma_{\mu\nu} T^A q^j_p \right) G^{\mu\nu}_A + \left(C^\star_{\substack{eB\\pr}}\, \overline{e}_r \sigma^{\mu\nu} \ell^j_p + C_{\substack{uB\\pr}}\, \overline{q}_{p,k} \sigma_{\mu\nu} u_r \epsilon^{kj} + C^\star_{\substack{dB\\pr}}\, \overline{d}_r \sigma_{\mu\nu}\, q^j_p \right) B_{\mu\nu}, \\
&+ \left(C^\star_{\substack{eW\\pr}} \overline{e}_r \sigma^{\mu\nu} \tau_I \ell^j_p + C_{\substack{uW\\pr}}\, \overline{q}_{p,k} \sigma_{\mu\nu} \tau^I u_r \epsilon^{kj} + C^\star_{\substack{dW\\pr}}\, \overline{d}_r \sigma_{\mu\nu} \tau_I q^j_p \right) W^I_{\mu\nu} + C_{\substack{eH\\pr}}\, H^j\, \overline{\ell}_p e_r H + C^\star_{\substack{eH\\pr}}\, H^j\, (\overline{e}_r H^\dagger \ell_p), \\
&+ C^\star_{\substack{eH\\pr}}\, (H^\dagger H)\, \overline{e}_r \ell^j_p + C_{\substack{dH\\pr}}\, H^j \left(\overline{q}_p d_r H \right) + C^\star_{\substack{dH\\pr}}\, H^j\, (H^\dagger \overline{d}_r q_p) + C^\star_{\substack{dH\\pr}}\, (H^\dagger H)\, \overline{d}_r q^j_p + C_{\substack{uH\\pr}}\, H^j \left(\overline{q}_p u_r \tilde{H} \right), \\
&+ C^\star_{\substack{uH\\pr}}\, H^j\, (\tilde{H}^\dagger \overline{u}_r q_p) + C_{\substack{uH\\pr}} (H^\dagger H) \overline{q}_{p,k} u_r \epsilon^{kj} + 2i (D_\mu H^j) \sum_{\psi=\{e,u,d\}} C_{\substack{H\psi\\pr}}\, J^{\psi\,\mu}_{pr} + 2i (D_\mu H^j) \sum_{\psi=\{\ell,q\}} C^{(1)}_{\substack{H\psi\\pr}}\, J^{\psi\,\mu}_{pr}, \\
&+ C^{(1)}_{\substack{H\ell\\pr}}\, H^j [Y_e]^\star_{mr} (\overline{\ell}_p e^m H) - C^{(1)}_{\substack{H\ell\\pr}}\, H^j [Y_e]_{sp} (H^\dagger \overline{e}_s \ell^r) + C^{(1)}_{\substack{Hq\\pr}}\, H^j [Y_u]^\star_{mr} (\overline{q}_p u^m \tilde{H}) - C^{(1)}_{\substack{Hq\\pr}}\, H^j [Y_u]_{mp} (\overline{u}_m q^r \tilde{H}^\dagger), \\
&+ C^{(1)}_{\substack{Hq\\pr}}\, H^j [Y_d]^\star_{mr} (\overline{q}_p d^m H) - C^{(1)}_{\substack{Hq\\pr}}\, H^j [Y_d]_{mp} (H^\dagger\, \overline{d}_m q^r) + C_{\substack{He\\pr}}\, H^j [Y_e]_{rm} (H^\dagger \overline{e}_p \ell^m) - C_{\substack{He\\pr}}\, H^j [Y_e]^\star_{pm} (\overline{\ell}^m H e^r), \\
&+ C_{\substack{Hu\\pr}}\, H^j [Y_u]_{rm} (\tilde{H}^\dagger \overline{u}_p\, q^m) - C_{\substack{Hu\\pr}}\, H^j [Y_u]^\star_{pm} (\overline{q}^m \tilde{H} u^r) + C_{\substack{Hd\\pr}}\, H^j [Y_d]_{rm} (H^\dagger \overline{d}_p q^m) - C_{\substack{Hd\\pr}}\, H^j [Y_d]^\star_{pm} (\overline{q}^m H d^r), \\
&+ i\, C^{(3)}_{\substack{H\ell\\pr}} \left[\{\tau_I, D_\mu\} H \right]^j J^{\ell,I,\mu}_{pr} + i\, C^{(3)}_{\substack{H\ell\\pr}} (\tau_I H)^j \partial_\mu J^{\ell,I,\mu}_{pr} + i\, C^{(3)}_{\substack{Hq\\pr}} \left[\{\tau_I, D^\mu\} H \right]^j J^{q,I,\mu}_{pr} + i\, C^{(3)}_{\substack{Hq\\pr}} (\tau_I H)^j \partial_\mu J^{q,I,\mu}_{pr}, \\
&+ i\, C^\star_{\substack{Hud\\pr}}\, (D_\mu \tilde{H})^j (\overline{d}_r \gamma^\mu u^p) + i\, C^\star_{\substack{Hud\\pr}}\, \tilde{H}^j \partial_\mu\, (\overline{d}_r \gamma^\mu u^p) - i\, C^\star_{\substack{Hud\\pr}}\, (D_\mu H)^\dagger_k \epsilon^{kj} (\overline{d}_r \gamma^\mu u^p) + 2\, C_{H\Box}\, H^j \Box (H^\dagger H), \\
&- C_{HD} \left[(D^\mu H)^j\, (H^\dagger \overleftrightarrow{D}_\mu H) + H^j \partial^\mu (H^\dagger \overrightarrow{D}_\mu H) \right]. \qquad (4.42)
\end{aligned}
$$

4.5 Matching

Matching of an EFT entails studying the predictions of the full theory in comparison to its low-energy Wilsonian approximation. Although an EFT is fully independent of its UV completion, in the sense of having different S-matrix elements for various processes and being renormalised separately with separate counterterms, it is usually constructed in a manner where it is expected to produce the low-energy limit of its UV completion. An EFT is built up of a tower of higher-dimensional operators and is valid in a given range of energies, denoted as a limit in the expansion parameters. However, it contains a large number of free parameters, namely the Wilson coefficients. A test of a given EFT could be to check its compatability with a weakly-coupled UV theory. This was the idea behind the diagrammatic large mass expansion discussed in Sec. 2.2, where we considered the low energy limit of an integral in a perturbative series and checked how we could obtain a similarly convergent integral that could capture the results of the original integral. This matching of S-matrix elements can be seen in the following manner:

$$
\langle p_1 \dots p_m | S | k_1 \dots k_n \rangle^{UV}_{p^2 \ll m^2} \to \langle p_1 \dots p_m | S | k_1 \dots k_n \rangle^{EFT}. \qquad (4.43)
$$

In the above, we essentially integrate out some heavy mass scale m as in the large mass expansion calculation. Now, as mentioned, EFTs contain a large number of parameters that

must be fixed by this matching procedure. As a result, for q free parameters, we require as many linearly independent matrix elements in order to make this comparison and fix the parameters. We can modify Eq. (4.43) as follows

$$\langle p_1 \dots p_m | S_{1\dots q} | k_1 \dots k_n \rangle^{UV}_{p^2 \ll m^2} \to \langle p_1 \dots p_m | S_{1\dots q} | k_1 \dots k_n \rangle^{EFT}. \tag{4.44}$$

As per Ref. [5], as compared to our discussion in Sec. 2.2, we only need to compare the convergent parts of the theories. This is due to the fact that UV divergences are dealt with on each side conventionally using counterterms. On the other hand, IR divergences are much more complex to deal with and we do so using factorisation and resummation. We can also simply see that the comparison between theories is made at the level of renormalised interactions and thus the divergences are irrelevant.

An effective field theory can be constructed in a bottom-up approach. This means that we have control of the IR theory, in this case the SM, and construct a Wilsonian OPE to introduce corrections to the SM without knowledge of the overarching UV theory. Ultimately, one has to make a match between the complex Wilson coefficients of the EFT to the parameters of the UV theory. In this section, we consider simple examples of UV theories in order to illustrate the novel subleading effects that arise due to the EOM corrections we worked out previously. In particular, we will look at theories which would be relevant to the B-meson anomalies, i.e., $B \to K^{(*)}\ell^+\ell^-$. This process consists of a bottom quark decaying into a strange quark and a lepton-anti-lepton pair, and thus would induce the following operators at dimension six in the EFT:

$$\mathcal{Q}^{(1)}_{\substack{lq \\ mmsb}} = (\bar{\ell}_m \gamma^\mu \ell_m)(\bar{s}\gamma_\mu b), \tag{4.45}$$

$$\mathcal{Q}^{(3)}_{\substack{lq \\ mmsb}} = (\bar{\ell}_m \, \tau^I \, \gamma^\mu \ell_m)(\bar{s} \, \tau_I \, \gamma_\mu b). \tag{4.46}$$

These processes are particularly interesting because they contain flavour changing neutral currents (FCNCs) which are known not to exist at tree level in the Standard Model. Thus, New Physics would be more visible here. There is also an existing tension between theory and experiment in these processes. Our interest here is merely to illustrate EOM effects. We will consider examples of heavy scalar, fermion, and vector fields with different representations under the SM gauge groups. The notation used has been borrowed from Ref. [55]. We consider the fields $\{\zeta, \beta, \mathcal{W}, \mathcal{U}_2, \xi\}$ whose $(SU(3)_C \times SU(2)_L)_{U(1)_Y}$ representations are

$$\{(3,3)^0_{-1/3},\ (1,1)^1_0,\ (1,3)^1_0,\ (3,1)^{1/2}_{2/3},\ (3,3)^{1/2}_{2/3}\}, \tag{4.47}$$

where the superscript denotes the spin. We have two approaches to integrating out these heavy fields, one where we find the EOM for the heavy field from the Lagrangian and plug it back in to obtain higher dimensional operators, and the other where we expand out the

propagators. The propagator expansions for fields of different spins are as follows:

$$\Delta = -\frac{1}{M^2}\left(1-\frac{D^2}{M^2}\right)+\mathcal{O}(1/M^6)(scalars), \tag{4.48}$$

$$\Delta = -\frac{i\not{D}+M}{M^2}\left(1-\frac{D^2}{M^2}\right)+\mathcal{O}(1/M^6)(fermions), \tag{4.49}$$

$$\Delta^{\mu\nu} = \frac{\eta^{\mu\nu}}{M^2}+\frac{D^\mu D^\nu-\eta^{\mu\nu}D^2}{M^4}.(vectors). \tag{4.50}$$

The explicit interaction Lagrangians coming from the general extensions described in Eq. (4.47) are given in Appendix A of Ref. [55]. Additionally, a full list of the EFT operators from the Warsaw basis that are introduced from these particles can be found in Table 7 of the same.

The interactions of the scalar field ζ induces the baryon-number violating operator $\mathcal{Q}_{qqq}$, which is known to have a small matching coefficient. $\mathcal{Q}_{qq}^{(1,3)}$ and $\mathcal{Q}_{lq}^{(1,3)}$ are also induced in tree level matching but here we are interested mainly in EOM effects. Scalar fields have an expansion as given in Eq. (4.48), where corrections of order p^2/m^4 appear, which is already subleading. Using the EOM for scalar particles, these corrections which are already subleading can be reduced. This means that the first irreducible corrections only appear at $\mathcal{O}(m^-6)$, which would correspond to a $\mathcal{L}^{(10)}$. Thus, we will neglect this.

The main example we will use to elucidate the example of EOM corrections is that of the heavy vector fields $\beta, \mathcal{W}$. β is a singlet field and it appears within a Proca Lagrangian with a mass introduced through the Stückelberg mechanism. The more interesting part is the interaction Lagrangian. The β field is coupled to the SM as:

$$\begin{aligned}\mathcal{L}_{int}^{\beta} = &-g_\beta^{RH}\,\beta^\mu H^\dagger i\overleftrightarrow{D}_\mu H + g_\beta^{IH}\beta^\mu\partial_\mu(H^\dagger H),\\ &-\sum_{\psi=\{\ell,q,e,d,u\}} g_{\beta\psi}^{mn}\,\beta^\mu\,\bar{\psi}_m\gamma_\mu\psi_n.\end{aligned} \tag{4.51}$$

We see that this field interacts with both the Higgs as well as various fermions. The interaction with the Higgs is expressed in terms of the real and imaginary part of the coupling constant. The non-interaction terms of the Lagrangian have a straightforward EOM called the Proca equation. Thus, the EOM for this Lagrangian takes the form:

$$\begin{aligned}(\Box+m_\beta^2)\beta_\mu = &-g_\beta^{RH}\,H^\dagger i\overleftrightarrow{D}_\mu H + g_\beta^{IH}\,\partial_\mu(H^\dagger H),\\ &-\sum_{\psi=\{\ell,q,e,d,u\}} g_{\beta\psi}^{mn}\,\bar{\psi}_m\gamma_\mu\psi_n.\end{aligned} \tag{4.52}$$

At the first approximation in the low momentum limit, we can simply set that $\Box = 0$, and obtain the expression:

$$\begin{aligned}\beta_\mu = &-\frac{g_\beta^{RH}}{m_\beta^2}\,H^\dagger i\overleftrightarrow{D}_\mu H + \frac{g_\beta^{IH}}{m_\beta^2}\,\partial_\mu(H^\dagger H),\\ &-\sum_{\psi=\{\ell,q,e,d,u\}}\frac{g_{\beta\psi}^{mn}}{m_\beta^2}\,\bar{\psi}_m\gamma_\mu\psi_n.\end{aligned} \tag{4.53}$$

Plugging the above in Eq. (4.51) gives us various combinations of operators. We clearly obtain four fermion operators. Making a simple comparison with the Warsaw basis gives us the following Wilson coefficients

$$C^{(1)}_{\substack{H\psi_1\\mp}} = -g^{RH}_\beta\, g^{\psi_1}_{mp}, \qquad\qquad C_{\substack{\psi_1\psi_2\\mpst}} = -g^{mp}_{\beta\psi_1}\, g^{\psi_2}_{st}, \tag{4.54}$$

in terms of the coupling of the heavy fields to the SM. Note that for the case that $\psi_1 = \psi_2$, we obtain an additional factor of 2 in the above. In addition, we have various combinations of Higgs fields which can be reduced to the Warsaw basis using intergration by parts and EOM to obtain

$$C_{H\Box} = -\frac{(g^{RH}_\beta)^2}{2} + \frac{(g^{IH}_\beta)^2}{2} \qquad\qquad C_{HD} = -2\,(g^{RH}_\beta)^2. \tag{4.55}$$

We are left with some combinations of operators that need to further be reduced using EOM methods

$$\begin{aligned}\mathcal{L}^{(6)}_\beta \supset\ & \frac{1}{m^2_\beta}\, g^{RH}_\beta\, g^{IH}_\beta (H^\dagger i\overleftrightarrow{D}_\mu H)\, \partial^\mu (H^\dagger H),\\ & + \frac{g^{IH}_\beta}{m^2_\beta}\, \partial_\mu (H^\dagger H) \sum_{\psi=\{\ell,q,e,d,u\}} g^{mn}_{\beta\psi}\, \bar\psi_m \gamma^\mu \psi_n.\end{aligned} \tag{4.56}$$

The corresponding Wilson coefficients are given by

$$\begin{aligned}C_{\substack{eH\\pr}} &= -i g^{IH}_\beta \left([Y_e]^\star_{rp}\, g^{RH}_\beta - [Y_e]^\star_{rm}\, g^{pm}_{\beta,\ell} + [Y_e]^\star_{mp}\, g^{mr}_{\beta,e} \right),\\ C_{\substack{dH\\pr}} &= -i g^{IH}_\beta \left([Y_d]^\star_{rp}\, g^{RH}_\beta - [Y_d]^\star_{rm}\, g^{pm}_{\beta,q} + [Y_d]^\star_{mp}\, g^{mr}_{\beta,d} \right),\\ C_{\substack{uH\\pr}} &= -i g^{IH}_\beta \left([Y_u]^\star_{rp}\, g^{RH}_\beta - [Y_u]^\star_{rm}\, g^{pm}_{\beta q} + [Y_u]^\star_{mp}\, g^{mr}_{\beta u} \right).\end{aligned} \tag{4.57}$$

At this stage, we will focus on the operators of interest in this example, given in Eq. (4.46) and show the results obtained from the subleading matching:

$$\begin{aligned}\mathcal{L}^{(8)}_\beta \supset\ & \frac{i g^{IH}_\beta g^{mn}_{\beta\ell}}{m^4_\beta} \left[C^{(1)}_{\substack{\ell q\\npst}}\, J^\ell_{mp,\mu} - C^{(1)}_{\substack{\ell q\\pmst}}\, J^\ell_{pn,\mu} \right] J^{q,\mu}_{st} H^\dagger H,\\ +\ & \frac{i g^{IH}_\beta g^{mn}_{\beta q}}{m^4_\beta} \left[C^{(1)}_{\substack{\ell q\\stnp}}\, J^q_{mp,\mu} - C^{(1)}_{\substack{\ell q\\stpm}}\, J^q_{pn,\mu} \right] J^{\ell,\mu}_{st} H^\dagger H.\end{aligned} \tag{4.58}$$

These results are subleading, proportional to the inverse power of the mass. The non-intuitive scalings of these couplings can be understood better in diagrammatic form.

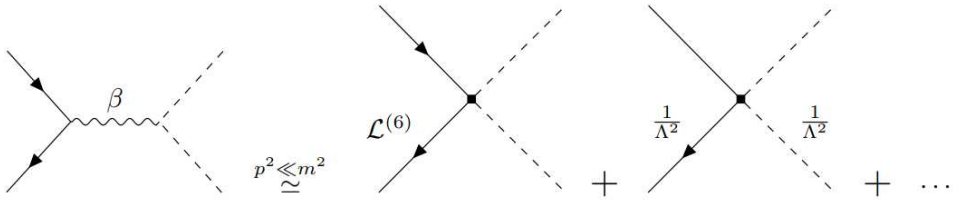

Figure 4.1: Integrating out heavy fields in EFTs

On one hand, in Fig. 4.1, we see the general expectation in an EFT. When a heavy propagator is integrated out, this results in a tower of local contact operators where we can systematically look at subleading terms as well. Essentially, we would be replacing the propagator with a Taylor series involving p^2/m_β^2 following Eq. (4.48). In Fig. 4.1, the black squares indicate expansions in β while the circle indicates the EOM matching correction of a singlet field $(1,1)_0$. However, the scaling of the couplings we obtained in Eq. (4.57) show a different type of effect, as seen in Fig. 4.2. At subleading order, we can find propagators of the heavy field that cannot be naively removed to obtain contact operators as in the previous case. The particular form of the scaling of the couplings elucidate these new effects. The presence of light propagators leads to subtleties.

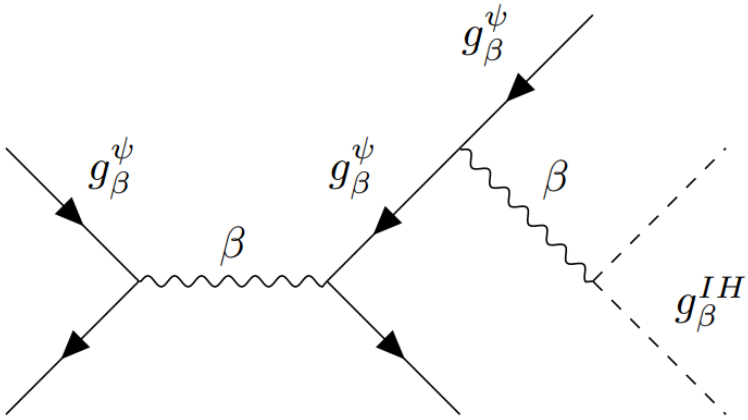

Figure 4.2: EOM effects on EFT calculations

A key thing to notice in Eq. (4.57) is the factor of i that appears, which implies that if one expands out the complex Wilson coefficients, it leads to cancellation in terms which are symmetric in the flavour indices. As per the discussion in Ref. [2], flavour indices that are bilinear in the same field of a self-Hermitian operator can be decomposed into a symmetric and antisymmetric part, which correspond to CP-even and CP-odd terms as

$$C_{pr} = S_{pr} + iA_{pr}, \tag{4.59}$$

where we can conclude that the symmetric components of the above, namely S_{pr} will cancel. Analogous results have been obtained for the $\mathcal{W}$ field, however now with $SU(2)$ indices

$$\begin{aligned} 2\,\mathcal{L}_{int}^{\mathcal{W}} = &-g_{\mathcal{W}}^{RH}\,\mathcal{W}_I^\mu H^\dagger i\overleftrightarrow{D}^I_\mu H + g_{\mathcal{W}}^{IH}\mathcal{W}_I^\mu \partial_\mu (H^\dagger \tau^I H), \\ &- \sum_{\psi=\{\ell,q\}} g_{\mathcal{W}\psi}^{mn}\,\mathcal{W}_I^\mu\,\bar{\psi}_m \tau^I\,\gamma_\mu \psi_n, \end{aligned} \tag{4.60}$$

which leads to similar contact operators as in the case of the heavy field β

$$\begin{aligned} \mathcal{L}_{\mathcal{W}}^{(6)} \supset \quad & \frac{1}{4\,m_{\mathcal{W}}^2}\,g_{\mathcal{W}}^{RH}\,g_{\mathcal{W}}^{IH}(H^\dagger i\overleftrightarrow{D}^I_\mu H)\,\partial^\mu (H^\dagger \tau^I H), \\ + \quad & \frac{g_{\mathcal{W}}^{IH}}{4\,m_{\mathcal{W}}^2}\,\partial^\mu (H^\dagger \tau^I H) \sum_{\psi=\{\ell,q\}} g_{\mathcal{W}\psi}^{mn}\,\bar{\psi}_m \tau^I \gamma_\mu \psi_n. \end{aligned} \tag{4.61}$$

This leads to subleading corrections in the SMEFT, where instead of operators such as $\mathcal{Q}_{lq}^{(1)}$, we obtain $\mathcal{Q}_{lq}^{(3)}$, which contains additional Pauli matrices. The detailed calculations can be found in Ref. [56].

4.6 Conclusions

In this section, we discussed the original work published in Ref. [2]. The full set of corrections to the Standard Model Equations of Motion due to dimension-6 operators in the War-

saw basis were listed. Note that in Ref. [57], a similar analysis was made for Low-Energy Effective Field Theory (LEFT) . The basis-dependence of these corrections was made evident, since we were exclusively using the operator structures that form the Warsaw basis. An example of a matching calculation where we discussed operators that can contribute to B-meson decays showed non-intuitive effects leading to subtleties when integrating out heavy fields to obtain local contact operators in an EFT basis. These effects were attributed to EOM corrections. Since these EOM corrections are basis-dependent, one can conclude that when calculating subleading corrections within the SMEFT framework, the basis choice at lower orders in the power counting of the heavy scale determines results at higher orders, or that matching coefficients for $\mathcal{L}^{(n)}$ terms are affected by basis choices for $\mathcal{L}^{(m<n)}$. These effects must be considered as we move towards higher order precision results in SMEFT.

Chapter 5

Gravity as an Effective Field Theory

Gravity has been studied since the 17th century, starting with Newton's initial theory of gravity, what we today call classical gravity. At an elementary level, this theory just began by describing the force that attracts massive particles or objects. However, this also is the first description of a binary system. Newtonian gravity was able to accurately predict the orbits of planetary systems, with some exceptions.
Classical gravity is considered to be an EFT of GR where we consider weak gravity at non-relativistic velocities and apply these limits to GR which we expect to reproduce classical gravity in the flat space non-relativistic limit. Einstein, in 1915, described gravity in a completely new way. Firstly, he described gravity in terms of differential geometry and geodesics, where mass and energy were said to warp spacetime itself. Compared to the simple calculations in Newtonian physics, the non-linear nature of Einstein's theory of General Relativity, has meant that the two-body problem in GR has not yet been fully solved.
Gravity has been fairly mysterious to quantum physicists for a long time. The major reason being that in quantum field theory one makes use of coupling constants as seen in the SM that do not have a unit once we make use of $\hbar = c = 1$. However, the Newtonian gravitational constant does have a unit which makes it difficult to incorporate into a quantum theory. One of the contemporary big pursuits has been to unify gravitation and quantum theory. There has been a revived interest in studying gravity due to the 2017 Nobel Prize to the Laser Interferometer Gravitational Wave Observatory (LIGO) collaboration for their discovery of gravitational waves (GW) from binary black holes (BHB). While Einstein's theory of General Relativity has existed since the first decade of the 20th century and has been validated in all kinds of experiments, most memorably where it correctly predicted the precession of the Mercury orbit, the final proof of its predictions came from the observation of tensor perturbations in the form of GWs. The first evidence of GWs appeared in 1974, when Hulse and Taylor [58] discovered the first example of a binary of pulsars. This lead to the building of more advanced detectors, finally resulting in the current configuration of the LIGO detector which is one of the most advanced and precise experiments that currently exists. LIGO is set to expand all over the globe in the next few years, including in India, where a detector called Indigo is being developed (See Ref. [59]), which means that we will have more precise statistics on GWs. Quantum theorists are now looking into a variety of approaches, combining effective field theories and amplitudes with gravity:

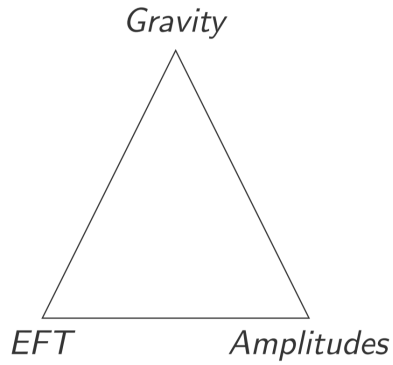

In this thesis, we will look at gravity from the perspective of particle physics, however, the interest in GWs also extends to cosmologists and astrophysicists. Potentially, a future GW telescope would be a probe of the earliest epochs of the universe [60], perhaps giving us more information about the mysterious period of inflation. From the astrophysical perspective, one would be hopeful for more information on stellar collapse and the fundamental structure of collapsed massive stars such as neutron stars and black holes. Thus, GWs have truly cemented gravity as a force of attraction and interaction between high-energy physicists from several different fields.

5.1 The Two-Body Problem

Since the main application of the work done in this thesis is to calculate the spacetime metric of black holes with different spin, we will focus on the binary mergers of these. In principle, these approaches can be extended to any kind of massive body under certain limits which will shortly be elaborated upon.
Black holes are some of the most mysterious objects in the universe, forming through the collapse of a massive star into a singular object whose gravitational strength ensures that even light cannot escape its limits. They are fully defined using three parameters– the mass, spin, and charge. This will allow us to calculate other important quantities, such as the radius of influence of the BH, which describes its event horizon. In the case of a BH with spin zero, we have the following result for the well-known Schwarzschild radius:

$$r_{schwarzschild} = \frac{2Gm}{c^2}, \tag{5.1}$$

where G is the Newtonian gravitational constant constrained to the value $6.6740810^{-11}m^3kg^{-1}s^{-2}$, and m is the mass of the black hole. Black holes are interesting to those studying gravity since they are perhaps one of the objects projecting the strongest gravitational force. GR is today assumed to be an EFT, breaking down in the limit of strong gravity, i.e., at the Planck scale. Thus, studying BHs is essential to testing any complete theory of gravity. In the following sections, we will look at how BHs affect the curvature of spacetime around them. Theories mediated by massless particles have the property that they can affect the curvature of spacetime even at far distances, so in particular, we will use EFT methods in gravity to compute corrections to the spacetime metric for Schwarzschild and Kerr black holes.

5.1.1 The LIGO discovery

The first discovery of GWs for a Binary Black hole Merger (BHB) showed the following experimental results:

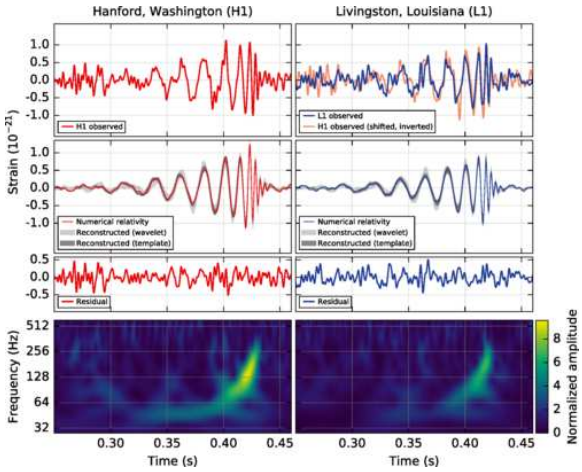

Figure 5.1: Source- LIGO Collaboration

The above picture describes the simultaneous detection of a BHB using experiments in two different parts of the United States. What we see is that the two L-shaped detectors experience a minor length change corresponding to length contractions. This is described in terms of the binary strain. A full review of the detection can be found in Ref. [61]. We see a similar pattern for both detectors where there is a gradual increase in frequency and amplitude as the black holes get closer to each other, resulting in a catastrophic merger where this pattern gradually crescendos, and concludes in a peaceful final state. This is also corroborated by the bottom two graphs of the figure, where we see a sudden increase in frequency that corresponds with the merger.

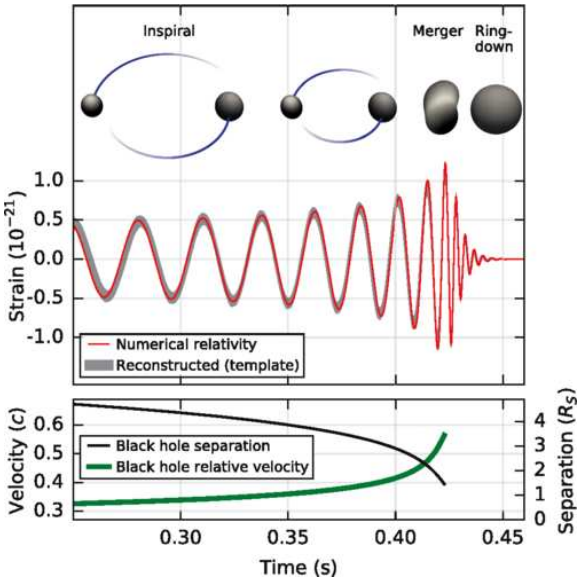

Figure 5.2: Source: LIGO Collaboration

The previous paragraph is made more concrete in the Fig. 5.2, where we see the agreement between theoretical predictions and experiment. The description of the BHB is considered in three regimes: the inspiral, merger and ringdown. An important observation to note is that the inspiral period comprises the majority of the graph, where we see a very gradual increase in the binary strain. The merger is the period where the GW radiation peaks. Following this, we see a dampening of the frequency as the single merged black hole "rings".

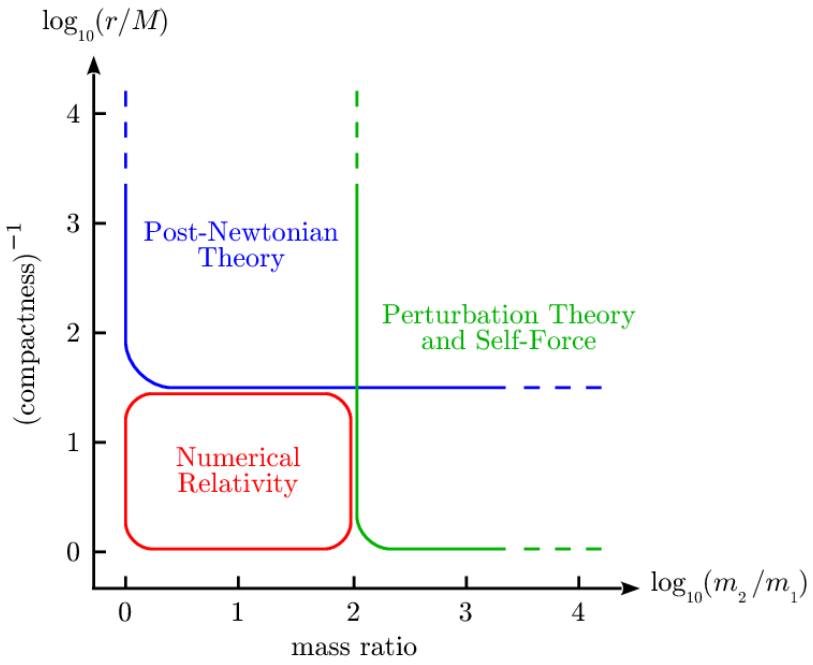

Figure 5.3: Source: Ref. [62]

We see in Fig. 5.3 that based on two parameters, the mass rations m_2/m_1 and what is called the inverse of the compactness r/M, where M is the total mass and r is the radius of separation, that these scales determine which approach best applies.
We are clearly looking at a multi-scale problem where the masses of the black holes as well as the radius of separation are some of the scales under consideration. In addition, we have the velocities and the value of the quantum constant $\hbar$, with the latter being relevant to quantum corrections to GR. Most studies operate under the assumption that the BHs are in similar mass range; in the case of the first LIGO discovery, GW150914, the masses of the BHs were found to be approximately 35 and 30 solar masses respectively. It is possible that large mass separations can be misinterpreted with the angular momentum of the black hole. In the catastrophic merger regime, one must apply numerical methods as analytical methods can be insufficient. However, it must be noted that most of the BHB can be described analytically using various perturbative methods. The longest time period is the inspiral, described by a post-Newtonian theory. Here, the radius of separation is relatively large. The final part of the merger is described best using a one-body effective approach to gravity as formulated by Buonanno and Damour, in Ref. [63–65]. This effective-one body approach, in fact, is used to validate the results from numerical calculations for the whole merger. The limitation of numerical methods in this case is the extensive time span of the inspiral of heavy bodies. This means that we need to run a simulation to describe very long periods of time, which is both expensive and cumbersome. Analytic approaches based on particle physics and scattering amplitudes can be employed to study most of the timeline of the merger. This is all succinctly expressed in Fig. 5.3. The commonly used approximations are the post-Newtonian and similarly post-Minkowskian limits. The former is a low-energy

expansion in velocity as well as $\hbar$, and additionally in flat space. The post-Minkowskian expansions are more advanced where we are looking at potentially special relativistic velocities while making a Taylor expansion around flat space. A thorough review of these limits can be found in Ref. [66].
Clearly, we see that effective field theory approaches based on expansions in velocities and the gravitational constant are being employed to theoretically predict GWs. A full review of post-Newtonian theory and its status is available in Ref. [62]. A public code for this is available, called `EFTofPNG`, which includes post-Newtonian corrections as well as the effects of spin in Ref. [67].The Effective One Body Formalism is discussed in Ref. [68], while the seminal results were presented in Ref. [63, 64]. In addition, a relevant EFT approach for extended objects was put forward by Goldberger and Rothstein in Refs. [69–71]. Effective approaches allow us to circumvent the non-renormalisability of the theory. As will be explained shortly, a combination of EFT and modern approaches to scattering amplitude computations may be optimal for the task.

5.2 Latest Results in PN and PM theories

The following are the state-of-the-art results in both PN and PM theory. These involve expansions in velocity, and further in flat spacetime itself. These results have also been verified by experiments.

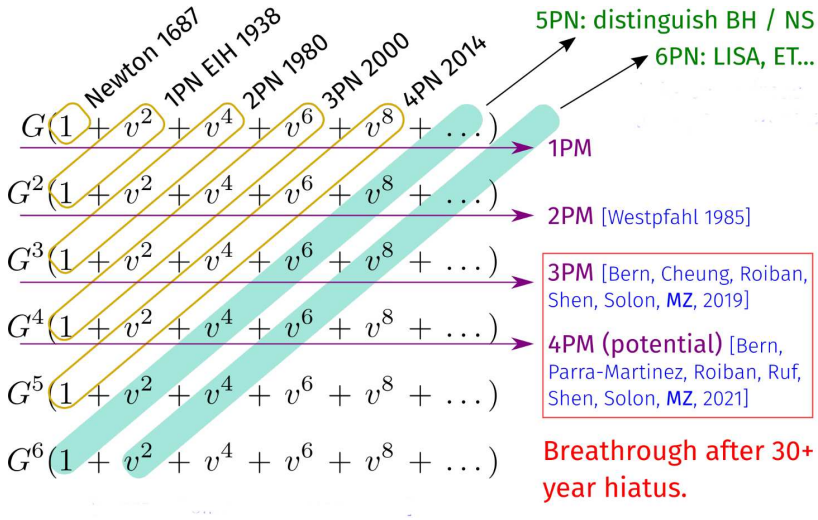

Figure 5.4: Source: Mao Zeng, GGI 2021 Slides

Fig. 5.4 begins on the top left corner with Newton's initial results, which would correspond to the leading order result in the post-Newtonian expansion of GR as expected. However, noting the timelines of the following results in PN theory, one can see the accelerated excitement in calculating PN expansions in recent years. Full results for the fourth order in the PN expansion were obtained in 2014, whereas we currently have partial results for the fifth

and sixth orders in Ref. [72] only this year. On the other hand, post-Minkowskian theory involves far more involved calculations. The most recent results are in the fourth order in the gravitational coupling G, obtained this year Ref. [73]. These higher-order computations are not at all easy, just as in the case of particle physics calculations. The 5th order in PN theory, as stated in Fig. 5.4, could be used to differentiate between neutron star and black hole mergers. Further, as per Ref. [66], higher order PN computations would be relevant for extreme mass ratio inspirals. Unitary-based approaches looking at different variables than in the traditional Feynman diagram approach have been found to make these calculations concise and easier to implement in automated programs. In Sec. 6.3, we briefly review the basic ideas behind such an approach.

5.3 An EFT Formalism for Gravity

The background developed in Sec. 2 will be used in the following sections to develop and apply an effective approach to gravity. The current results that were reviewed in Sec. 5.2 showed us that the EFTs based on post-Newtonian and post-Minkowskian expansions, as well as other expansions, are already an important part of gravitational studies. We are motivated to believe that the traditional thinking that gravity is different from the forces in the SM and cannot be quantised is in fact wrong. On the contrary, gravity may be even better suited to an EFT-based quantum treatment since we believe that the quantum corrections to GR below the Planck scale are very small, thus implying that GR is unlikely to break down at lower energies. In this case, we can use the low-energy DOFs in GR to extract these quantum corrections as is a standard approach in the EFT. On the other hand, we are still unsure of the scales at which the SM would break down, as was seen in the exclusion limit study for exotics at ATLAS given in Fig. 3.3.

In this case, we consider a particular class of post-Newtonian corrections where we examine the long-range effects of massless force carriers, namely the graviton. To be more precise, we will look at a range of non-analytic contributions to the metric tensor in the case of Schwarzschild and Kerr black holes involving the functions $\ln -q^2$ and $1/\sqrt{-q^2}$. The metric is an inherently classical quantity, coming from GR. However, long-range effects using an effective quantum approach result in both quantum as well as classical corrections to these quantities. It must be emphasised that we are not studying quantum gravity here- a theory that would probe gravity at short distances, i.e., strong gravity. Instead, we are studying objects such as black holes by looking at them as a form of quantum matter which interacts with gravity. To this effect, we are studying BHs as point particles with extremely large mass. EFTs are able to handle such multi-scale problems, as has been clearly established. We study the effect of such massive point particles coupling with the energy-momentum tensor $T_{\mu\nu}$ in gravity. These effects are also seen in the case of other massless force carriers such as the photon in the case of theories like QED. Gravitational theories experience such corrections when we see photon-graviton interactions. Results for the Reissner-Nordström and Kerr-Newmann metrics are found in Ref. [74], where we see corrections to the Schwarzschild and Kerr metrics proportional to the QED coupling α. Specifically, we will consider both quantum and classical corrections to gravity. We will be looking at simplified methods to study the classical limit, where we have $q/m \to 0$. In accordance, we will be making an expansion around the flat Minkowski metric at first order.

These non-analytic computations are very interesting, since we are using quantum field theoretical methods to obtain results in a classical gravitational theory. This method allows us to obtain fundamental quantities such as the spacetime metric, and the Newtonian potentials. These results are available in Refs. [75–77]. In the following, we will begin by considering the EFT formalism that is used here in order to quantise gravity and explain the procedure of obtaining Feynman rules. Then, after a brief study of the difference between analytic and non-analytic corrections and the implications of the latter, we will explain the procedure of independently reproducing some of the results in Ref. [75], using the full formalism. A separate approach involving residue theorem, which attempts to simplify these calculations, will be studied in Sec. 6.2. We will end the discussion with a review of other modern approaches to such calculations, which use scattering amplitudes instead of the standard Feynman approach.

It should be noted that a full loop computation involves several diagrams, as can be seen in Refs. [75, 76]. In addition, one must consider renormalisation and vacuum polarisation diagrams. Such diagrams can also contribute to corrections to the metric. We restricted our case here to classical corrections, however, there are quantum contributions due to several diagrams. Given the limited nature of the corrections we are interested in, we will ignore spurious infinities, since they do not appear here.

5.4 General Relativity as an EFT

The Einstein equations for GR are

$$R_{\mu\nu} - \frac{1}{2}Rg_{\mu\nu} = 16\pi G T_{\mu\nu} - \lambda g_{\mu\nu}. \tag{5.2}$$

While $g_{\mu\nu}$ is the metric tensor, $R_{\mu\nu}$ and R are respectively the Ricci tensor and the Ricci scalar, which describe the curvature of spacetime. On the right hand side, we have $T_{\mu\nu}$, the energy-momentum tensor. Thus, the equations essentially relate the curvature of spacetime to the energy/mass content. We are going to ignore the λ term now, which is related to the cosmological constant but not relevant to this discussion. Cosmological bounds on this have that $|\lambda/8\pi G| \sim 10^{-66} eV^4$, as per Ref. [78]. The curvature tensors are written explicitly as follows:

$$\begin{aligned}
\Gamma^{\lambda}_{\mu\nu} &= \frac{1}{2}g^{\lambda\sigma}\left[\partial_\mu g_{\sigma\nu} + \partial_\nu g_{\sigma\mu} - \partial_\sigma g_{\mu\nu}\right] \\
R^{\lambda}_{\sigma\mu\nu} &= \partial_\mu \Gamma^{\lambda}_{\sigma\nu} - \partial_\nu \Gamma^{\lambda}_{\sigma\mu} + \Gamma^{\rho}_{\sigma\nu}\Gamma^{\lambda}_{\rho\mu} - \Gamma^{\rho}_{\sigma\mu}\Gamma^{\lambda}_{\rho\nu} \\
R_{\mu\nu} &= R^{\lambda}_{\mu\nu\lambda} \\
R &= g^{\mu\nu}R_{\mu\nu},
\end{aligned} \tag{5.3}$$

where we begin by defining the Christoffel symbol that appears in the various other objects, followed respectively by the Riemann tensor, Ricci tensor, and Ricci scalar. These curvature tensors are equated to the energy-momentum tensor $T_{\mu\nu}$ on the right-hand side, which describes the mass/energy content– thus relating the effect of matter and energy to the geometry of spacetime. This is a non-linear equation in the tensors described in Eq. (5.3). The additional relevant quantity is the Einstein-Hilbert action for GR

$$S = \int d^4x \sqrt{-g}\frac{2}{\kappa^2}R, \tag{5.4}$$

where $g = det(g_{\mu\nu})$ is the determinant of the metric, R is the Ricci scalar, and $\kappa^2 = 32\pi G$, G being the Newtonian gravitational constant. This action is based on the idea of general covariance. However, this invance also allows higher order terms systematic in an EFT expansion. We can add to the gravitational part above by considering different combinations of curvature tensors and possibly derivatives on them. As stated in Ref. [79], these terms are ordered according to derivatives acting on them, based on the idea of general covariance. Derivatives on light fields produce powers of momentum when Fourier transformed, while those for massive fields will generate powers of the mass. In general, we work in the limit q/m being small, since we are concerned with very heavy objects whose momentum is small in comparison. Thus, the masses that are generated tend to offer the leading contribution to the results. We can write the following infinite EFT expansion, based on general coordinate invariance

$$\mathcal{L} = \sqrt{-g}\left[\frac{2R}{\kappa^2} + c_1 R^2 + c_2 R_{\mu\nu}R^{\mu\nu} + \cdots + \mathcal{L}_{matter}\right]. \tag{5.5}$$

The ordering in the above terms can be reconsidered by looking at the expressions for the tensors we see above, which were detailed in Eq. (5.3). We can see above that since the

Christoffel symbol comes with one derivative, all the curvatures involve two derivatives of the metric field. Thus, we see in Eq. (5.6) that our first term proportionate to just R is of order ∂^2, while R^2 terms are proportionate to four powers of the derivative. We have certain experimental limits from cosmology on the Wilson coefficients $c_1, c_2, \cdots$, etc. mentioned above where a matched result of $c_1, c_2 > 10^{70}$ would imply deviations from GR [80].
It turns out conveniently, that in the low energy case, we only need to concern ourselves with the Einstein-Hilbert action and matter that we started off with. By working out the equations of motion and the associated propagator when considering an $R + R^2$ type action, we see that the only effect the higher order operators have are to weakly modify the gravitational potential, to the extent that it can be neglected from consideration. This can be understood using EOM arguments. Further discussion of why we can neglect other terms can be found in Ref. [81].

Ultimately, we will restrict this case to the Lagrangian

$$\mathcal{L} = \sqrt{-g}\left[\frac{2R}{\kappa^2} + \mathcal{L}_{matter}\right]. \tag{5.6}$$

In the following, we will discuss how to treat the gravitational component in an appropriate power series in κ. We will also discuss some interesting matter Lagrangians, how they couple with gravity, and how to obtain Feynman rules. This will set up the framework for applying this to relevant computations in gravity.

5.5 Quantisation of Gravity

The first step of constructing an EFT is to construct an action that contains all of the field content and interactions within the theory. General relativity in itself is known to have issues with renormalisability, and in previous sections we have touched upon the fact that treating it as an EFT is a way of circumventing this issue. Now that we have a Lagrangian, we can consider the problem of quantising the gravitational metric field. This is traditionally done using the background field method, where at lowest order, the metric tensor expanded as

$$g_{\mu\nu}(x) \equiv \bar{g}_{\mu\nu}(x) + \kappa h_{\mu\nu}. \tag{5.7}$$

In the above, we have expanded around a classical background field denoted with the bar and the quantum component appears within $h_{\mu\nu}$. We explicitly note that the expanded field $h_{\mu\nu}$ is always proportional to one order in κ. These factors are put in only when the power counting needs to be seen exactly, and will be ignored otherwise. Although the following expansions contain higher order terms, we will be neglecting terms from the second order in κ since this is a weak field expansion . We need to use $\bar{g}_{\mu\nu}$, the background field, to raise and lower indices. The above definition in Eq. (5.7) can be used to find the following functions:

$$\begin{aligned} g^{\mu\nu} &= \bar{g}^{\mu\nu} - \kappa h^{\mu\nu} + h^{\mu}_{\alpha} h^{\alpha\nu} + \dots \\ \sqrt{-g} &= \sqrt{-\bar{g}}\left[1 + \frac{1}{2}\kappa h - \frac{1}{4} h^{\alpha}_{\beta} h^{\beta}_{\alpha} + \frac{1}{8} h^2 + \dots\right]. \end{aligned} \tag{5.8}$$

The first equation above is obtained simply by inverting the metric. The determinant in the latter is obtained by using the relation $det(A) = \exp(Tr(\ln(A)))$ and subsequently using

the weak field expansion. We also define the following:

$$h^{\mu\nu} = \bar{g}^{\mu\alpha}\bar{g}^{\nu\beta}h_{\alpha\beta} \tag{5.9}$$

$$h = \bar{g}^{\mu\nu}h_{\mu\nu}. \tag{5.10}$$

The above allows us to expand the Lagrangian around the quantum field $h_{\mu\nu}$

$$\begin{aligned}
\sqrt{-g}\frac{2R}{\kappa^2} &= \sqrt{-g}\left[\frac{2\bar{R}}{\kappa^2} + \mathcal{L}_g^{(1)} + \mathcal{L}_g^{(2)} + \cdots\right] \\
\mathcal{L}_g^{(1)} &= \frac{1}{\kappa}h_{\mu\nu}\left[\bar{g}^{\mu\nu}\bar{R} - 2\bar{R}^{\mu\nu}\right] \\
\mathcal{L}_g^{(2)} &= \frac{1}{2}D_\alpha h_{\mu\nu}D^\alpha h^{\mu\nu} - \frac{1}{2}D_\alpha h D^\alpha h + D_\alpha h D_\beta h^{\alpha\beta} \\
&\quad - D_\alpha h_{\mu\beta}D^\beta h^{\nu\alpha} + \bar{R}\left(\frac{1}{2}h^2 - \frac{1}{2}h_{\mu\nu}h^{\mu\nu}\right) + \bar{R}^{\mu\nu}\left(2h^\lambda_\mu h_{\nu\alpha} - h h_{\mu\nu}\right).
\end{aligned} \tag{5.11}$$

where the superscripts on the Lagrangians denote the order in κ we are working with. On the other hand, we can use an EFT approach and expand out the matter Lagrangian to find Feynman rules. If we are looking at the simple case where our sources are scalar particles, the matter Lagrangian looks as follows

$$\sqrt{-g}\mathcal{L}_m = \sqrt{-g}\left(\frac{1}{2}\partial_\mu\varphi g^{\mu\nu}\partial_\nu\varphi - \frac{1}{2}m^2\varphi^2\right). \tag{5.12}$$

Here, $\sqrt{-g}$ is the determinant of the metric tensor. Plugging this into the above, it is clear that at zeroeth order, we will simply obtain the standard scalar Lagrangian for flatspace with no gravitational interactions, namely

$$\sqrt{-g}\mathcal{L}_m^{(0)} = \frac{1}{2}\partial_\mu\varphi\partial^\mu\varphi - \frac{1}{2}m^2\varphi^2. \tag{5.13}$$

However, at first order, we do find gravitational interactions. This is expected, since we only expect quantum contributions to GR at higher orders in the theory. In this case, we stick to the first order in κ in Eqs. (5.8). For the scalar theory under consideration, we have

$$\sqrt{-g}\mathcal{L}_m^{(1)} = -\frac{\kappa}{2}\left[\partial_\mu\varphi h^{\mu\nu}\partial_\nu\varphi - \frac{h}{2}\left(\partial_\alpha\varphi\partial^\alpha\varphi - m^2\varphi^2\right)\right]. \tag{5.14}$$

Given that $h = h^{\mu\nu}\eta_{\mu\nu}$, this can be rewritten as

$$\sqrt{-g}\mathcal{L}_m^{(1)} = \frac{-\kappa h^{\mu\nu}}{2}\left[\partial_\mu\varphi\partial_\nu\varphi - \frac{1}{2}\eta_{\mu\nu}\left(\partial_\alpha\varphi\partial^\alpha\varphi - m^2\varphi^2\right)\right]. \tag{5.15}$$

The above form for interactions between matter Lagrangians and gravity can be used to derive Feynman rules. In fact, the explicit expression for the scalar-graviton interaction appearing from this is explicitly derived in Appendix A. This formalism can be extended to a variety of matter Lagrangians. This could include particles of different spins as well as complex scalars and so on. It should be noted that there is additional complexity when including a matter Lagrangian which contains fermions. In this case, a direct coupling through a

metric is not possible and a new formalism needs to be introduced. In this context, a vierbein field is introduced. Essentially, we are consistently expressing a Dirac Lagrangian in curved space. At zeroeth order, the Dirac Lagrangian coupled to gravity is expressed as

$$\sqrt{e}\mathcal{L}_m^{(0)} = \bar{\psi}\left(\frac{i}{2}\gamma^\alpha \delta_\alpha^\mu \partial_\mu^{LR} - m\right)\psi. \tag{5.16}$$

The partial derivative above is explicitly defined as

$$\bar{\psi}\partial_\mu^{LR}\psi \equiv \bar{\psi}\partial_\mu\psi - (\partial_\mu\bar{\psi})\psi. \tag{5.17}$$

This field has to be introduced in order to obtain Feynman rules. Detailed explanation is available in Refs. [79, 82].

5.6 Analytic and Non-Analytic Contributions

In the following sections, we will devote our interest to certain non-analytic structures that appear in the effective field theoretical description of gravity. These effects correspond to long-range effects arising from massless propagators. Gravitons and photons are examples of force carriers that are massless, thus calculations involving such particles produce non-analytic structures. This can be understood naively by considering what happens when one expands massive and massless propagators respectively. Consider the expansion of a massive propagator in the low momentum limit

$$\frac{1}{q^2 - m^2} = -\frac{1}{m^2}\left(1 + \frac{q^2}{m^2} + \cdots\right), \tag{5.18}$$

where we can see that it is not possible to obtain terms of the form $(\sim 1/q^2)$. We have instead, a steady analytic expansion in powers of the momentum q. However, a massless propagator is already of the form $(1/q^2)$ and is able to produce non-analytic structures, mainly of the form $(1/\sqrt{-q^2})$ and $(\ln(-q^2))$.

One must go through a power-counting procedure to meticulously examine powers of $\hbar$ in order to determine which of these corrections are quantum and classical. By carefully examining the dimensions of the quantities in question, it can be determined that the logarithmic terms correspond to quantum corrections and the square-root terms correspond with classical corrections. This is the specific feature of theories involving massless propagators. By looking at the Fourier transforms of the aforementioned terms, one can see that these contribute to long-range effects in gravity. Thus, while classical corrections are simply a power series in the gravitational constant, quantum corrections are also proportional to factors in $\hbar$.

The following Fourier transformations exist for various classical non-analytic terms:

$$\begin{aligned}
&\int \frac{d^3q}{(2\pi)^3} e^{i\vec{q}\cdot\vec{r}}|\vec{q}| = -\frac{1}{\pi^2 r^4}, \\
&\int \frac{d^3q}{(2\pi)^3} e^{i\vec{q}\cdot\vec{r}} q_j|\vec{q}| = \frac{-4ir_j}{\pi^2 r^6}, \\
&\int \frac{d^3q}{(2\pi)^3} e^{i\vec{q}\cdot\vec{r}} \frac{q_i q_j}{|\vec{q}|} = \frac{1}{\pi^2 r^4}\left(\delta_{ij} - 4\frac{r_i r_j}{r^2}\right),
\end{aligned} \tag{5.19}$$

as well as the corresponding integrals for the quantum terms which involve the logarithms:

$$\begin{aligned}
&\int \frac{d^3q}{(2\pi)^3} e^{i\vec{q}\cdot\vec{r}} \vec{q}^2 \ln \vec{q}^2 = \frac{3}{\pi r^5}, \\
&\int \frac{d^3q}{(2\pi)^3} e^{i\vec{q}\cdot\vec{r}} q_j \vec{q}^2 \ln \vec{q}^2 = \frac{i15 r_j}{\pi r^7}, \\
&\int \frac{d^3q}{(2\pi)^3} e^{i\vec{q}\cdot\vec{r}} q_i q_j \ln \vec{q}^2 = \frac{-3}{2\pi r^5} \left(\delta_{ij} - 5\frac{r_i r_j}{r^2} \right).
\end{aligned} \tag{5.20}$$

These results were shown in Ref. [79]. The presence of inverse r on the right-hand side clearly show us that we are looking at long-range effects that vanish only in the limit of $r \to \infty$. In general, form factors show the general momentum space structure of a particle, excluding certain structures. So far, non-analytic terms have been found in the case of QED and χPT, where in the latter case, we see non-analytic terms connected to the pion mass. Of course, as we will see shortly, such terms are also seen in the case of gravity as an EFT. As per Ref. [74], in the case of QED being the matter Lagrangian interacting with gravity, we have the following corrections for charged black holes:

$$F(q^2) = 1 + a\alpha \frac{q^2}{m^2} \sqrt{\frac{m^2}{-q^2}} + b\alpha \frac{q^2}{m^2} \ln(-q^2) + c\alpha \frac{q^2}{m^2} + \cdots . \tag{5.21}$$

These results represent the Reissner-Nordström black holes and the presence of the factor α shows the charge parameter of the black hole. Using this, we can find the metric, as per Eq. (5.19), to obtain that

$$metric \sim Gm \int \frac{d^3q}{(2\pi)^3} \frac{1}{\mathbf{q}^2} \left[1 - b\alpha \frac{\mathbf{q}}{m^2} \frac{m^2}{q^2} - \frac{\mathbf{q}^2}{m^2} \ln(q^2) - c\alpha \frac{\mathbf{q}^2}{m^2} + \cdots \right]. \tag{5.22}$$

Solving the 3-dim integrals results in

$$metric \sim GM \left[\frac{1}{r} + \frac{a\alpha}{mr^2} + \frac{b\alpha h}{m^2 r^3} + \frac{c\alpha}{m^2} \delta^3(x) + \cdots \right]. \tag{5.23}$$

Thus, we see that the logarithmic terms correspond to terms proportional to $\hbar$, thus showing themselves to be quantum contributions. As in Ref. [74], the numerical factors of order 1 have been ignored for this discussion. The proof of the methods employed lies in the fact that the non-analytic terms proportional to $\sqrt{1 \,/\, -q^2}$ accurately reproduce the classical results from GR. In addition, we obtain quantum corrections that naturally vanish in the limit of $\hbar \to 0$ to give us the results from classical GR. However, it is interesting to see how quantum effects compare with these long-range effects. To this end, the power counting is as follows

$$\frac{G\alpha}{r^2} \to \frac{G^2 m^2}{r^2}, \tag{5.24}$$

$$\frac{G\alpha\hbar}{mr^3} \to \frac{G^2 m\hbar}{r^3}. \tag{5.25}$$

Thus, as per Ref. [74], we can conclude that in the limit that $Gm^2 < \alpha$, charge-related effects due to QED dominate any effects due to quantum gravity. It should be noted that

if we had massless neutrinos, as in the SM, the weak interaction could contribute to long-distance effects. However, neutrino oscillations and the very probable case that neutrinos are indeed massive, eliminate this worry. In addition, as per Ref. [74], these effects would still be very small when compared to photonic effects. The major source of interest in this is that Feynman diagram calculations are able to reproduce classical effects within gravity. As per Ref. [74], we see that this procedure is independent of the absolute structure of the particle involved, and thus does not involve the quantum physics of black holes. It is purely a long-range effect, and replacing the electron with a proton, that does have a deeper structure, results in a further Taylor series in the form factors involving analytic terms due to the mass of the proton.

Chapter 6

Metric Corrections for Schwarzschild and Kerr Black holes

6.1 Full Feynman Computation

6.1.1 Outline of Procedure

The Schwarzschild and Kerr metrics respectively describe the curvature of spacetime around black holes without and with spin, respectively. These metrics were found as classical solutions to the Einstein field equations under the assumptions of zero charge and no contribution from the cosmological constant λ that often appears in the field equations. The following are the classical solutions for the Schwarzschild metric in harmonic gauge:

$$g_{00} = 1 - \frac{2GM}{r} + \dots \tag{6.1}$$

$$g_{0i} = 0 \tag{6.2}$$

$$g_{ij} = -\delta_{ij}\left(1 + \frac{2GM}{r}\right) + \dots \tag{6.3}$$

The related expression for Kerr BHs is:

$$g_{00} = 1 - \frac{2GM}{r} + \dots \tag{6.4}$$

$$g_{0i} = \frac{2G}{r^2}(\vec{S} \times \vec{r}) + \dots \tag{6.5}$$

$$g_{ij} = -\delta_{ij}\left(1 + \frac{2GM}{r}\right) + \dots \tag{6.6}$$

Firstly, we should note that the g_{00} and g_{ij} terms are identical in the above. Since the only difference between these two types appears in the off-diagonal terms, one can conclude that the effect of spin appears exclusively in these off-diagonal terms.

In QED, results are often expressed in terms of form factors that appear as coefficients when one makes a general Lorentz expansion on a specified quantity (in the case of gravity, $T_{\mu\nu}$). This was seen in Section 5.6. These form factors are functions of the momenta and usually are restricted by conditions based on momentum limits. These terms cannot appear from effective Lagrangians, and hence form a special class of corrections. The results for the case of pure gravity will also be expressed in terms of form factors with a different power counting and which are independent of the QED coupling α. The general approach is as follows:

The full loop computation to obtain corrections to the metrics of Schwarzschild and Kerr BHs is explained here. As mentioned, we considered the BHs at lowest order to be point

particles interacting with the energy momentum tensor $\langle p_2|T^{\mu\nu}|p_1\rangle$. This particular result will be expressed in terms of form factors which will then be used to reproduce the metric.

In terms of the field $h_{\mu\nu}$, one can rewrite the Einstein equations in harmonic gauge as

$$\Box h_{\mu\nu} = -16\pi G\left(T_{\mu\nu}(x) - \frac{1}{2}\eta_{\mu\nu}T(x)\right), \tag{6.7}$$

where $T = \eta^{\mu\nu}T_{\mu\nu}$. This can then be rewritten using the Green's function as

$$h_{\mu\nu}(x) = -16\pi G\int \frac{d^3q}{(2\pi)^3}e^{i\mathbf{q}\cdot\mathbf{r}}\frac{1}{\mathbf{q}^2}\left(T_{\mu\nu}(q) - \frac{1}{2}\eta_{\mu\nu}T(q)\right). \tag{6.8}$$

The above equation exemplifies why we looked at the Fourier transformations of the non-analytic terms under consideration in Eq. (5.19) and Eq. (5.20). The results obtained for the energy-momentum tensor, when Fourier transformed, are directly connected to corrections to the metric. Thus, our aim here is to find the energy momentum tensor in momentum space. Essentially, we look at the various Lorentz structures that the matrix elements of the energy-momentum tensor allow. We consider two large masses described by momenta p_1 and p_2 respectively, where $q = p_1 - p_2$ and $P = 1/2(p_1 + p_2)$. In the scalar case, we have the following transition amplitude describing the interactions of these masses with the EM tensor:

$$\langle p_2|T_{\mu\nu}|p_1\rangle = \frac{e^{-iqx}}{\sqrt{4E_1E_2}}\left[2P_\mu P_\nu F_1(q^2) + (q_\mu q_\nu - g_{\mu\nu}q^2)F_2(q^2)\right]. \tag{6.9}$$

We also have the normalisation condition

$$\langle p_2|p_1\rangle = 2E_1(2\pi)^3\delta^3(\mathbf{p_2} - \mathbf{p_1}). \tag{6.10}$$

In the fermion case, we have some additional structures that are allowed, which describe spin and thus are related to the gamma matrices, and further the Pauli matrices.

$$\begin{aligned}\langle p_2|T_{\mu\nu}|p_1\rangle = \overline{u}(p_2)\Bigg[&\frac{1}{m}P_\mu P_\nu F_1(q^2) - \left(\frac{i}{4m}\sigma_{\mu\lambda}q^\lambda P_\nu + \frac{i}{4m}\sigma_{\nu\lambda}q^\lambda P_\mu\right)F_2(q^2)\\ &+(q_\mu q_\nu - g_{\mu\nu}q^2)F_3(q^2)\Bigg]\,u(p_1).\end{aligned} \tag{6.11}$$

Here, we have

$$\sigma^{\mu\nu} = \frac{i}{2}[\gamma^\mu, \gamma^\nu]. \tag{6.12}$$

In the calculation that follows, the Gordon identity is employed in simplification.

$$\bar{u}(p_2)\gamma^\mu u(p_1) = \bar{u}(p_2)\left[\frac{(p_1+p_2)^\mu}{2m} + i\sigma^{\mu\nu}\frac{(p_2-p_1)_\nu}{2m}\right]. \tag{6.13}$$

We can see that F1 and F2 in the scalar case correspond to F1 and F3 in the fermion case up to factors of 2, while F2 completely contains the spin component.

In essence, we are looking to calculate the form factors that describe the energy momentum tensor associated with this metric.

This calculation will be specifically undertaken at the one-loop level. In principle, there are several subtleties to such a calculation. For one, there are a large number of diagrams at

one loop. However, we will focus on one of two diagrams that produce the non-analytical terms of interest. In addition, we have to examine divergences and renormalisability. A full study of the relevant diagrams, including vacuum polarisation, is presented in Ref. [75]. Here, we simply focus on making a comparison of methods used to study classical corrections to the metric.

Thus, a full example of an independent calculation of the form factors that come from the only relevant diagram that produces classical (as well as quantum) corrections is undertaken. Using the procedure described, this leads us back to results for corrections to the metric that are higher order in the gravitational constant.

A different approach follows, where the calculation is undertaken using a Feynman rule approach, and however replaces matter-graviton vertices with simplified versions. This results in simplifications in the three-graviton vertex which leads to a smaller expression for the full Feynman integral associated with this process. Then, instead of calculating these integrals in dimensional regularisation,, it's possible to use the residue theorem to obtain three-dimensional integrals that can then be associated with a tree-level process involving two heavy sources and their interaction with gravity.

In general, improvements on the standard approach have two major motivations. One of these will be evident from the tediousness of such a calculation in gravity when compared to equivalent processes in QCD and other theories. The complicated form of the 3-graviton vertex, given the spin-2 nature of the graviton, as well as the formalism demanding that larger multiplicity graviton vertices be present, motivates us to find simpler solutions to the problem. The final results make clear that large parts of the expressions for the Feynman amplitude do not in fact contribute to the fairly succinct result ultimately obtained. Another motivation is to find connections between classical quantities and their quantum counterparts. Within this formalism, Kerr black holes are interpreted as spin-1/2 quantum particles. Thus, simplified approaches using the classical limit of the theory can perhaps shine light on the connection between spin, a deeply quantum quantity, and its classical counterpart– the angular momentum. In general, there is motivation in understanding the deeper structure of gravity and why the results appearing from calculations appear as they are. To this end, the amplitudes approach is hoping to highlight new patterns within gravitational theory.

In Ref. [76], results were obtained for such source terms for the scalar metric, where the scalar-graviton vertex simply reduces to $-i\kappa m^2 \delta^0_\mu \delta^0_\nu$, which results in the correct form factors. However, an independent analysis of these calculations found errors, and with only partially accurate results. Current work is aimed at producing an analogous calculation for the case of fermionic sources. This involves on one hand showing that we can consistently produce the spin-independent form factors F1 and F3, but also produce a spin term that correctly gives us the classical angular momentum of a Kerr black hole.

The approach undertaken is to firstly produce the full loop computation as done in Ref. [75] and then to try to make a term-by-term comparison in order to obtain the source term. The full calculation has been produced to complete accuracy using a program called `FORM`. In addition, a reproduction of the calculation in Ref. [76] was made both by hand, as well as using `Mathematica`.

6.1.2 Results

To begin with, the full loop computation using the complete Feynman rules was reproduced, and a comparison made with [75]. A list of the Feynman rules can be found in Appendix A, and the full derivations of these can be found in [82]. The full three-graviton vertex is split into five parts, denoted by square brackets, as in Ref. [75]. The fifth part does not contribute non-analytic terms, so is neglected. The computation was done twice, once using the identity

$$\mathcal{P}^{\alpha\beta}_{\rho\sigma}\tau^{\mu\nu}_{\alpha\beta,\gamma\delta}\mathcal{P}^{\gamma\delta}_{\lambda\xi} = \tau^{\mu\nu}_{\rho\sigma,\lambda\xi}, \tag{6.14}$$

and once without. Note that although both the quantum and the classical corrections were reproduced, here we only show the results for the classical terms, and ignore the log terms. The classical corrections are reproduced from just one diagram, 6.1.

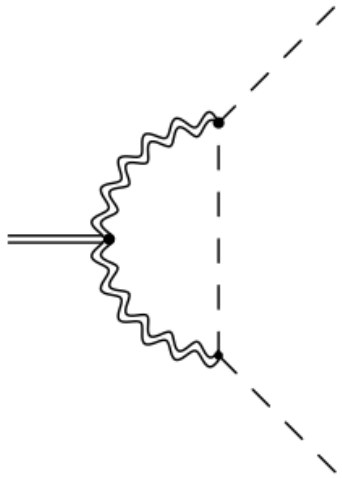

Figure 6.1: The only one-loop diagram for classical corrections

The entire computation was done in the Breit frame, described by

$$\begin{aligned} p_1 &= (E, \vec{q}/2) \\ p_2 &= (E, -\vec{q}/2) \\ q &= (0, \vec{q}) \\ q &= p_1 - p_2. \end{aligned}$$

Integrals from Ref. [79] were verified and used. The procedure here follows that of Ref. [75]. We begin with Feynman rules and restrict our case to the single diagram that has both

classic and quantum corrections The initial expression for the Feynman rules is

$$\mathcal{M}^{\mu\nu} = \int \frac{d^4k}{(2\pi)^4} \tau_6^{\lambda\xi}(p_1, k+p_2)\tau_6^{\rho\sigma}(k+p_2, p_2)\tau_3(k,q)^{\mu\nu}_{\alpha\beta,\gamma\delta} \tag{6.15}$$

$$\times \frac{i\mathcal{P}^{\alpha\beta}_{\rho\sigma}}{k^2+i\varepsilon} \frac{i\mathcal{P}^{\gamma\delta}_{\lambda\xi}}{(k-q)^2+i\varepsilon} \frac{i}{(k+p_2)^2-m^2.+i\varepsilon}. \tag{6.16}$$

The above expression is fully expanded out; the relevant relations between momenta from Eq. (6.15) were used. The form factors were projected out and leading results for them were obtained. The full code for these calculations is available in Appendix B. The integrals from Ref. [79] are expressions from dimensional regularisation which are the given in the form of the non-analytic functions of interest and ignores other terms. The results were obtained for each term within square brackets in the three-graviton vertex for gravity. Note that the fifth term within square brackets which is proportionate to $k + (k-q)^2$ does not contribute to the result so we only look at the first four terms. The results obtained are given in the following tables.

6.1.3 Scalar Case

		Line 1	Line 2	Line 3	Line 4	Total
Paper	F1	1/16	−1	1	0	1/16
	F2	7/8	−1	2	−1	7/8
Using id	F1	1/16	0	−1	1	1/16
	F2	7/8	0	0	0	7/8
Not using id	F1	1/16	−1	1	0	1/16
	F2	7/8	−1	2	−1	7/8

6.1.4 Fermion Case

		Line 1	Line 2	Line 3	Line 4	Total
Paper	F1	1/16	−1	1	0	1/16
	F2	0	0	−1/2	3/4	1/4
	F3	7/16	0	0	0	7/16
Using id	F1	1/16	0	−1	1	1/16
	F2	0	0	−1/2	3/4	1/4
	F3	7/16	0	0	0	7/16
Not using id	F1	1/16	−1	1	0	1/16
	F2	0	−1/2	1/2	1/4	1/4
	F3	7/16	−1/2	1	−1/2	7/8

Although the original results were derived both by hand as well as with `Mathematica`, these results were reproduced using a different program, `FORM`. Coefficients for the form factors were obtained and were seen to be coherent with the results in Ref. [75]. Ultimately, the final results are consistent. However, we see that the usage of the identity changes intermediate results, for the different terms within the 3-graviton vertex. It leads to a shuffling of terms within the 3-graviton vertex, though it does not affect the final result. This leads us to believe that a large part of the 3-graviton vertex is ultimately inconsequential to the results obtained.

As we can see above, the total results for F1 and F2 in the scalar case, and F1, F2, and F3 in the fermion case are identical to the paper, both when the identity is used and also when it isn't. Additionally, the spin component associated with the fermion case is completely described by F2. Thus, we expect that F1 and F2 in the scalar case should match F1 and F3 in the fermion case, which turns out to be true. There's factors of two that differ between the results, this is expected if one looks at the definitions in 6.9 and 6.11

Additionally, we can make a comparison with each line of the three graviton vertex. Clearly, in the scalar case, the results from the paper match exactly with the case where the identity has not been used. However, in the fermion case, we can see that F1 was calculated without making use of the identity, while F2 and F3 match the case where the identity was used.

As a final consistency check, we can see that F1 and F2 in the scalar case match F1 and F3 in the fermion case in a line-by-line comparison in both cases, where the identity has and has not been used. Thus, we can say confidently that these results are fully accurate.

6.2 Approaches Based on the Residue Theorem

In this section, we will look into an alternate approach to the previous calculation. There were two diagrams that contributed to non-analytic corrections to the black hole metrics. However, in this case we will look into a simplified approach to exclusively obtain the results for the classical corrections. Of the two diagrams, one resulted in both log as well as square root terms, however the second only created quantum corrections. Thus, in this section, the focus will only be on the diagram that was considered:

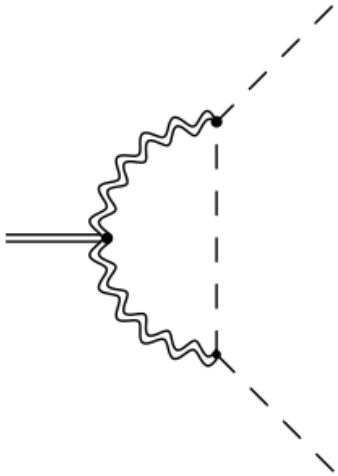

Figure 6.2: One-loop triangle integral which contributes to classical corrections to the metric

The aim of this project is to simplify the previous calculation and interpret the connections between the quantum calculation and the classical results that were ultimately obtained. We will consider a parallel example within scalar QED to elucidate the method being used here. This will then be extended to gravity. The previous calculation showed us that using Feynman rules for gravity can be very cumbersome. The vertex containing three gravitons has a very complicated form, that nevertheless leads us to fairly simple results. Thus, one can make the fair assumption that most of the components within this vertex do not contribute to the final result. This cannot be made very evident using numerical computations, so analytical methods will be employed to simplify the vertex rules in order to reproduce the classical terms. This section is based on Ref. [76]. Note that Ref. [76] uses scalar results and also goes further to extend the approach to higher loop orders. Here we will consider NLO scalar results and possible extensions to higher spin forms.

6.2.1 Outline of Procedure

We will now consider the example of scalar QED. As mentioned in Sec. 5.6, quantum approaches can be used to obtain both classical as well as quantum corrections to theories with massless mediators. The scalar QED Lagrangian is defined as

$$\mathcal{L} - (D^\mu \varphi)^\dagger (D_\mu \varphi) - m^2 \varphi^\dagger \varphi - \frac{1}{4} F^{\mu\nu} F_{\mu\nu}. \tag{6.17}$$

Here, $F_{\mu\nu}$ is the usual field strength tensor given by $F_{\mu\nu} = \partial_\mu A_\nu - \partial_\nu A_\mu$, and the interaction terms occur through the covariant derivative defined as

$$D_\mu \equiv \partial_\mu + ieA_\mu. \tag{6.18}$$

One way to calculate the matrix element we are interested in, namely $\langle p_2 | T^{\mu\nu} | p_1 \rangle$, would be to look at the explicit field content. $T^{\mu\nu}$ corresponds to the conserved current associated with the Poincare symmetry under translation

$$T^{\mu\nu} = \frac{\delta \mathcal{L}}{\delta(\partial_\mu \varphi_a)} \delta^\nu \varphi_a - \eta^{\mu\nu} \mathcal{L}. \tag{6.19}$$

Unfortunately, this approach is cumbersome and not so easy to generalise. The form we obtain for $T^{\mu\nu}$ from the above prescription need not be gauge invariant or symmetric in its indices and would need to be suitably modified by adding derivative terms that preserve other conserved charges. However, once we have such a form, it is possible to write out the wave expansions for the fields involved. Then, with appropriate normalisations for the commutation relations for a and $a^\dagger$, as well as for $\langle p_2 | p_1 \rangle$, we can find the required solution. Note that for regular QED with fermions, we would need to have anticommutation relations instead. Eq. (6.19) can be explicitly calculated for the Lagrangian we have and is found to be

$$T^{\mu\nu} = (D^\mu \varphi)^\dagger \partial^\nu \varphi + (D^\mu \varphi) \partial^\nu \varphi^\dagger - \eta^{\mu\nu} (D^\rho \varphi)^\dagger (D_\rho \varphi) \tag{6.20}$$

$$+ \frac{1}{4} \eta^{\mu\nu} F^{\rho\sigma} F_{\rho\sigma} - F^{\mu\rho} \partial^\nu A_\rho + \eta^{\mu\nu} (m^2 \varphi^\dagger \varphi). \tag{6.21}$$

The above can be symmetrised and simplified using the fact that $\partial_\mu T^{\mu\nu} = 0$, since this is a conserved quantity. However, the essence behind the procedure at one loop is to replace the loop diagram with one containing classical source terms. This would involve simplifying the vertices as follows. A similar calculation is given in Ref. [76] for the conserved current based on the $U(1)$ symmetry of the diagram

$$\varphi(x) \to e^{i\alpha}\varphi(x). \tag{6.22}$$

Using Noether's theorem, the conserved current associated with this symmetry is

$$j^\mu = \frac{\partial \mathcal{L}}{\partial(\partial_\mu \varphi_a)}\Delta\varphi_a = i\left(\varphi\partial^\mu\varphi^\dagger - \varphi^\dagger\partial^\mu\varphi\right) + 2eA^\mu\varphi^\dagger\varphi. \tag{6.23}$$

This is explicitly calculated in the classical limit and the result obtained for the transition amplitude involving this conserved current is:

$$\langle p_2|j_\mu|p_1\rangle \sim 2\pi\delta^\mu_0. \tag{6.24}$$

Now, we look at the one-loop corrections to $\langle p_2|T^{\mu\nu}|p_1\rangle$. To begin with, we have a Feynman integral similar to that in Eq. (6.16):

$$\begin{aligned} D(p_1,p_2) = 2\int \frac{d^4k}{(2\pi)^4}\left[\frac{-ig^{\rho\delta}}{(k-p_1)^2+i\varepsilon}\right]\left[\frac{-ig^{\sigma\lambda}}{(k-p_2)^2+i\varepsilon}\right]\left[\frac{i}{k^2-m^2+i\varepsilon}\right] \\ \times\left[-ie(p_1+k)_\delta\right]\left[-ie(k+p_2)_\lambda\right]V(k-p_1,k-p_2)^{\mu\nu}_{\rho\sigma}. \end{aligned} \tag{6.25}$$

Here, we have two photon propagators and one scalar propagator. We also have three interaction vertices, where two of them involve two scalars interacting with a photon, and we have a third vertex involving multiple photons. The photon vertex can be read off a symmetric version of Eq. (6.21) which looks like

$$T^{\mu\nu}_{sym} = (D^\mu\varphi)^\dagger D^\nu\varphi + (D^\mu\varphi)D^\nu\varphi^\dagger - \eta^{\mu\nu}(D^\rho\varphi)^\dagger D_\rho\varphi \tag{6.26}$$

It looks as follows

$$\begin{aligned} V(k-p_1,k-p_2)^{\mu\nu}_{\rho\sigma} = -\frac{1}{2}\Big(&\eta^{\mu\nu}\left[\eta_{\rho\sigma}(k-p_1)\cdot(k-p_2) - (k-p_1)_\sigma\cdot(k-p_2)_\rho\right] \\ &- \eta_{\rho\sigma}\left[(k-p_1)^\mu(k-p_2)^\nu + (k-p_1)^\nu(k-p_2)^\mu\right] \\ &+ \left[(k-p_1)^\mu(k-p_2)_\rho\eta^\nu{}_\sigma + (k-p_2)^\mu(k-p_1)_\sigma\eta^\nu{}_\rho\right] \\ &+ \left[(k-p_1)_\sigma(k-p_2)^\nu\eta^\mu_\rho + (k-p_2)_\rho(k-p_1)^\nu\eta^\mu_\sigma\right] \\ &-(k-p_1)\cdot(k-p_2)(\eta^\mu_\rho\eta^\nu_\sigma + \eta^\mu_\sigma\eta^\nu_\rho)\Big). \end{aligned} \tag{6.27}$$

The idea behind this approach is that the above gets simplified by making use of the fact that $\partial_\mu T^{\mu\nu} = 0$, we can use that $k_1^\rho V(k_1,k_2)^{\mu\nu}_{\rho\sigma} = 0$ and similarly $k_2^\rho V(k_1,k_2)^{\mu\nu}_{\rho\sigma} = 0$. This results in a simplified version where we have, as per Ref. [76], that

$$V^{\mu\nu}_{00}(\mathbf{k}+\frac{\mathbf{q}}{2},\mathbf{k}-\frac{\mathbf{q}}{2}) = -\frac{1}{2}\left(2\delta^\mu_0\delta^\nu_0 - \eta^{\mu\nu}\right)\left(\mathbf{k}^2 - \frac{\mathbf{q}^2}{4} + \delta^\mu_i\delta^\nu_j\left(k^ik^j - \frac{1}{4}q^iq^j\right)\right). \tag{6.28}$$

This allows to represent $\langle p_2|T^{\mu\nu}|p_1\rangle$in terms of a three-dimensional integral

$$\langle T^{\mu\nu}\rangle = e^2\left(3\delta_0^\mu\delta_0^\nu q^2 + \left(q^\mu q^\nu - \eta^{\mu\nu}q^2\right)\right)\frac{1}{8}\int\frac{d^3k}{(2\pi)^3}\frac{1}{(\mathbf{k}+\frac{\mathbf{q}}{2})^2(\mathbf{k}-\frac{\mathbf{q}}{2})^2} \tag{6.29}$$

Note that these results are again applicable in the Breit frame that we were using. Following this, Feynman parameters can be employed in order to simplify the above integral. In general, the classical limit of the triangle integral under consideration is looked at. Thus, we are looking at the limit where $q/m \to 0$ for the integral

$$I = \int\frac{d^4k}{(2\pi)^4}\frac{1}{[((k-p_1)^2+i\varepsilon)((k-p_2)^2+i\varepsilon)(k^2-m^2+i\varepsilon)]}. \tag{6.30}$$

We will use the residue theorem to find the behaviour of the above integral. The details follow in the explicit calculation in the case of gravity. However, we are able to obtain that

$$I \simeq \frac{i}{4m}\int\frac{d^3k}{(2\pi)^3}\frac{1}{(\mathbf{k}+\frac{\mathbf{q}}{2})^2(\mathbf{k}-\frac{\mathbf{q}}{2})^2}. \tag{6.31}$$

This leads us to conclude that the one-loop diagram can be replaced with a tree-level diagram where gravity interacts with classical sources. Thus, we can replace the loop diagram with

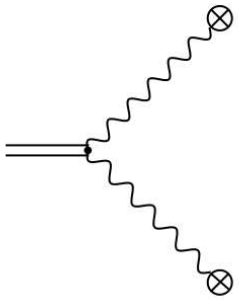

Figure 6.3: Replacement Feynman diagram- classical sources vs. loops

6.2.2 Results

The previous procedure is now generalised to gravity. Explicit calculations of the full Feynman integral were previously shown, now we look at using the methods illustrated to simplify the three-graviton vertex and use residue theorem in order to reproduce the corrections to the Schwarzschild and Kerr metrics for black holes. An analytic computation of Ref. [76] was made using `Mathematica`. To begin with, the complete matrix elements we are calculating for the triangle graph are, as in the loop calculation:

$$\mathcal{M}^{\mu\nu} = \int\frac{d^4k}{(2\pi)^4}\tau_6^{\lambda\xi}(p_1,k+p_2)\tau_6^{\rho\sigma}(k+p_2,p_2)\tau_3(k,q)^{\mu\nu}_{\alpha\beta,\gamma\delta} \tag{6.32}$$

$$\times\frac{i\mathcal{P}^{\alpha\beta}_{\rho\sigma}}{k^2+i\varepsilon}\frac{i\mathcal{P}^{\gamma\delta}_{\lambda\xi}}{(k-q)^2+i\varepsilon}\frac{i}{(k+p_2)^2-m^2+i\varepsilon}. \tag{6.33}$$

Firstly, the above is simplified using the usual identity

$$\mathcal{P}^{\alpha\beta}_{\rho\sigma}\tau^{\mu\nu}_{\alpha\beta,\gamma\delta}\mathcal{P}^{\gamma\delta}_{\lambda\xi} = \tau^{\mu\nu}_{\rho\sigma,\lambda\xi}. \tag{6.34}$$

Further, as per Ref. [76], we only consider an approximation on 2-scalar 1-graviton vertices τ_6^{00}, and the $\tau^{\mu\nu}_{00,00}$ components of the 3-graviton vertex. This yields the following simplifications

$$\tau_6^{00}(p_1, k+p_2) = \tau_6^{00}(k+p_2, p_2) \quad \approx i\kappa m^2, \tag{6.35}$$

$$\tau^{\mu\nu}_{00,00}(k,q) \quad \approx \frac{-i\kappa}{2}\left(\frac{1}{2}k^\mu k^\nu + (k-q)^\mu(k-q)^\nu + q^\mu q^\nu - \frac{3}{2}\eta^{\mu\nu}q^2\right). \tag{6.36}$$

It is reiterated that given that we are only interested in the classical limit of computations in the context of replacing loop diagrams with classical sources, we confine our attention to the single diagram that produces classical corrections to GR. Although there are several diagrams, there were three that contributed non-analytic corrections. Two of these were however, fully quantum. within this formalism, the numerators we are working with are hugely simplified. In addition, we work only in the region of the integral where the integrated momentum $k \ll m$ and so we can make a simplification as in Ref. [77] that

$$(k+p_2)^2 - m^2 \approx k^2 + 2k\cdot p_1 \approx 2mk_0. \tag{6.37}$$

which leads to a simplification on the denominator. Thus, the hugely simplified expression we are working with is

$$\mathcal{M}^{\mu\nu} = -\frac{\kappa^3 m^4}{4}\int \frac{d^4k}{(2\pi)^4}\frac{\left(k^\mu k^\nu + (k-q)^\mu(k-q)^\nu + q^\mu q^\nu - \frac{3}{2}\eta^{\mu\nu}q^2\right)}{[2mk_0 + i\varepsilon][k^2+i\varepsilon][(k-q)^2+i\varepsilon]}. \tag{6.38}$$

Since we are planning to do a contour integral over k_0 in order to solve the above, it becomes convenient to also express the denominator in terms of k_0.

$$\mathcal{M}^{\mu\nu} = -\frac{\kappa^3 m^4}{4}\int \frac{d^4k}{(2\pi)^4}\frac{\left(k^\mu k^\nu + (k-q)^\mu(k-q)^\nu + q^\mu q^\nu - \frac{3}{2}\eta^{\mu\nu}q^2\right)}{[2mk_0 + i\varepsilon][k_0^2 - \vec{k}^2 + i\varepsilon][k_0^2 - \vec{k}^2 - \vec{q}^2 + 2\vec{k}\cdot\vec{q} + i\varepsilon]}. \tag{6.39}$$

In order to use the residue theorem, we also require the poles of the above denominators. We consider all poles lying on the lower half of the complex plane and thus obtain

$$k_{0a} = -\frac{i\varepsilon}{2m}, \tag{6.40}$$

$$k_{0b} = +\sqrt{\vec{k}^2 - i\varepsilon}, \tag{6.41}$$

$$k_{0c} = +\sqrt{\vec{k}^2 + \vec{q}^2 - 2\vec{k}\cdot\vec{q} - i\varepsilon}. \tag{6.42}$$

Now, we look at the individual components of the above expression, which we can later relate to the matrix elements using the structure of the latter (Eq. 6.9 and Eq. 6.11). Now, when looking at these various components, we can make certain simplifications based on

the fact that we are working in the Breit frame (6.15). This includes that $q_0 = 0$ and $q^2 = -\vec{q}^2$. Putting these in, we have for the (0,0) component:

$$\mathcal{M}^{00} = -\frac{\kappa^3 m^4}{4} \int \frac{d^4k}{(2\pi)^4} \frac{2k_0^2 + \frac{3}{2}\vec{q}^2}{[2mk_0 + i\varepsilon][k_0^2 - \vec{k}^2 + i\varepsilon][k_0^2 - \vec{k}^2 - \vec{q}^2 + \vec{k}\cdot\vec{q} + i\varepsilon]}. \tag{6.43}$$

Applying the residue theorem on the above expression is fairly straightforward, and results in the following three-dimensional integral

$$-\frac{3}{16} i\pi\kappa^3 m^3 \int \frac{d^3\vec{k}}{(2\pi)^3} \frac{\vec{q}^2}{(\vec{k}^2)(\vec{k} - \vec{q}^2)}. \tag{6.44}$$

We do not expect the $(0, i)$ components to contribute, since they are related to the spin component. The numerator turns out to be odd in k_0 and k^i and thus, we can neglect this case. However, for $\mathcal{M}^{ij}$, following an identical procedure, we get the following expression

$$\mathcal{M}^{ij} = -\frac{\kappa^3 m^4}{4} \int \frac{d^4k}{(2\pi)^4} \frac{k^i k^j + (k-q)^i (k-q)^j + q^i q^j - \frac{3}{2}\vec{q}^2}{[2mk_0 + i\varepsilon][k_0^2 - \vec{k}^2 + i\varepsilon][k_0^2 - \vec{k}^2 - \vec{q}^2 + \vec{k}\cdot\vec{q} + i\varepsilon]}. \tag{6.45}$$

And applying the residue theorem gives us the result

$$\mathcal{M}^{ij} = -\frac{1}{16} i\pi\kappa^3 m^3 \int \frac{d^3\vec{k}}{(2\pi)^3} \frac{\vec{q}^2}{(\vec{k}^2)(\vec{k} - \vec{q})^2}. \tag{6.46}$$

Now, in order to solve the above three dimensional integrals, we follow the usual procedure of dimensional regularisation to convert the above to Feynman integrals. The above are fairly simple since we only have two denominators. We simplify the denominator by completing the square as follows:

$$k^2(k-q)^2 \to (1-x)k^2 + x(k-q)^2, \tag{6.47}$$

where x is our Feynman parameter. Completing the square in k, we get that the denominator becomes

$$(k - xq)^2 + q^2 x(1-x). \tag{6.48}$$

Thus, wherever a factor of k in the numerator appears, we need to transform it as $k \to k + xq$ and we obtain that $\Delta = q^2 x(x-1)$ to get the following Feynman integrals:

$$\mathcal{M}^{00} = -\frac{3}{16} i\pi\kappa^3 m^3 \int_0^1 dx \int \frac{d^3\vec{k}}{(2\pi)^3} \frac{\vec{q}^2}{\vec{k}^2 - \Delta}, \tag{6.49}$$

$$\mathcal{M}^{ij} = -\frac{1}{16} i\pi\kappa^3 m^3 \int_0^1 dx \int \frac{d^3\vec{k}}{(2\pi)^3} \frac{4k^i k^j + 4(1 - x + x^2) q^i q^j - 3\vec{q}^2}{\vec{k}^2 - \Delta}. \tag{6.50}$$

Note that for the $\mathcal{M}^{ij}$ case, since dimensional regularisation produces spherically symmetric integrals, we eliminated odd integrals with only a single power of k in the numerator. We can clearly see that there is some trouble in the second result since the coefficients of the $q^i q^j$ and δ^{ij} terms should be identical in order to obtain a reasonable form factor. The three-dimensional integrals were calculated slightly differently where the denominators

were simplified as in Ref. [76] and identical results were obtained. Thus, the issue lies somewhere in the initial expression for the matrix elements or the calculation of the residues. In particular, the residue calculation for $\mathcal{M}^{ij}$ produces a term $-3\vec{q}^2$ which could be a possible source of trouble. The issue does not seem to be that we made the approximation in the integral parameter $k \ll m$ in a different manner than as seen in Ref. [76].

We will make note of some of the errors present in the calculation in Ref. [76]. Firstly, in the full loop computation, the terms in the three-graviton vertex that are proportional to k^2 and $(k-q)^2$ that appear in the fifth square bracket of the full expression, are neglected. These are known not to produce any non-analytic contributions due to their cancellations with denominators. Ref. [76] does not do this and this leads to an accidental correct result in the case of $\mathcal{M}^{00}$. One can see where the three-dimensional integrals are evaluated that in the $\mathcal{M}^{00}$ case a numerator is present of the form $-3/2\vec{k}^2 + 3/8\vec{q}^2$, that when evaluated coincidentally produce two factors of $3/8\vec{q}^2$ in the numerator. The term $3/2\vec{k}^2$ appears due to the contribution from the three graviton vertex. This seems to be compensated for by the missing prefactor in the three-graviton vertex itself of $-i\kappa/2$. The simplified versions of the 3-graviton vertex contain spurious terms due to the contributions from the fifth square bracket. Particularly troublesome is the expression for τ^{ij} in Ref. [76], where it is unclear how the factor of $7/8$ is obtained proportional to $\eta^{ij}\vec{q}^2$. This leads to the desired results in for $\mathcal{M}^{ij}$. However, in the calculation detailed above, we can clearly see that the result is not symmetric as expected.

We can note that an identical result for M^{00} was obtained and a slightly different result for M^{ij}, which comes with an overall prefactor of $7/256$. This will be investigated further by looking at [77].

This entire calculation is interesting because it provides a general understanding of the underlying physics of calculations in gravity. Replacing loop diagrams with simplified vertex functions which translate to classical source terms offer a good interpretation of the theory behind these gravitational calculations. The procedures we have seen have been able to produce both quantum as well as classical corrections to gravity using a quantum formulation. Thus, it is very relevant to look at what this really means; this result looks at a comparison between classical and quantum physics. There is a lot of interesting physics to be understood when one goes to higher spins. As we know, spin is a very fundamental quantity within quantum physics, with no direct interpretation in classical physics. However, within this formalism, we are looking at spin in connection with the angular momentum of black holes. Therefore, the hope is that one can understand this connection at a deeper level. By extending the procedure to spin-1/2 particles, we will be looking at classical source terms that represent the angular momentum of Kerr black holes but also function as the quantum compatriot of this, representing spin. Thus, this work needs to be developed further to find this simplification of the classical source term for non-zero angular momentum black holes. In addition, we note that we used a particular limit of the integral where $k \ll m$. A full analysis using the method of regions needs to be done to examine the validity of this hypothesis. Ultimately, we hope to find a method that is able to reduce complex loop diagrams to simple loop diagrams involving classical source terms. The knowledge that results from this will be extremely valuable to understanding the physics behind gravity.

6.3 Gravity from Scattering Amplitudes

Scattering amplitudes represent a new method to calculate physical variables in any arbitrary QFT. It has heavily been inspired by methods of calculation in String Theory. String theory is traditionally based not on Feynman-rule calculations, but on looking at physical quantities such as amplitudes based on the principle of generalised unitarity. These methods combine an effort to have symmetries and simple formulae being explicitly manifest, as well as being practical and useful to current calculations in particle physics. These methods can be conveniently extended to theories like QCD. The basis of such methods is to divide a QCD amplitude into a colour and kinematic part.

$$\mathcal{A}_n^{tree}(k_i, \lambda_i, a_i) = g^{(n-2)} \sum_{\sigma \epsilon S_n / Z_n} Tr\left(T^{a_{\sigma(1)}} \dots T^{a_{\sigma(n)}} \right) A_n^{tree}(\sigma(1^{\lambda_1}), \dots, \sigma(n^{\lambda_n})). \tag{6.51}$$

We are considering an n-particle amplitude, which is a function of the momenta, helicities, and colour factors of the particles involved. The first part of the right-hand-side consists of traces of Gell-Mann matrices, which describes the colour of the gluons. These terms generally are of other forms involving the colour factors f^{abc} which are reduced to the above form. On the other hand, the momenta are fully separated from the colour part of the amplitude and thus, we consider from here on, a colour-stripped amplitude. The above formula has been thoroughly reviewed in Refs. [83,84]. However, the essence of the above equation, and modern scattering amplitudes in general, is to choose what variables are used to describe the kinematic part. In this case, the kinematic part is described in terms of Lorentz-invariant Weyl spinor products

$$\langle i \ j \rangle \equiv \varepsilon^{\alpha\beta}(\lambda)_\alpha(\lambda_j)_\beta \tag{6.52}$$

$$[i \ j] = \varepsilon^{\dot{\alpha}\dot{\beta}}, \tag{6.53}$$

where, we use the above products to describe two-dimensional versions of Dirac spinors in terms of these Lorentz-contracted forms. A major development in the field of scattering amplitudes was the Parke- Taylor formula, which is essentially a formula that allows us to calculate without calculating. At tree level, we're able to determine the kinematic part of a massless, tree-level, n-gluon amplitude in a particular configuration of the helicities, i.e., the projection of spin onto the momentum. In this case, we look at the configuration that maximally violates the helicity, also known as the MHV amplitude. The Parke-Taylor formula for a massless, tree-level, MHV, n-gluon amplitude looks as:

$$A(1^-, 2^-, 3^+, \cdots, n^+) = i \frac{\langle 12 \rangle^4}{\langle 12 \rangle \langle 23 \rangle \cdots \langle n1 \rangle}. \tag{6.54}$$

The Parke-Taylor formula [85] was expressed in the above more readable form by Mangano, Parke and Xu [86]. This was a very revolutionary development in the field of QCD. However, we should make note that the above expression only applies to tree-level diagrams. In addition, it applies to massless particles with specific helicities. A reason why it was considered impractical is that at the LHC one requires a calculation for all helicities and also at higher orders in perturbation theory, to compete with the high precision data available. Historically, recursive approaches were considered to deal with this, due to the relative

simplicity of numerically programming such approaches. E.g., the QCD β-functions were calculated using such methods, and it turned out that for certain helicity configurations, there were extremely simple formulae that could describe the amplitudes [87]. In this context, Britto, Cachazo, Feng, and Witten came up with the BCFW relations in 2005 [88]. Essentially, one is considering the fact that the residue theorem can be used by examining the infinities of an amplitude and this can be employed to reconstruct the full physical amplitude on the basis of Cauchy's Residue theorem. The basis of this method is using the on-shell properties of particles and equivalently saying that when a propagator diverges, the amplitude can be reconstructed based on the structure of these divergences. Essentially, one can express an n-loop amplitude in terms of $(m < n)$-loop amplitudes using on-shell cuts and recursive properties. This further deals with the general issue of having to deal with difficult integrals in QCD computations.
Two major advantages of using an amplitudes-based approach are as follows:

- Amplitudes are looking at physical quantities. Thus, one can avoid gauge-dependent intermediate results and look directly at physical, gauge-invariant quantities.
- The Feynman-rule-based approach is often very complicated due to the presence of complex loop integrals as well as the final step of integrating over final states. Amplitudes are inherently better suited to calculating higher-multiplicity processes.

To those working on gravity this field is particularly interesting due to a fundamental connection that was found by Kawai, Lewellen, and Tye in 1985 [89]. QCD is mediated by a spin-1 particle, the gluon. On the other hand, gravity is mediated by a spin-2 particle, the graviton. The KLT relations, named after the aforementioned authors, show that gravity in fact is a square of gauge theory.

$$\mathcal{M}_4^{tree}(1,2,3,4) = -is_{12}\mathcal{A}_4^{tree}(1,2,3,4)\mathcal{A}_4^{tree}(1,2,4,3) \tag{6.55}$$

$$\begin{aligned}\mathcal{M}_5^{tree}(1,2,3,4,5) = &-is_{12}s_{34}\mathcal{A}_5^{tree}(1,2,3,4,5)\mathcal{A}_5^{tree}(2,1,4,3,5)\\ &+is_{13}s_{24}\mathcal{A}_5^{tree}(1,3,2,4,5)\mathcal{A}_5^{tree}(3,1,4,2,5).\end{aligned} \tag{6.56}$$

Eqs.(6.56) show some limited examples of what was stated. We clearly see that amplitudes within gravity are connected to a product of amplitudes in QCD. The combination of the Parke-Taylor formula, the BCFW relations, and the KLT formula means that we can use amplitude based methods to compute formulae in gravity at higher-loop orders based on recursive relations. We should also note that such connections were also found between $N = 4$-SYM theories and $N = 8$-Supergravity. In addition, there have been further developments in this field, most notably, the BCJ relations, named after Bern, Carrasco, and Johansson from 2008 [90]. Here, relations between colour-stripped amplitudes were made based on the idea that the sum of the Mandelstam variables $s + t + u = 0$, analogous to a Jacobi identity. This was generalised to higher loop order and connected to the KLT relations. A full review of the historical progress in this field can be found in Ref. [91].
Amplitude-based approaches have gradually become more common as a go-to approach for practical calculations. To exemplify this, a slide from Ref. [91] is reproduced in Fig. 6.4, where we see that a majority of the current state-of-the-art results in QCD have been computed using automated unitarity-based methods, rather than traditional Feynman-rule-based methods. This has clearly lead to accelerated progress in precision calculations.

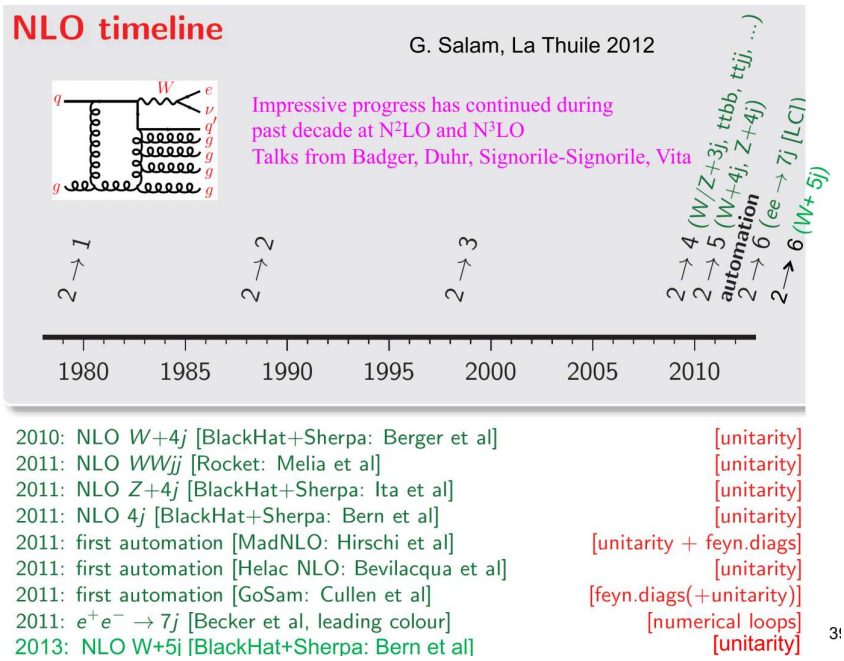

Figure 6.4: Source: Zvi Bern, Amplitudes 2021 slides

Ultimately, we are able to choose between a three-gluon-vertex and a three-graviton-vertex. The latter is very long as compared to the former. The KLT relations make amplitudes and gravity computable, especially numerically. This is what we can look forward to in the future!

Chapter 7

Conclusion

In this thesis, we consider some of the most important aspects and applications of effective field theories. Scale separation, encapsulated in the Appelquist-Carrazone theorem, is the key idea that allows us to examine different ranges of energies independent of each other. This is the main reason that EFTs are a universal tool to understand any physical theory. After obtaining a brief understanding of the ideas and properties of EFTs, we went on to look at two big fields in EFTs today- the EFT of the Standard Model as well as some of the different effective approaches to gravity. The existence of highly precise and advanced experiments, mainly the Large Hadron Collider at CERN and the LIGO experiment, have made necessary that we have increasingly precise predictions of particle physics and gravitational waves. The main motivation of using EFTs in these theoretical studies was elucidated. All the particles in the Standard Model of particle physics have been discovered, but there are several reasons to believe that it is incomplete and New Physics lies beyond it. The large amount of statistics at the LHC contrasted with the difficulty of building colliders with a higher centre-of-mass energy has meant that EFTs are well suited to finding traces of New Physics. This can be done in the most general way possible while making only minimal restrictions on the potential UV theory. On the other hand, the LIGO collaboration has given us the opportunity to probe the regime of strong gravity in the form of binary mergers of massive bodies such as black holes and neutron stars. This is the next step to improving our understanding of General Relativity and testing a full theory of gravity. It is slowly expanding to more countries around the world, which will lead to more precise data collection. Thus, we are at the stage where simpler analytic and numeric methods are not only essential but indispensable to the future of high-energy physics.
Due to these motivations, we looked deeper into some applications of EFTs.

A short overview of the Standard Model Effective Field Theory allowed us to see that not only is it a very general theory, suited to studying almost all collider processes but also that there are challenges that stem from having such a general and multifunctional theory. Furthermore, although effective approaches to gauge theories were a part of the early explorations into quantum field theories, SMEFT was neglected for many years. Now, parallel to SM studies, deeper investigations into the fundamental properties of SMEFT are being made, such as understanding the RGE evolution of the SMEFT Wilson coefficients and looking to match these coefficients universally to obtain limits on their values. A major goal of SMEFT studies is to be able to numerically calculate higher order processes in this theory. In this context, novel advancements were made in which the Euler-Lagrange equations of motion for the SMEFT at dimension six were calculated and added as corrections to the well-known Standard Model equations of motion. An example of how these results are relevant to calculating B-meson decays, a process potentially in conflict with current theoretical predictions in the SM, was explained. Thus, sub-leading corrections due to the

subtleties of an EFT were discussed, which are relevant to any future high-precision study. The conclusion was that the power counting of EFTs means that there is a class of corrections due to EOM effects that result in a basis dependence in the results.
On the other hand, we looked at a few of the modern effective approaches to gravity. In attempting to make theoretical predictions of binary black hole mergers, one must consider different regimes, and some of these are particularly suited to analytic calculations. These analytic calculations apply to certain limits of the scales of the problem. Current results in the main two types of approximations– the post-Newtonian and post-Minkowskian approximations– were shown. One example of an EFT approach to gravity was considered, where we systematically used the steps that go into constructing an EFT and derived Feynman rules to show how one can obtain important quantities, such as a limit of the spacetime metric of gravity. A full NLO computation of a particular class of both quantum and classical corrections was reproduced independently. However, due to the limitations of using Feynman diagram approaches, an alternative method was discussed using Cauchy's residue theorem. Finally, we discussed the progressions in scattering amplitude methods as a modern alternative that is gaining traction as potentially being able to greatly simplify numerical computations.
The last few years have shown significant developments in both the fields of particle physics and gravity that are based on effective field theory approaches. As we gradually obtain more statistics in the incredible experiments we have at CERN and the LIGO collaboration, there is great reason to be optimistic that we will find results that succeed two of the most important theories of our time- the Standard Model of particle physics and General Relativity.

Chapter 8

Outlook

Effective field theory approaches have been seen for both their generality to different applications in particle physics, as well as gravity. In both these contexts, we have seen that EFTs offer a general, minimal explanation for the unknown. At this stage, the hope is to have more automated programs to calculate scattering amplitudes in these theories, in order to compete with the experimental data available today and in the coming years. In the case of SM, unitarity-based approaches provide some of the most precise calculations available today. We hope to extend these to SMEFT and gravitational EFTs.
When considering SMEFT, we already have candidate programs for NLO calculations, however, it is an aim to reach a similar level of precision as that of the SM. Perhaps, amplitude-based methods, when applied to SMEFT, will offer a simplified manner of doing such calculations. This can be a simple extension of existing programs for the SM, but is of course complicated by operator-mixing in the SMEFT. There is a lot of hope that future studies will bridge this gap so that automated programs for the SM can be generalised to theories such as SMEFT and HEFT, so that data from the LHC and LEP can be maximised to find any potential deviation from the SM. In addition, one of the major goals of this programme is to consider universal matching coefficients of all the operators within the Warsaw basis. Non-zero results for Wilson coefficients are indicative of New Physics.
Amplitude and particle-physics-based calculations in gravity have seen a lot of growth in the last few years. However, it is clear that a standard Feynman-rule based approach is sub-optimal for gravity, given the complexity of the vertex functions, and the fact that these vertex functions get more complicated as we go to higher order in EFTs. The KLT and BCJ theorems offer an opportunity to do calculations in gravity parallel to those in QCD, by making use of the relations. In addition, developments that are able to use the KLT relations in a recursive manner offer a lot of insight and optimism into the future of particle-physics-based calculations in gravity.
Amplitudes offer a different perspective– we consider structure and symmetry and examine patterns to arrive at results. However, this field is in its infancy, with a lot of its applications being in planar and massless theories. Parallel approaches to make integrations within amplitudes easier as well as extending these theories to further applications, is a step towards finding a complete theory of gravity, and perhaps finding a theory to unite quantum physics and gravity. It must be stated that such calculations have their primary application in finding precise predictions within particle physics. On the flipside, gravity is a good crossover between quantum and classical theory. There is a lot of optimism towards better understanding both quantum theories, as we well as gravity, using studies in quantum effects within gravity.

Effective-field-theory-based approaches are indispensable to the future of high-energy physics and the following years augur significant developments in theoretical predictions

and a step into a new and unknown paradigm within high-energy physics.

Appendix A

Feynman Rules for GR EFT

The general definition of a vertex rule in momentum space is

$$\mathcal{V}_{\mu_1\nu_1\ldots\mu_m\nu_m} = +i\int d^4x d^4x_1\cdots d^4x_n d^4y_1\cdots d^4y_m \exp[i(p_1x_1+\cdots+p_nx_n+q_1y_1\cdots+q_my_m)]$$
$$\times\frac{\delta}{\delta\varphi_1(x_1)}\times\cdots\times\frac{\delta}{\delta\varphi_n(x_n)}\times\frac{\delta}{\delta\mathcal{H}_1^{\mu_1\nu_1}(y_1)}\times\cdots\times\frac{\delta}{\delta\mathcal{H}_m^{\mu_m\nu_m}(y_m)}\mathcal{L}_{int}(\varphi_1,\cdots,\varphi_n,\mathcal{H}_1,\cdots,\mathcal{H}_m)(x).$$

Here, we start with the interaction Lagrangian in position space and take functional derivatives over it with all the source fields $\varphi_1,\cdots,\varphi_n$ and the associated positions $x_1,\cdots,x_n$; and graviton fields $\mathcal{H}_1^{\mu_1\nu_1},\cdots,\mathcal{H}_m^{\mu_m\nu_m}$ and the corresponding positions $y_1,\cdots,y_m$. Finally, we perform a Fourier transformation to replace an expression that is in terms of the positions x and y to momenta $p_1,\cdots,p_n$ for the source fields, and $q_1,\cdots,q_n$ for the graviton fields. Note that the incoming momenta are denoted with a positive sign, and consequently the outgoing ones are with a negative sign. The final expression will contain two Lorentz indices for every graviton field in the interaction Lagrangian, and one per spin-1 vector field. Note that to complete the expression, we would need to have a delta function containing all the momenta p and q associated with the vertex.

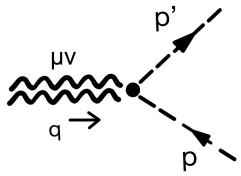

Figure A.1: Graviton-scalar interaction

We derived the following matter-graviton interacting Lagrangian at $\mathcal{O}(\kappa)$ in Eq. (5.15),

$$\mathcal{L}_m^{(1)} = -\frac{\kappa}{2}h^{\mu\nu}(x)\left[\partial_\mu\varphi(x)\partial_\nu\varphi(x)-\frac{1}{2}\eta_{\mu\nu}\left\{\partial_\alpha\varphi(x)\partial^\alpha\varphi(x)-m^2\varphi(x)^2\right\}\right]. \tag{A.1}$$

We simply need to insert it into Eq. (**??**) to obtain the expression we are looking for. Since we have two scalar fields and one graviton field, the expression will have two Lorentz indices

associated with it, as follows:

$$\tau_{\mu\nu} = -\frac{i\kappa}{2}\int d^4x d^4x_1 d^4x_2 d^4y\ \exp(i(p_1x_1 - p_2x_2 + qy)) \tag{A.2}$$

$$\times \frac{\delta}{\delta\varphi(x_1)}\frac{\delta}{\delta\varphi(x_2)}\frac{\delta}{\varphi\mathcal{H}^{\mu\nu}(y)}h^{\alpha\beta}(x)\left[\partial_\alpha\varphi(x)\partial_\beta\varphi(x) - \frac{1}{2}\eta_{\alpha\beta}\left\{\partial_\rho\varphi(x)\partial^\rho\varphi(x) - m^2\varphi(x)^2\right\}\right] \tag{A.3}$$

Working out the functional derivatives yields the following

$$= -\frac{i\kappa}{2}\int d^4x d^4x_1 d^4x_2 d^4y\ \exp(i(p_1x_1 - p_2x_2 + qy))\delta(x-y)\left[\partial_\mu\delta(x-x_2)\partial_\nu\delta(x-x_1)\right. \tag{A.4}$$

$$\left.+\partial_\mu\delta(x-x_1)\partial_\nu\delta(x-x_2) - \eta_{\mu\nu}\left\{\partial_\rho\delta(x-x_1)\partial^\rho\delta(x-x_2) - m^2\delta(x-x_1)\delta(x-x_2)\right\}\right].$$

In order to deal with the δ-functions, we expand them as Fourier functions. E.g.,

$$\partial_\mu\delta(x-x_1) \to \delta_\mu\int\frac{d^4k_1}{(2\pi)^4}e^{ik_1(x-x_1)} \to \int\frac{d^4k_1}{(2\pi)^4}ik_{1\mu}e^{ik_1(x-x_1)}. \tag{A.5}$$

Since every term contained δ-functions in both x_1 as well as x_2, we can pull out the associated exponentials, yielding

$$\tau_{\mu\nu} = -\frac{i\kappa}{2}\int d^4x d^4x_1 d^4x_2 d^4y\frac{d^4k_1}{(2\pi)^4}\frac{d^4k_2}{(2\pi)^4}\exp[i((p_1-k_1)x_1 - (p_2+k_2)x_2 + (k_1+k_2+q)y)]$$

$$[-k_{1\mu}k_{2\nu} - k_{1\nu}k_{2\mu} - \eta_{\mu\nu}\{k_1\cdot k_2 - m^2\}]. \tag{A.6}$$

Integrating over x_1 and x_2 simply gives us more delta functions:

$$= -\frac{i\kappa}{2}\int d^4x\frac{d^4k_1}{(2\pi)^4}\frac{d^4k_2}{(2\pi)^4}\delta(k_1-p_1)\delta(k_2+p_2)\exp(i(p_1-p_2+q)x)[-k_{1\mu}k_{2\nu} - k_{1\nu}k_{2\mu}.$$

$$= +\frac{i\kappa}{2}\int d^4x\exp(i(p_1-p_2+q)x)[p_{1\mu}p_{2\nu} + p_{1\nu}p_{2\mu}$$

$$-\eta_{\mu\nu}(p_1\cdot p_2 - m^2)]$$

$$= \frac{i\kappa}{2}[p_{1\mu}p_{2\nu} + p_{1\nu}p_{2\mu} - \eta_{\mu\nu}(p_1\cdot p_2 - m^2)]\delta(p_1-p_2+q). \tag{A.7}$$

In the final step, we simply pulled out a δ-function describing the conservation of momentum, which we will leave out of the expression for the vertex rule henceforth.

In a similar manner, matter Lagrangians for all kinds of gravitational interactions can be derived and we simply list several Feynman rules, as per Ref. [82].

2-scalar-1-photon vertex

Scalar QED has interactions between vector bosons and scalars, and the following results have been expressly derived in Ref. [20]:

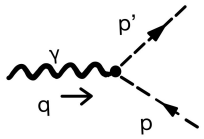

$$= \tau_1^{\gamma}(p, p', e)$$

where:

$$\tau_1^{\gamma}(p, p', e) = -ie\left(p + p'\right)^{\gamma}. \tag{A.8}$$

2-scalar-1-photon-1-graviton vertex

For the 2-scalar-1-photon-1-graviton vertex we have derived:

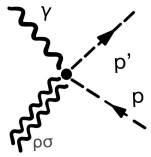

$$= \tau_5^{\rho\sigma(\gamma)}(p, p', e)$$

where:

$$\tau_5^{\rho\sigma(\gamma)}(p, p', e) = ie\kappa\left[\mathcal{P}^{\rho\sigma\alpha\gamma}(p + p')_{\alpha}\right], \tag{A.9}$$

and $\mathcal{P}^{\rho\sigma\alpha\gamma}$ is defined as usual.

2-photon-1-graviton vertex

For the 2-photon-1-graviton vertex we have derived:

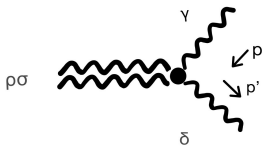

$$= \tau_3^{\rho\sigma(\gamma\delta)}(p, p')$$

where:

$$\begin{aligned}\tau_3^{\rho\sigma(\gamma\delta)}(p, p') = i\kappa\Big[&\mathcal{P}^{\rho\sigma(\gamma\delta)}(p \cdot p') + \frac{1}{2}\Big(\eta^{\rho\sigma}p^{\delta}p'^{\gamma} + \eta^{\gamma\delta}(p^{\rho}p'^{\sigma} + p^{\sigma}p'^{\rho}) \\ &- (p'^{\gamma}p^{\sigma}\eta^{\rho\delta} + p'^{\gamma}p^{\rho}\eta^{\sigma\delta} + p'^{\rho}p^{\delta}\eta^{\sigma\gamma} + p'^{\sigma}p^{\delta}\eta^{\rho\gamma})\Big)\Big].\end{aligned} \tag{A.10}$$

The following results are shown from Ref. [79], and they were explicitly derived in Ref. [82].

2-scalar-2-photon vertex

The following results are available and fully derived in Ref. [20]

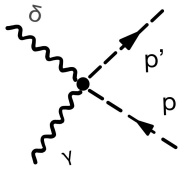

$$= \tau_4^{\gamma\delta}(p, p', e)$$

where:

$$\tau_4^{\gamma\delta}(p, p', e) = 2ie^2\eta^{\gamma\delta}. \tag{A.11}$$

2-scalar-1-graviton vertex

This Feynman rule has been systematically derived and we reproduce our expression from Eq. (A.7) here:

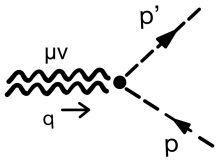

$$= \tau_6^{\mu\nu}(p, p', m)$$

where:

$$\tau_6^{\mu\nu}(p, p', m) = -\frac{i\kappa}{2}\left[p^\mu p'^\nu + p^\nu p'^\mu - \eta^{\mu\nu}\left((p\cdot p') - m^2\right)\right]. \tag{A.12}$$

2-scalar-2-graviton vertex

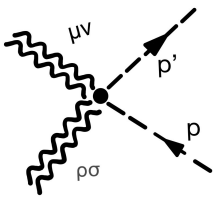

$$= \tau_8^{\eta\lambda\rho\sigma}(p, p', m)$$

where:

$$\begin{aligned}\tau_8^{\eta\lambda\rho\sigma}(p, p') = i\kappa^2\Bigg[&\left\{I^{\eta\lambda\alpha\delta}I^{\rho\sigma\beta}_{\ \ \ \delta} - \frac{1}{4}\left\{\eta^{\eta\lambda}I^{\rho\sigma\alpha\beta} + \eta^{\rho\sigma}I^{\eta\lambda\alpha\beta}\right\}\right\}\left(p_\alpha p'_\beta + p'_\alpha p_\beta\right)\\ &- \frac{1}{2}\left\{I^{\eta\lambda\rho\sigma} - \frac{1}{2}\eta^{\eta\lambda}\eta^{\rho\sigma}\right\}\left[(p\cdot p') - m^2\right]\Bigg].\end{aligned} \tag{A.13}$$

2-fermion-1-graviton vertex

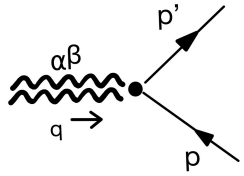

$$= \tau_7^{\alpha\beta}(p, p', m)$$

where:

$$\tau_7^{\alpha\beta}(p, p', m) = \frac{-i\kappa}{2}\left[\frac{1}{4}(\gamma^\alpha(p+p')^\beta + \gamma^\beta(p+p')^\alpha) - \frac{1}{2}\eta^{\alpha\beta}(\frac{1}{2}(\not{p}+\not{p}') - m)\right]. \quad \text{(A.14)}$$

2-fermion-2-graviton vertex

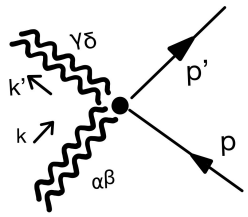

$$= \tau_9^{\alpha\beta,\gamma\delta}(p, p', m)$$

where:

$$\begin{aligned}\tau_9^{\alpha\beta,\gamma\delta}(p, p', m) = i\kappa^2 \Big\{ &-\frac{1}{2}(\frac{1}{2}(\not{p}+\not{p}') - m)\mathcal{P}^{\alpha\beta,\gamma\delta} - \frac{1}{16}[\eta^{\alpha\beta}(\gamma^\gamma(p+p')^\delta + \gamma^\delta(p+p')^\gamma) \\ &+ \eta^{\gamma\delta}(\gamma^\alpha(p+p')^\beta + \gamma^\beta(p+p')^\alpha)] + \frac{3}{16}(p+p')_\epsilon\gamma^\xi(I^{\xi\phi,\alpha\beta}I_\phi{}^{\epsilon,\gamma\delta} + I^{\xi\phi,\gamma\delta}I_\phi{}^{\epsilon,\alpha\beta}) \\ &+ \frac{i}{16}\epsilon^{\rho\sigma\eta\lambda}\gamma_\lambda\gamma_5(I^{\alpha\beta}{}_{,\eta\nu}I^{\gamma\delta}{}_{,\sigma\nu}k'_\rho - I^{\gamma\delta}{}_{,\eta\nu}I^{\alpha\beta}{}_{,\sigma\nu}k_\rho)\Big\}.\end{aligned}$$

3-graviton vertex

The three-graviton vertex is complex and we have made extensive use of it in our calculations. The following describes its form

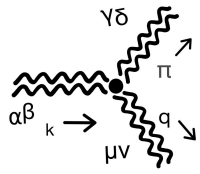

$$= \tau_{10}{}^{\mu\nu}_{\alpha\beta\gamma\delta}(k, q)$$

where:

$$\begin{aligned}
\tau_{10}{}^{\mu\nu}_{\alpha\beta\gamma\delta}(k,q) = -\frac{i\kappa}{2} \times \Bigg(& \mathcal{P}_{\alpha\beta\gamma\delta}\Big[k^\mu k^\nu + (k-q)^\mu (k-q)^\nu + q^\mu q^\nu - \frac{3}{2}\eta^{\mu\nu} q^2\Big] \\
& + 2q_\lambda q_\sigma \Big[I_{\alpha\beta}{}^{\sigma\lambda} I_{\gamma\delta}{}^{\mu\nu} + I_{\gamma\delta}{}^{\sigma\lambda} I_{\alpha\beta}{}^{\mu\nu} - I_{\alpha\beta}{}^{\mu\sigma} I_{\gamma\delta}{}^{\nu\lambda} - I_{\gamma\delta}{}^{\mu\sigma} I_{\alpha\beta}{}^{\nu\lambda} \Big] \\
& + \Big[q_\lambda q^\mu \Big(\eta_{\alpha\beta} I_{\gamma\delta}{}^{\nu\lambda} + \eta_{\gamma\delta} I_{\alpha\beta}{}^{\nu\lambda} \Big) + q_\lambda q^\nu \Big(\eta_{\alpha\beta} I_{\gamma\delta}{}^{\mu\lambda} + \eta_{\gamma\delta} I_{\alpha\beta}{}^{\mu\lambda} \Big) \\
& - q^2 \Big(\eta_{\alpha\beta} I_{\gamma\delta}{}^{\mu\nu} + \eta_{\gamma\delta} I_{\alpha\beta}{}^{\mu\nu} \Big) - \eta^{\mu\nu} q_\sigma q_\lambda \Big(\eta_{\alpha\beta} I_{\gamma\delta}{}^{\sigma\lambda} + \eta_{\gamma\delta} I_{\alpha\beta}{}^{\sigma\lambda} \Big) \Big] \\
& + \Big[2q_\lambda \big(I_{\alpha\beta}{}^{\lambda\sigma} I_{\gamma\delta\sigma}{}^{\nu} (k-q)^\mu + I_{\alpha\beta}{}^{\lambda\sigma} I_{\gamma\delta\sigma}{}^{\mu} (k-q)^\nu - I_{\gamma\delta}{}^{\lambda\sigma} I_{\alpha\beta\sigma}{}^{\nu} k^\mu - I_{\gamma\delta}{}^{\lambda\sigma} I_{\alpha\beta\sigma}{}^{\mu} k^\nu \big) \\
& + q^2 \Big(I_{\alpha\beta\sigma}{}^{\mu} I_{\gamma\delta}{}^{\nu\sigma} + I_{\alpha\beta}{}^{\nu\sigma} I_{\gamma\delta\sigma}{}^{\mu} \Big) + \eta^{\mu\nu} q_\sigma q_\lambda \Big(I_{\alpha\beta}{}^{\lambda\rho} I_{\gamma\delta\rho}{}^{\sigma} + I_{\gamma\delta}{}^{\lambda\rho} I_{\alpha\beta\rho}{}^{\sigma} \Big) \Big] \\
& + \Big\{ (k^2 + (k-q)^2) \big[I_{\alpha\beta}{}^{\mu\sigma} I_{\gamma\delta\sigma}{}^{\nu} + I_{\gamma\delta}{}^{\mu\sigma} I_{\alpha\beta\sigma}{}^{\nu} - \frac{1}{2}\eta^{\mu\nu} \mathcal{P}_{\alpha\beta\gamma\delta} \big] \\
& - \Big(I_{\gamma\delta}{}^{\mu\nu} \eta_{\alpha\beta} k^2 + I_{\alpha\beta}{}^{\mu\nu} \eta_{\gamma\delta} (k-q)^2 \Big) \Big\} \Bigg).
\end{aligned} \tag{A.15}$$

It must be noted that the above derivations are not simple and in the fermion case require that the vierbein formalism is employed. We make use of the master equation in order to obtain the above. Note that any vertices that do not include gravitons are derived in Ref. [20]. Once again, the full derivations are available in Ref. [82].

Appendix B

FORM Codes for Full Loop Computation

I wrote four similar codes in FORM: two each for the scalar and fermion case, and further one each where the identity [] is used and is not used. Here they are reproduced in full:

B.0.1 Scalar Case without Identity

```
Off Statistics;

\textit{*Declare variables}
Symbol kap,m,TAG,pi,A1,A2,G;
dimension 4;
Vector p1, p2, q1, q2, q,l, l1,l2,k,l3,l4,Q;
index mu,nu,alpha,beta,gamma,delta,rho,xsi,lam,sig,kappa,eta,zeta;
CFunction L, S,I,P;
*NTensor;
Tensor T7,K;

#message This is the initial expression.
*Expression
local scalar1 = i_*P(alpha,beta,lam,kappa)*i_*P(gamma,delta,rho,sig)*i_*T7(alpha,beta,p1,l1)*T7(ga
P(rho,sig,lam,kappa)*(l3(mu)*l3(nu)+l4(mu)*l4(nu)+q(mu)*q(nu)-3/2*d_(mu,nu)*q.q);
local scalar2 = i_*P(alpha,beta,lam,kappa)*i_*P(gamma,delta,rho,sig)*i_*T7(alpha,beta,p1,l1)*T7(ga
2*q(xsi)*q(eta)*(I(rho,sig,eta,xsi)*I(lam,kappa,mu,nu)+I(lam,kappa,eta,xsi)*I(rho,sig,mu,nu) - I(
local scalar3 = i_*P(alpha,beta,lam,kappa)*i_*P(gamma,delta,rho,sig)*i_*T7(alpha,beta,p1,l1)*T7(ga
(q(xsi)*q(mu)*(d_(rho,sig)*I(lam,kappa,nu,xsi)+d_(lam,kappa)*I(rho,sig,nu,xsi))+q(xsi)*q(nu)*(d_(
local scalar4 = i_*P(alpha,beta,lam,kappa)*i_*P(gamma,delta,rho,sig)*i_*T7(alpha,beta,p1,l1)*T7(ga
(2*q(xsi)*(I(rho,sig,xsi,eta)*I(lam,kappa,eta,nu)*l4(mu)+I(rho,sig,xsi,eta)*I(lam,kappa,eta,mu)*l
-I(lam,kappa,xsi,eta)*I(rho,sig,eta,nu)*l3(mu)-I(lam,kappa,xsi,eta)*I(rho,sig,eta,mu)*l3(nu))
+q.q*(I(rho,sig,xsi,mu)*I(lam,kappa,nu,xsi)+I(rho,sig,xsi,nu)*I(lam,kappa,xsi,mu))+d_(mu,nu)*q(xs
local scalar5 = i_*P(alpha,beta,lam,kappa)*i_*P(gamma,delta,rho,sig)*i_*T7(alpha,beta,p1,l1)*T7(ga
((l1.l1 + l2.l2)*(I(eta,mu,rho,sig)*I(lam,kappa,eta,nu)+I(eta,nu,rho,sig)*I(lam,kappa,eta,mu)-1/2

.sort;
print;

sum alpha,beta,gamma,delta;
```

```
#message The functions P and I are expanded, so only mu, nu, alpha->delta indices remain
id P(alpha?,beta?,gamma?,delta?)=1/2*(d_(alpha,gamma)*d_(beta,delta)+d_(alpha,delta)*d_
id I(alpha?,beta?,gamma?,delta?) = 1/2*(d_(alpha,gamma)*d_(beta,delta)+d_(alpha,delta)*d
.sort;
print;

*Expand out all functions and express everything in terms of p1 and p2
id T7(mu?,nu?,p1?,p2?)=-i_*kap/2*(p1(mu)*p2(nu)+p1(nu)*p2(mu)-d_(mu,nu)*(p1.p2-m^2));
id l3 =l;
id l4 = l-q;
*id l3 = l+q/2;
*id l4 = l-q/2;
id q = p2 - p1;
id l1 = p2 -l;
*id l1=1/2*p1 + 1/2*p2-l;
id p1.p1 = m^2;
id p2.p2=m^2;
.sort;
sum alpha,beta,gamma,delta;
*Express everything in terms of q and P
id p1 = 1/2*(2*Q-q);
id p2=1/2*(2*Q+q);
id q.Q=0;
.sort;
#message summing over all indices other than mu and nu:
print;
.sort;
*id K(mu?)= i_/(32*pi^2*m^2)*(p2(mu)*((1+q.q/(2*m^2))*L+1/4*(q.q/m^2)*S)+q(mu)*(-L-S/2))
#message These are the integrals in the problem
*Express everything in terms of tensors of the integration variable
toTensor l,K;
Multiply TAG;
id TAG*K(?args)=K(?args);
Bracket l,K;
.sort;
print;
.sort;

*Integral simplifications
*id K(q)=q.q/2*TAG;
*id q(mu?)*K(mu?,nu?)=q.q/2*K(nu);
*id q(mu?)*K(mu?,nu?,alpha?)=q.q/2*K(nu,alpha);

\textit{*Integral Solutions}
id K(mu?,nu?,alpha?,beta?)=0;
.sort;
```

```
id K(mu?,nu?,alpha?)=i_/(32*pi^2*m^2)*(p2(mu)*p2(nu)*p2(alpha)*(1/6*q.q/m^2*L)+(p2(mu)*p2(nu)*
q(alpha)+p2(mu)*p2(alpha)*q(nu)+p2(nu)*p2(alpha)*q(mu))*(-1/3*q.q/m^2*L-q.q/(16*m^2)*S)+
(q(mu)*q(nu)*p2(alpha)+q(mu)*q(alpha)*p2(nu)+q(nu)*q(alpha)*p2(mu))*(1/3*L)+
q(mu)*q(nu)*q(alpha)*(-L-5/16*S)+(d_(mu,nu)*p2(alpha)+d_(mu,alpha)*p2(nu)+d_(nu,alpha)*p2(mu))*
(-q.q/12*L)+(d_(mu,nu)*q(alpha)+d_(mu,alpha)*q(nu)+d_(nu,alpha)*q(mu))*(q.q/6*L+q.q/16*S));
.sort;
id K(mu?,nu?)=i_/(32*pi^2*m^2)*(p2(mu)*p2(nu)*(-q.q/(2*m^2)*L-q.q/(8*m^2)*S)+(p2(mu)*q(nu)+
p2(nu)*q(mu))*(1/2*(1+q.q/m^2)*L+3/16*q.q/m^2*S)+q(mu)*q(nu)*(-L-3/8*S)+q.q*d_(mu,nu)*(L/4+S/8))
.sort;
id K(mu?)= i_/(32*pi^2*m^2)*(p2(mu)*((1+q.q/(2*m^2))*L+1/4*(q.q/m^2)*S)+q(mu)*(-L-S/2));
.sort;
id TAG = i_/(32*pi^2*m^2)*(-L-S);
Bracket L,S;
.sort;
#message Solved integrals, independent of k
print;
.sort;

*id p2.q = q.q/2;
id p2 = 1/2*(2*Q+q);
id q.Q=0;
.sort;
Bracket L,S;
print;
.sort;

id Q = 1/2*(p2+p1);
id q = p2-p1;
id p1.p1 = m^2;
id p2.p2 = m^2;
.sort;

id p1 = 1/2*(2*Q-q);
id p2=1/2*(2*Q+q);
id q.Q=0;
id Q.Q=m^2-q.q/4;
.sort;
Bracket L,S;
print;
.sort;

local test = 1/2/m*(2*Q(mu)*Q(nu)*A1 +(q(mu)*q(nu)-d_(mu,nu)*q.q)*A2);
local F11 = (3/4/Q.Q^2 *Q(mu)*Q(nu) - 1/(4*Q.Q)*d_(mu,nu) )*scalar1;
local F21 = (1/2/Q.Q/q.q *Q(mu)*Q(nu) - 1/(2*q.q)*d_(mu,nu) )*scalar1;
local F12 = (3/4/Q.Q^2 *Q(mu)*Q(nu) - 1/(4*Q.Q)*d_(mu,nu) )*scalar2;
local F22 = (1/2/Q.Q/q.q *Q(mu)*Q(nu) - 1/(2*q.q)*d_(mu,nu) )*scalar2;
```

```
local F13 = (3/4/Q.Q^2 *Q(mu)*Q(nu) - 1/(4*Q.Q)*d_(mu,nu) )*scalar3;
local F23 = (1/2/Q.Q/q.q *Q(mu)*Q(nu) - 1/(2*q.q)*d_(mu,nu) )*scalar3;
local F14 = (3/4/Q.Q^2 *Q(mu)*Q(nu) - 1/(4*Q.Q)*d_(mu,nu) )*scalar4;
local F24 = (1/2/Q.Q/q.q *Q(mu)*Q(nu) - 1/(2*q.q)*d_(mu,nu) )*scalar4;
local F15 = (3/4/Q.Q^2 *Q(mu)*Q(nu) - 1/(4*Q.Q)*d_(mu,nu) )*scalar5;
local F25 = (1/2/Q.Q/q.q *Q(mu)*Q(nu) - 1/(2*q.q)*d_(mu,nu) )*scalar5;

sum mu,nu;
Multiply 2*m;
id kap^3 = 32*pi*G;
id Q.Q=m^2-q.q/4;
id q.Q=0;
Bracket L,S;
print;
.sort;

local F1 = F11+F12+F13+F14;
local F2=F21+F22+F23+F24;
local fullscalar=scalar1+scalar2+scalar3+scalar4+scalar5;
local test2 = F21+F22+F23+F24+F25;
.sort;
Bracket L,S;
print;
.end;
```

The following final output was obtained

```
F11 =
    + L * ( 1/4*q.q*i_*m*pi^-1*G + 43/96*q.q^2*Q.Q^-1*i_*m*pi^-1*G - 11/24*
      q.q^2*i_*m^-1*pi^-1*G - 1/32*q.q^3*Q.Q^-1*i_*m^-1*pi^-1*G + 1/12*
      q.q^3*i_*m^-3*pi^-1*G - 5/64*q.q^4*Q.Q^-1*i_*m^-3*pi^-1*G )

    + S * ( 1/16*q.q*i_*m*pi^-1*G + 17/128*q.q^2*Q.Q^-1*i_*m*pi^-1*G - 3/32
      *q.q^2*i_*m^-1*pi^-1*G - 1/128*q.q^3*Q.Q^-1*i_*m^-1*pi^-1*G + 1/64*
      q.q^3*i_*m^-3*pi^-1*G - 3/128*q.q^4*Q.Q^-1*i_*m^-3*pi^-1*G );

F21 =
    + L * ( 13/3*i_*m^3*pi^-1*G - 37/48*q.q*i_*m*pi^-1*G - 13/24*q.q^2*i_*
      m^-1*pi^-1*G + 1/32*q.q^3*i_*m^-3*pi^-1*G )

    + S * ( 7/8*i_*m^3*pi^-1*G - 19/64*q.q*i_*m*pi^-1*G - 7/32*q.q^2*i_*
      m^-1*pi^-1*G + 3/128*q.q^3*i_*m^-3*pi^-1*G );

F12 =
    + L * (  - 2*q.q*i_*m*pi^-1*G - 1/8*q.q^2*i_*m^-1*pi^-1*G + 1/4*q.q^3*
      i_*m^-3*pi^-1*G )
```

```
    + S * (  - q.q*i_*m*piˆ-1*G - 1/8*q.qˆ2*i_*mˆ-1*piˆ-1*G + 3/32*q.qˆ3*i_
      *mˆ-3*piˆ-1*G );

F22 =
    + L * (  - i_*mˆ3*piˆ-1*G + 1/16*q.qˆ2*i_*mˆ-1*piˆ-1*G )

    + S * (  - i_*mˆ3*piˆ-1*G + 1/32*q.qˆ2*i_*mˆ-1*piˆ-1*G );

F13 =
    + L * ( q.q*i_*m*piˆ-1*G + 1/2*q.qˆ2*i_*mˆ-1*piˆ-1*G + 3/8*q.qˆ3*i_*
      mˆ-3*piˆ-1*G )

    + S * ( q.q*i_*m*piˆ-1*G + 1/4*q.qˆ2*i_*mˆ-1*piˆ-1*G + 5/32*q.qˆ3*i_*
      mˆ-3*piˆ-1*G );

F23 =
    + L * ( 1/4*q.qˆ2*i_*mˆ-1*piˆ-1*G + 1/16*q.qˆ3*i_*mˆ-3*piˆ-1*G )

    + S * ( 2*i_*mˆ3*piˆ-1*G + 1/8*q.qˆ2*i_*mˆ-1*piˆ-1*G + 1/64*q.qˆ3*i_*
      mˆ-3*piˆ-1*G );

F14 =
    + L * (  - q.qˆ2*i_*mˆ-1*piˆ-1*G + 1/3*q.qˆ3*i_*mˆ-3*piˆ-1*G )

    + S * (  - 13/32*q.qˆ2*i_*mˆ-1*piˆ-1*G + 3/64*q.qˆ3*i_*mˆ-3*piˆ-1*G );

F24 =
    + L * (  - i_*mˆ3*piˆ-1*G + 1/6*q.q*i_*m*piˆ-1*G + 1/12*q.qˆ2*i_*mˆ-1*
      piˆ-1*G - 1/8*q.qˆ3*i_*mˆ-3*piˆ-1*G )

    + S * (  - i_*mˆ3*piˆ-1*G + 1/16*q.q*i_*m*piˆ-1*G + 1/64*q.qˆ2*i_*mˆ-1*
      piˆ-1*G - 5/128*q.qˆ3*i_*mˆ-3*piˆ-1*G );

F15 =
    + L * ( 5/2*i_*mˆ3*piˆ-1*G - 1/16*q.q*Q.Qˆ-1*i_*mˆ3*piˆ-1*G - 1/2*q.q*
      i_*m*piˆ-1*G - 3/8*q.qˆ2*l2.l2*i_*mˆ-3*piˆ-1*G - 5/48*q.qˆ2*Q.Qˆ-1*i_
      *m*piˆ-1*G - 19/12*q.qˆ2*i_*mˆ-1*piˆ-1*G - 1/48*q.qˆ3*Q.Qˆ-1*i_*mˆ-1*
      piˆ-1*G + 3/16*l2.l2*Q.Qˆ-1*i_*mˆ3*piˆ-1*G + 3/2*l2.l2*i_*m*piˆ-1*G
       + 5/16*Q.Qˆ-1*i_*mˆ5*piˆ-1*G )

    + S * ( 1/2*i_*mˆ3*piˆ-1*G + 1/32*q.q*l2.l2*i_*mˆ-1*piˆ-1*G + 1/32*q.q*
      i_*m*piˆ-1*G - 5/32*q.qˆ2*l2.l2*i_*mˆ-3*piˆ-1*G - 9/256*q.qˆ2*Q.Qˆ-1*
      i_*m*piˆ-1*G - 31/64*q.qˆ2*i_*mˆ-1*piˆ-1*G + 1/512*q.qˆ3*l2.l2*Q.Qˆ-1
      *i_*mˆ-3*piˆ-1*G - 1/256*q.qˆ3*Q.Qˆ-1*i_*mˆ-1*piˆ-1*G + 1/16*l2.l2*
      Q.Qˆ-1*i_*mˆ3*piˆ-1*G + 1/2*l2.l2*i_*m*piˆ-1*G + 1/16*Q.Qˆ-1*i_*mˆ5*
```

```
        pi^-1*G );

   F25 =
       + L * (  - 19/24*i_*m^3*pi^-1*G + 9/8*q.q^-1*l2.l2*i_*m^3*pi^-1*G + 15/
          8*q.q^-1*i_*m^5*pi^-1*G - 1/4*q.q*l2.l2*i_*m^-1*pi^-1*G - 25/24*q.q*
          i_*m*pi^-1*G + 1/16*q.q^2*l2.l2*i_*m^-3*pi^-1*G + 1/4*q.q^2*i_*m^-1*
          pi^-1*G - 1/4*l2.l2*i_*m*pi^-1*G )

       + S * (  - 1/16*i_*m^3*pi^-1*G + 3/8*q.q^-1*l2.l2*i_*m^3*pi^-1*G + 3/8*
          q.q^-1*i_*m^5*pi^-1*G - 7/64*q.q*l2.l2*i_*m^-1*pi^-1*G - 45/128*q.q*
          i_*m*pi^-1*G + 7/256*q.q^2*l2.l2*i_*m^-3*pi^-1*G + 5/64*q.q^2*i_*m^-1
          *pi^-1*G - 1/16*l2.l2*i_*m*pi^-1*G );

   F1 =
       + L * (  - 3/4*q.q*i_*m*pi^-1*G + 43/96*q.q^2*Q.Q^-1*i_*m*pi^-1*G - 13/
          12*q.q^2*i_*m^-1*pi^-1*G - 1/32*q.q^3*Q.Q^-1*i_*m^-1*pi^-1*G + 25/24*
          q.q^3*i_*m^-3*pi^-1*G - 5/64*q.q^4*Q.Q^-1*i_*m^-3*pi^-1*G )

       + S * ( 1/16*q.q*i_*m*pi^-1*G + 17/128*q.q^2*Q.Q^-1*i_*m*pi^-1*G - 3/8*
          q.q^2*i_*m^-1*pi^-1*G - 1/128*q.q^3*Q.Q^-1*i_*m^-1*pi^-1*G + 5/16*
          q.q^3*i_*m^-3*pi^-1*G - 3/128*q.q^4*Q.Q^-1*i_*m^-3*pi^-1*G );

   F2 =
        + L * ( 7/3*i_*m^3*pi^-1*G - 29/48*q.q*i_*m*pi^-1*G - 7/48*q.q^2*i_*
          m^-1*pi^-1*G - 1/32*q.q^3*i_*m^-3*pi^-1*G )

        + S * ( 7/8*i_*m^3*pi^-1*G - 15/64*q.q*i_*m*pi^-1*G - 3/64*q.q^2*i_*
          m^-1*pi^-1*G );
```

where we only consider the leading terms.

B.0.2 Scalar Case with Identity

```
#-


Off Statistics;

*Declare variables
Symbol kap,m,TAG,pi,A1,A2,G;
dimension 4;
Vector p1, p2, q1, q2, q,l, l1,l2,k,l3,l4,Q;
index mu,nu,alpha,beta,gamma,delta,rho,xsi,lam,sig,kappa,eta,zeta;
CFunction L, S,I,P;
```

```
*NTensor;
Tensor T7,K;

#message This is the initial expression.
*Expression
local scalar1 = i_*i_*i_*T7(lam,kappa,p1,l1)*T7(rho,sig,l1,p2)*i_*kap/2*
P(rho,sig,lam,kappa)*(l3(mu)*l3(nu)+l4(mu)*l4(nu)+q(mu)*q(nu)-3/2*d_(mu,nu)*q.q);
local scalar2 = i_*i_*i_*T7(lam,kappa,p1,l1)*T7(rho,sig,l1,p2)*i_*kap/2*
2*q(xsi)*q(eta)*(I(rho,sig,eta,xsi)*I(lam,kappa,mu,nu)+I(lam,kappa,eta,xsi)*I(rho,sig,mu,nu) - I(
local scalar3 = i_*i_*i_*T7(lam,kappa,p1,l1)*T7(rho,sig,l1,p2)*i_*kap/2*
(q(xsi)*q(mu)*(d_(rho,sig)*I(lam,kappa,nu,xsi)+d_(lam,kappa)*I(rho,sig,nu,xsi))+q(xsi)*q(nu)*(d_
local scalar4= i_*i_*i_*T7(lam,kappa,p1,l1)*T7(rho,sig,l1,p2)*i_*kap/2*
(2*q(xsi)*(I(rho,sig,xsi,eta)*I(lam,kappa,eta,nu)*l4(mu)+I(rho,sig,xsi,eta)*I(lam,kappa,eta,mu)*l
-I(lam,kappa,xsi,eta)*I(rho,sig,eta,nu)*l3(mu)-I(lam,kappa,xsi,eta)*I(rho,sig,eta,mu)*l3(nu))
+q.q*(I(rho,sig,xsi,mu)*I(lam,kappa,nu,xsi)+I(rho,sig,xsi,nu)*I(lam,kappa,xsi,mu))+d_(mu,nu)*q(xs
local scalar5 = i_*P(alpha,beta,lam,kappa)*i_*P(gamma,delta,rho,sig)*i_*T7(alpha,beta,p1,l1)*T7(ga
((l1.l1 + l2.l2)*(I(eta,mu,rho,sig)*I(lam,kappa,eta,nu)+I(eta,nu,rho,sig)*I(lam,kappa,eta,mu)-1/2

.sort;
print;

sum alpha,beta,gamma,delta;
#message The functions P and I are expanded, so only mu, nu, alpha->delta indices remain
id P(alpha?,beta?,gamma?,delta?)=1/2*(d_(alpha,gamma)*d_(beta,delta)+d_(alpha,delta)*d_(beta,gamm
id I(alpha?,beta?,gamma?,delta?) = 1/2*(d_(alpha,gamma)*d_(beta,delta)+d_(alpha,delta)*d_(beta,gam
.sort;
print;

*Expand out all functions and express everything in terms of p1 and p2
id T7(mu?,nu?,p1?,p2?)=-i_*kap/2*(p1(mu)*p2(nu)+p1(nu)*p2(mu)-d_(mu,nu)*(p1.p2-m^2));
id l3 =l;
id l4 = l-q;
*id l3 = l+q/2;
*id l4 = l-q/2;
id q = p2 - p1;
id l1 = p2 -l;
*id l1=1/2*p1 + 1/2*p2-l;
id p1.p1 = m^2;
id p2.p2=m^2;
.sort;
sum alpha,beta,gamma,delta;
*Express everything in terms of q and P
id p1 = 1/2*(2*Q-q);
id p2=1/2*(2*Q+q);
id q.Q=0;
.sort;
```

```
#message summing over all indices other than mu and nu:
print;
.sort;
*id K(mu?)= i_/(32*pi^2*m^2)*(p2(mu)*((1+q.q/(2*m^2))*L+1/4*(q.q/m^2)*S)+q(mu)*(-L-S/2))
#message These are the integrals in the problem
*Express everything in terms of tensors of the integration variable
toTensor l,K;
Multiply TAG;
id TAG*K(?args)=K(?args);
Bracket l,K;
.sort;
print;
.sort;

*Integratal simplifications
*id K(q)=q.q/2*TAG;
*id q(mu?)*K(mu?,nu?)=q.q/2*K(nu);
*id q(mu?)*K(mu?,nu?,alpha?)=q.q/2*K(nu,alpha);

*Integral Solutions
id K(mu?,nu?,alpha?,beta?)=0;
.sort;
id K(mu?,nu?,alpha?)=i_/(32*pi^2*m^2)*(p2(mu)*p2(nu)*p2(alpha)*(1/6*q.q/m^2*L)+(p2(mu)*
q(alpha)+p2(mu)*p2(alpha)*q(nu)+p2(nu)*p2(alpha)*q(mu))*(-1/3*q.q/m^2*L-q.q/(16*m^2)*S)
(q(mu)*q(nu)*p2(alpha)+q(mu)*q(alpha)*p2(nu)+q(nu)*q(alpha)*p2(mu))*(1/3*L)+
q(mu)*q(nu)*q(alpha)*(-L-5/16*S)+(d_(mu,nu)*p2(alpha)+d_(mu,alpha)*p2(nu)+d_(nu,alpha)*
(-q.q/12*L)+(d_(mu,nu)*q(alpha)+d_(mu,alpha)*q(nu)+d_(nu,alpha)*q(mu))*(q.q/6*L+q.q/16*
.sort;
id K(mu?,nu?)=i_/(32*pi^2*m^2)*(p2(mu)*p2(nu)*(-q.q/(2*m^2)*L-q.q/(8*m^2)*S)+(p2(mu)*q(
p2(nu)*q(mu))*(1/2*(1+q.q/m^2)*L+3/16*q.q/m^2*S)+q(mu)*q(nu)*(-L-3/8*S)+q.q*d_(mu,nu)*(
.sort;
id K(mu?)= i_/(32*pi^2*m^2)*(p2(mu)*((1+q.q/(2*m^2))*L+1/4*(q.q/m^2)*S)+q(mu)*(-L-S/2));
.sort;
id TAG = i_/(32*pi^2*m^2)*(-L-S);
Bracket L,S;
.sort;
#message Solved integrals, independent of k
print;
.sort;

*id p2.q = q.q/2;
id L=0;
id p2 = 1/2*(2*Q+q);
id q.Q=0;
.sort;
Bracket L,S;
```

```
print;
.sort;

id Q = 1/2*(p2+p1);
id q = p2-p1;
id p1.p1 = m^2;
id p2.p2 = m^2;
.sort;

id p1 = 1/2*(2*Q-q);
id p2=1/2*(2*Q+q);
id q.Q=0;
id Q.Q=m^2-q.q/4;
.sort;
Bracket L,S;
print;
.sort;

local test = 1/2/m*(2*Q(mu)*Q(nu)*A1 +(q(mu)*q(nu)-d_(mu,nu)*q.q)*A2);
local F11 = (3/4/Q.Q^2 *Q(mu)*Q(nu) - 1/(4*Q.Q)*d_(mu,nu) )*scalar1;
local F21 = (1/2/Q.Q/q.q *Q(mu)*Q(nu) - 1/(2*q.q)*d_(mu,nu) )*scalar1;
local F12 = (3/4/Q.Q^2 *Q(mu)*Q(nu) - 1/(4*Q.Q)*d_(mu,nu) )*scalar2;
local F22 = (1/2/Q.Q/q.q *Q(mu)*Q(nu) - 1/(2*q.q)*d_(mu,nu) )*scalar2;
local F13 = (3/4/Q.Q^2 *Q(mu)*Q(nu) - 1/(4*Q.Q)*d_(mu,nu) )*scalar3;
local F23 = (1/2/Q.Q/q.q *Q(mu)*Q(nu) - 1/(2*q.q)*d_(mu,nu) )*scalar3;
local F14 = (3/4/Q.Q^2 *Q(mu)*Q(nu) - 1/(4*Q.Q)*d_(mu,nu) )*scalar4;
local F24 = (1/2/Q.Q/q.q *Q(mu)*Q(nu) - 1/(2*q.q)*d_(mu,nu) )*scalar4;
*local F15 = (3/4/Q.Q^2 *Q(mu)*Q(nu) - 1/(4*Q.Q)*d_(mu,nu) )*scalar5;
*local F25 = (1/2/Q.Q/q.q *Q(mu)*Q(nu) - 1/(2*q.q)*d_(mu,nu) )*scalar5;

sum mu,nu;
Multiply 2*m;
id kap^3 = 32*pi*G;
id Q.Q=m^2-q.q/4;
id q.Q=0;
id q.q^2=0;
Bracket L,S;
print;
.sort;

local F1 = F11+F12+F13+F14;
local F2=F21+F22+F23+F24;
*local fullscalar=scalar1+scalar2+scalar3+scalar4+scalar5;
*local test2 = F21+F22+F23+F24+F25;
.sort;
Bracket L,S;
```

```
print;
.end;
```

The results obtained in this case were much simpler:

```
$ F11 =
       + S * ( 1/16*q.q*i_*m*pi^-1*G );

   F21 =
       + S * ( 7/8*i_*m^3*pi^-1*G - 19/64*q.q*i_*m*pi^-1*G );

   F12 = 0;

   F22 = 0;

   F13 =
       + S * (  - q.q*i_*m*pi^-1*G );

   F23 = 0;

   F14 =
       + S * ( q.q*i_*m*pi^-1*G );

   F24 =
       + S * ( 1/16*q.q*i_*m*pi^-1*G );

   F1 =
       + S * ( 1/16*q.q*i_*m*pi^-1*G );

   F2 =
       + S * ( 7/8*i_*m^3*pi^-1*G - 15/64*q.q*i_*m*pi^-1*G );
```

B.0.3 Fermion Case without Identity

```
Off Statistics;

dimension 4;
symbol m,TAG,kappa,G,pi;
index alpha, beta, gamma, delta,rho,sig,kap,lam, xsi, eta,mu,nu,eps;
Vector q1,q2,l1,l2,l3,l4,Q,q,k1,k2,l;
NTensor SIG;
Tensor K,X;
CFunction L, S,P,I;
Function Ubar, U,T7;
```

```
local dirac1 = Ubar(k2)*T7(gamma,delta,l1,k2)*i_*(g_(1,l1)+m)*T7(alpha,beta,k1,l1)*U(k1)*i_*P(lam
(P(rho,sig,lam,kap)*(l2(mu)*l2(nu)+l3(mu)*l3(nu)+q(mu)*q(nu)-3/2*d_(mu,nu)*q.q));
local dirac2 = Ubar(k2)*T7(gamma,delta,l1,k2)*i_*(g_(1,l1)+m)*T7(alpha,beta,k1,l1)*U(k1)*i_*P(lam
(2*q(xsi)*q(eta)*(I(rho,sig,eta,xsi)*I(lam,kap,mu,nu)+I(lam,kap,eta,xsi)*I(rho,sig,mu,nu)-I(rho,s
local dirac3 = Ubar(k2)*T7(gamma,delta,l1,k2)*i_*(g_(1,l1)+m)*T7(alpha,beta,k1,l1)*U(k1)*i_*P(lam
(q(xsi)*q(mu)*(d_(rho,sig)*I(lam,kap,nu,xsi)+d_(lam,kap)*I(rho,sig,nu,xsi))+q(xsi)*q(nu)*(d_(rho
-q.q*(d_(rho,sig)*I(lam,kap,mu,nu)+d_(lam,kap)*I(rho,sig,mu,nu))-d_(mu,nu)*q(xsi)*q(eta)*(d_(rho
local dirac4 = Ubar(k2)*T7(gamma,delta,l1,k2)*i_*(g_(1,l1)+m)*T7(alpha,beta,k1,l1)*U(k1)*i_*P(lam
(2*q(xsi)*(I(rho,sig,xsi,eta)*I(lam,kap,eta,nu)*l3(mu)+I(rho,sig,xsi,eta)*I(lam,kap,eta,mu)*l3(nu
+q.q*(I(rho,sig,xsi,mu)*I(lam,kap,nu,xsi)+I(rho,sig,nu,xsi)*I(lam,kap,xsi,mu))+d_(mu,nu)*q(xsi)*
local dirac11 = Ubar(k2)*T7(rho,sig,l1,k2)*i_*(g_(1,l1)+m)*T7(lam,kap,k1,l1)*U(k1)*i_*i_*-i_*kapp
(P(rho,sig,lam,kap)*(l2(mu)*l2(nu)+l3(mu)*l3(nu)+q(mu)*q(nu)-3/2*d_(mu,nu)*q.q));
local dirac22 = Ubar(k2)*T7(rho,sig,l1,k2)*i_*(g_(1,l1)+m)*T7(lam,kap,k1,l1)*U(k1)*i_*i_*-i_*kapp
(2*q(xsi)*q(eta)*(I(rho,sig,eta,xsi)*I(lam,kap,mu,nu)+I(lam,kap,eta,xsi)*I(rho,sig,mu,nu)-I(rho,s
local dirac33 = Ubar(k2)*T7(rho,sig,l1,k2)*i_*(g_(1,l1)+m)*T7(lam,kap,k1,l1)*U(k1)*i_*i_*-i_*kappa
(q(xsi)*q(mu)*(d_(rho,sig)*I(lam,kap,nu,xsi)+d_(lam,kap)*I(rho,sig,nu,xsi))+q(xsi)*q(nu)*(d_(rho
-q.q*(d_(rho,sig)*I(lam,kap,mu,nu)+d_(lam,kap)*I(rho,sig,mu,nu))-d_(mu,nu)*q(xsi)*q(eta)*(d_(rho
local dirac44 = Ubar(k2)*T7(rho,sig,l1,k2)*i_*(g_(1,l1)+m)*T7(lam,kap,k1,l1)*U(k1)*i_*i_*-i_*kapp
(2*q(xsi)*(I(rho,sig,xsi,eta)*I(lam,kap,eta,nu)*l3(mu)+I(rho,sig,xsi,eta)*I(lam,kap,eta,mu)*l3(nu
+q.q*(I(rho,sig,xsi,mu)*I(lam,kap,nu,xsi)+I(rho,sig,nu,xsi)*I(lam,kap,xsi,mu))+d_(mu,nu)*q(xsi)*
.sort;
Bracket Ubar, U;
print;
.sort;

id P(alpha?,beta?,gamma?,delta?)=1/2*(d_(alpha,gamma)*d_(beta,delta)+d_(alpha,delta)*d_(beta,gamm
id I(alpha?,beta?,gamma?,delta?)=1/2*(d_(alpha,gamma)*d_(beta,delta)+d_(alpha,delta)*d_(beta,gamm
.sort;
Bracket Ubar, U;
print;
.sort;

id T7(alpha?,beta?,k1?,k2?)=-i_*kappa/2*(1/4*g_(1,alpha)*(k1(beta)+k2(beta))+1/4*g_(1,beta)*(k1(a
id g_(1,mu?,mu?)=4;
id g_(1,mu?,nu?,mu?)=-2*g_(1,nu);
.sort;
Bracket Ubar, U;
print;
.sort;

*Express all momenta in terms of k1 and k2
id l1=l+k2;
id l2 = l;
id l3=l-q;
id q = k1-k2;
```

```
.sort;
*Dirac Equation
repeat;
id g_(1,mu?,k2)=-g_(1,k2,mu)+2*k2(mu);
id Ubar(k2)*g_(1,k2)=Ubar(k2)*m;
endrepeat;
repeat;
id g_(1,k1,mu?)=-g_(1,mu,k1)+2*k1(mu);
id g_(1,k1)*U(k1)=m*U(k1);
endrepeat;
id g_(1,l,l)=l.l;
.sort;
Bracket Ubar, U;
print;
.sort;

id k1 = (q+2*Q)/2;
id k2 = (2*Q-q)/2;
id q.Q=0;
.sort;
*print;
Bracket Ubar,U;
print;
.sort;

toTensor l,K;
Multiply TAG;
id TAG*K(?args)=K(?args);
.sort;
Bracket K,Ubar,U;
*print;
.sort;

*Solve Integrals
*Concerned that q.q/16*S != q.q*S/16 or something similar
id K(mu?,nu?,alpha?,delta?,delta?)=X(mu,nu,alpha);
id X(mu?,nu?,alpha?)=0;
id K(mu?,nu?,alpha?,beta?)=0;
id K(mu?,nu?,alpha?)=i_/32/pi^2/m^2*(-k2(mu)*k2(nu)*k2(alpha)*(q.q/6/m^2*L)+(k2(mu)*k2(
-(q(mu)*q(nu)*k2(alpha)+q(nu)*q(alpha)*k2(mu)+q(mu)*q(alpha)*k2(nu))*L/3 + q(mu)*q(nu)*
+(d_(mu,nu)*q(alpha)+d_(mu,alpha)*q(nu)+d_(nu,alpha)*q(mu))*(q.q/6*L+q.q/16*S));
id K(mu?,nu?)=i_/32/pi^2/m^2*(k2(mu)*k2(nu)*(-q.q*L/(2*m^2)-q.q/8/m^2*S)-(k2(mu)*q(nu)+
+q.q*d_(mu,nu)*(L/4+S/8));
id K(mu?)=i_/32/pi^2/m^2*(-k2(mu)*((1+q.q/2/m^2)*L+1/4*q.q/m^2*S)+q(mu)*(-L-S/2));
id TAG=i_/32/pi^2/m^2*(-L-S);
.sort;
```

```
id q = k1-k2;
id Q=1/2*(k1+k2);
repeat;
id g_(1,mu?,k2)=-g_(1,k2,mu)+2*k2(mu);
id Ubar(k2)*g_(1,k2)=Ubar(k2)*m;
endrepeat;
repeat;
id g_(1,k1,mu?)=-g_(1,mu,k1)+2*k1(mu);
id g_(1,k1)*U(k1)=m*U(k1);
endrepeat;
id k1 = (q+2*Q)/2;
id k2 = (2*Q-q)/2;
id q.Q=0;
.sort;
Bracket Ubar,U,L,S;
print;
.sort;

*id g_(1,mu?,nu?)=d_(mu,nu)-i_*SIG(mu,nu);
*id g_(1,nu,mu)=-g_(1,mu,nu)+2*d_(mu,nu);
*id Ubar(k2)*g_(1,mu?)*U(k1)=Ubar(k2)*(Q(mu)/m-i_*SIG(mu,eps)*q(eps)/m)*U(k1);
id q.Q=0;
id kappa^3=32*pi*G;
id Q.Q=m^2-q.q/4;
id q.q/m^2=0;
id q.q^2=0;
Multiply 2*i_;
id L=0;
.sort;
*Gordon Identity
local dirac = dirac1+dirac2+dirac3+dirac4;
*local diractest1 = dirac1-dirac11;
*local diractest2 = dirac2-dirac22;
*local diractest3 = dirac3-dirac33;
*local diractest4 = dirac4-dirac44;
*local diractest = dirac1+dirac2+dirac3+dirac4-dirac11-dirac22-dirac33-dirac44;
Bracket Ubar,U,L,S;
print;
.sort;
*
.end;
```

The following results were obtained:

```
   dirac1 =
```

```
      + Ubar(k2)*U(k1)*S * ( 1/16*Q(mu)*Q(nu)*q.q*m^-1*G*pi^-1 + 7/16*q(mu)*
        q(nu)*m*G*pi^-1 - 47/128*q(mu)*q(nu)*q.q*m^-1*G*pi^-1 - 7/16*
        d_(mu,nu)*q.q*m*G*pi^-1 );

   dirac2 =
      + Ubar(k2)*g_(1,mu)*U(k1)*S * (  - 1/4*Q(nu)*q.q*G*pi^-1 )

      + Ubar(k2)*g_(1,nu)*U(k1)*S * (  - 1/4*Q(mu)*q.q*G*pi^-1 )

      + Ubar(k2)*U(k1)*S * (  - 1/2*Q(mu)*Q(nu)*q.q*m^-1*G*pi^-1 - 1/2*q(mu)*
        q(nu)*m*G*pi^-1 - 1/32*q(mu)*q(nu)*q.q*m^-1*G*pi^-1 + 1/2*d_(mu,nu)*
        q.q*m*G*pi^-1 );

   dirac3 =
      + Ubar(k2)*g_(1,mu)*U(k1)*S * ( 1/4*Q(nu)*q.q*G*pi^-1 )

      + Ubar(k2)*g_(1,nu)*U(k1)*S * ( 1/4*Q(mu)*q.q*G*pi^-1 )

      + Ubar(k2)*U(k1)*S * ( 1/2*Q(mu)*Q(nu)*q.q*m^-1*G*pi^-1 + q(mu)*q(nu)*m
        *G*pi^-1 + 3/32*q(mu)*q(nu)*q.q*m^-1*G*pi^-1 - d_(mu,nu)*q.q*m*G*
        pi^-1 );

   dirac4 =
      + Ubar(k2)*g_(1,mu)*U(k1)*S * ( 1/8*Q(nu)*q.q*G*pi^-1 )

      + Ubar(k2)*g_(1,nu)*U(k1)*S * ( 1/8*Q(mu)*q.q*G*pi^-1 )

      + Ubar(k2)*U(k1)*S * (  - 1/4*Q(mu)*Q(nu)*q.q*m^-1*G*pi^-1 - 1/2*q(mu)*
        q(nu)*m*G*pi^-1 + 7/128*q(mu)*q(nu)*q.q*m^-1*G*pi^-1 + 1/2*d_(mu,nu)*
        q.q*m*G*pi^-1 );

   dirac11 =
      + Ubar(k2)*U(k1)*S * ( 1/16*Q(mu)*Q(nu)*q.q*m^-1*G*pi^-1 + 7/16*q(mu)*
        q(nu)*m*G*pi^-1 - 47/128*q(mu)*q(nu)*q.q*m^-1*G*pi^-1 - 7/16*
        d_(mu,nu)*q.q*m*G*pi^-1 );

   dirac22 = 0;

   dirac33 =
      + Ubar(k2)*g_(1,mu)*U(k1)*S * (  - 1/4*Q(nu)*q.q*G*pi^-1 )

      + Ubar(k2)*g_(1,nu)*U(k1)*S * (  - 1/4*Q(mu)*q.q*G*pi^-1 )

      + Ubar(k2)*U(k1)*S * (  - 1/2*Q(mu)*Q(nu)*q.q*m^-1*G*pi^-1 + 1/32*q(mu)
        *q(nu)*q.q*m^-1*G*pi^-1 );
```

```
   dirac44 =
       + Ubar(k2)*g_(1,mu)*U(k1)*S * ( 3/8*Q(nu)*q.q*G*pi^-1 )

       + Ubar(k2)*g_(1,nu)*U(k1)*S * ( 3/8*Q(mu)*q.q*G*pi^-1 )

       + Ubar(k2)*U(k1)*S * ( 1/4*Q(mu)*Q(nu)*q.q*m^-1*G*pi^-1 + 11/128*q(mu)*
         q(nu)*q.q*m^-1*G*pi^-1 );

   dirac =
       + Ubar(k2)*g_(1,mu)*U(k1)*S * ( 1/8*Q(nu)*q.q*G*pi^-1 )

       + Ubar(k2)*g_(1,nu)*U(k1)*S * ( 1/8*Q(mu)*q.q*G*pi^-1 )

       + Ubar(k2)*U(k1)*S * (  - 3/16*Q(mu)*Q(nu)*q.q*m^-1*G*pi^-1 + 7/16*
         q(mu)*q(nu)*m*G*pi^-1 - 1/4*q(mu)*q(nu)*q.q*m^-1*G*pi^-1 - 7/16*
         d_(mu,nu)*q.q*m*G*pi^-1 );
```

B.0.4 Fermion Case with Identity

```
Off Statistics;

dimension 4;
symbol m,TAG,kappa,G,pi;
index alpha, beta, gamma, delta,rho,sig,kap,lam, xsi, eta,mu,nu,eps;
Vector q1,q2,l1,l2,l3,l4,Q,q,k1,k2,l;
NTensor SIG;
Tensor K,X;
CFunction L, S,P,I;
Function Ubar, U,T7;

local dirac11 = Ubar(k2)*T7(rho,sig,l1,k2)*i_*(g_(1,l1)+m)*T7(lam,kap,k1,l1)*U(k1)*i_*i_*-i_*kapp
(P(rho,sig,lam,kap)*(l2(mu)*l2(nu)+l3(mu)*l3(nu)+q(mu)*q(nu)-3/2*d_(mu,nu)*q.q));
local dirac22 = Ubar(k2)*T7(rho,sig,l1,k2)*i_*(g_(1,l1)+m)*T7(lam,kap,k1,l1)*U(k1)*i_*i_*-i_*kapp
(2*q(xsi)*q(eta)*(I(rho,sig,eta,xsi)*I(lam,kap,mu,nu)+I(lam,kap,eta,xsi)*I(rho,sig,mu,nu)-I(rho,s
local dirac33 = Ubar(k2)*T7(rho,sig,l1,k2)*i_*(g_(1,l1)+m)*T7(lam,kap,k1,l1)*U(k1)*i_*i_*-i_*kappa
(q(xsi)*q(mu)*(d_(rho,sig)*I(lam,kap,nu,xsi)+d_(lam,kap)*I(rho,sig,nu,xsi))+q(xsi)*q(nu)*(d_(rho
-q.q*(d_(rho,sig)*I(lam,kap,mu,nu)+d_(lam,kap)*I(rho,sig,mu,nu))-d_(mu,nu)*q(xsi)*q(eta)*(d_(rho
local dirac44 = Ubar(k2)*T7(rho,sig,l1,k2)*i_*(g_(1,l1)+m)*T7(lam,kap,k1,l1)*U(k1)*i_*i_*-i_*kapp
(2*q(xsi)*(I(rho,sig,xsi,eta)*I(lam,kap,eta,nu)*l3(mu)+I(rho,sig,xsi,eta)*I(lam,kap,eta,mu)*l3(nu
+q.q*(I(rho,sig,xsi,mu)*I(lam,kap,nu,xsi)+I(rho,sig,nu,xsi)*I(lam,kap,xsi,mu))+d_(mu,nu)*q(xsi)*
.sort;
Bracket Ubar, U;
print;
.sort;
```

```
id P(alpha?,beta?,gamma?,delta?)=1/2*(d_(alpha,gamma)*d_(beta,delta)+d_(alpha,delta)*d_
id I(alpha?,beta?,gamma?,delta?)=1/2*(d_(alpha,gamma)*d_(beta,delta)+d_(alpha,delta)*d_
.sort;
Bracket Ubar, U;
print;
.sort;

id T7(alpha?,beta?,k1?,k2?)=-i_*kappa/2*(1/4*g_(1,alpha)*(k1(beta)+k2(beta))+1/4*g_(1,b
id g_(1,mu?,mu?)=4;
id g_(1,k1?,k1?)=k1.k1;
id g_(1,mu?,nu?,mu?)=-2*g_(1,nu);
.sort;
Bracket Ubar, U;
print;
.sort;
*
*Express all momenta in terms of k1 and k2
id l1=l+k2;
id l2 = l;
id l3=l-q;
id q = k1-k2;
id g_(1,mu?,mu?)=4;
id g_(1,k1?,k1?)=k1.k1;
id g_(1,mu?,nu?,mu?)=-2*g_(1,nu);
.sort;
print;
Bracket Ubar, U;
.sort;
*Dirac Equation
repeat;
id g_(1,mu?,k2)=-g_(1,k2,mu)+2*k2(mu);
id Ubar(k2)*g_(1,k2)=Ubar(k2)*m;
endrepeat;
repeat;
id g_(1,k1,mu?)=-g_(1,mu,k1)+2*k1(mu);
id g_(1,k1)*U(k1)=m*U(k1);
endrepeat;
id g_(1,l,l)=l.l;
.sort;
Bracket Ubar, U;
print;
.sort;

id k1 = (q+2*Q)/2;
id k2 = (2*Q-q)/2;
id q.Q=0;
```

```
.sort;
print;
Bracket Ubar,U;
print;
.sort;

toTensor l,K;
Multiply TAG;
id TAG*K(?args)=K(?args);
.sort;
Bracket K,Ubar,U;
print;
.sort;

*Solve Integrals
*Concerned that q.q/16*S != q.q*S/16 or something similar
id K(mu?,nu?,alpha?,delta?,delta?)=X(mu,nu,alpha);
id X(mu?,nu?,alpha?)=0;
id K(mu?,nu?,alpha?,beta?)=0;
id K(mu?,nu?,alpha?)=i_/32/pi^2/m^2*(-k2(mu)*k2(nu)*k2(alpha)*(q.q/6/m^2*L)+(k2(mu)*k2(nu)*q(alph
-(q(mu)*q(nu)*k2(alpha)+q(nu)*q(alpha)*k2(mu)+q(mu)*q(alpha)*k2(nu))*L/3 + q(mu)*q(nu)*q(alpha)*(
+(d_(mu,nu)*q(alpha)+d_(mu,alpha)*q(nu)+d_(nu,alpha)*q(mu))*(q.q/6*L+q.q/16*S));
id K(mu?,nu?)=i_/32/pi^2/m^2*(k2(mu)*k2(nu)*(-q.q*L/(2*m^2)-q.q/8/m^2*S)-(k2(mu)*q(nu)+k2(nu)*q(m
+q.q*d_(mu,nu)*(L/4+S/8));
id K(mu?)=i_/32/pi^2/m^2*(-k2(mu)*((1+q.q/2/m^2)*L+1/4*q.q/m^2*S)+q(mu)*(-L-S/2));
id TAG=i_/32/pi^2/m^2*(-L-S);
.sort;
id q = k1-k2;
id Q=1/2*(k1+k2);
repeat;
id g_(1,mu?,k2)=-g_(1,k2,mu)+2*k2(mu);
id Ubar(k2)*g_(1,k2)=Ubar(k2)*m;
endrepeat;
repeat;
id g_(1,k1,mu?)=-g_(1,mu,k1)+2*k1(mu);
id g_(1,k1)*U(k1)=m*U(k1);
endrepeat;
id k1 = (q+2*Q)/2;
id k2 = (2*Q-q)/2;
id q.Q=0;
.sort;
Bracket Ubar,U,L,S;
print;
.sort;

**Gordon Identity
```

```
**id g_(1,mu?,nu?)=d_(mu,nu)-i_*SIG(mu,nu);
***id g_(1,nu,mu)=-g_(1,mu,nu)+2*d_(mu,nu);
***id Ubar(k2)*g_(1,mu?)*U(k1)=Ubar(k2)*(Q(mu)/m-i_*SIG(mu,eps)*q(eps)/m)*U(k1);
*id q.Q=0;
id kappa^3=32*pi*G;
id Q.Q=m^2-q.q/4;
*id q.q/m^2=0;
id q.q^2=0;
Multiply 2*i_;
id L=0;
.sort;
*local dirac = dirac1+dirac2+dirac3+dirac4;
**local diractest1 = dirac1-dirac11;
**local diractest2 = dirac2-dirac22;
**local diractest3 = dirac3-dirac33;
**local diractest4 = dirac4-dirac44;
**local diractest = dirac1+dirac2+dirac3+dirac4-dirac11-dirac22-dirac33-dirac44;
Bracket Ubar,U,L,S;
print;
.sort;
**
*Notes on extracting Form factors: F3 is directly proportional to q(mu)q(nu)-d_(mu,nu)q.q.
*F2 is one half of the coefficient of either g_(1,mu) terms or g_(1,nu) terms.
*F1 is the sum of F2+the term proportional to Q(mu)Q(nu)
.end;
```

The results obtained were:

```
   dirac11 =
       + Ubar(k2)*U(k1)*S * ( 1/16*Q(mu)*Q(nu)*q.q*m^-1*G*pi^-1 + 7/16*q(mu)*
         q(nu)*m*G*pi^-1 - 47/128*q(mu)*q(nu)*q.q*m^-1*G*pi^-1 - 7/16*
         d_(mu,nu)*q.q*m*G*pi^-1 );

   dirac22 = 0;

   dirac33 =
       + Ubar(k2)*g_(1,mu)*U(k1)*S * (  - 1/4*Q(nu)*q.q*G*pi^-1 )

       + Ubar(k2)*g_(1,nu)*U(k1)*S * (  - 1/4*Q(mu)*q.q*G*pi^-1 )

      + Ubar(k2)*U(k1)*S * (  - 1/2*Q(mu)*Q(nu)*q.q*m^-1*G*pi^-1 + 1/32*q(mu)
         *q(nu)*q.q*m^-1*G*pi^-1 );

   dirac44 =
       + Ubar(k2)*g_(1,mu)*U(k1)*S * ( 3/8*Q(nu)*q.q*G*pi^-1 )
```

```
 + Ubar(k2)*g_(1,nu)*U(k1)*S * ( 3/8*Q(mu)*q.q*G*piˆ-1 )

+ Ubar(k2)*U(k1)*S * ( 1/4*Q(mu)*Q(nu)*q.q*mˆ-1*G*piˆ-1 + 11/128*q(mu)*
   q(nu)*q.q*mˆ-1*G*piˆ-1 );
```

Bibliography

[1] T. Kajita, "Discovery of Atmospheric Neutrino Oscillations, Nobel Lecture." https://www.nobelprize.org/uploads/2018/06/kajita-lecture.pdf, Dec, 2015.

[2] A. Barzinji, M. Trott, and A. Vasudevan, *Equations of motion for the standard model effective field theory: Theory and applications*, *Physical Review D* **98** (Dec, 2018).

[3] B. Abbott, R. Abbott, T. Abbott, M. Abernathy, F. Acernese, K. Ackley, C. Adams, T. Adams, P. Addesso, R. Adhikari, and et al., *Observation of gravitational waves from a binary black hole merger*, *Physical Review Letters* **116** (Feb, 2016).

[4] T. Appelquist and J. Carazzone, *Infrared singularities and massive fields*, *Phys. Rev. D* **11** (May, 1975) 2856–2861.

[5] I. Brivio and M. Trott, *The Standard Model as an Effective Field Theory*, *Phys. Rept.* **793** (2019) 1–98, [arXiv:1706.0894].

[6] J. C. Collins, *Renormalization: An Introduction to Renormalization, The Renormalization Group, and the Operator Product Expansion*, vol. 26 of *Cambridge Monographs on Mathematical Physics*. Cambridge University Press, Cambridge, 1986.

[7] M. J. G. Veltman, *Mass Scale of Weak Interactions*, *Conf. Proc. C* **7707112** (1977) 116–142.

[8] D. Toussaint, *Renormalization effects from superheavy higgs particles*, *Phys. Rev. D* **18** (Sep, 1978) 1626–1631.

[9] J. Collins, F. Wilczek, and A. Zee, *Low-energy manifestations of heavy particles: Application to the neutral current*, *Phys. Rev. D* **18** (Jul, 1978) 242–247.

[10] M. Neubert, *Heavy quark effective theory*, *Subnucl. Ser.* **34** (1997) 98–165, [hep-ph/9610266].

[11] E. E. Jenkins, A. V. Manohar, and P. Stoffer, *Low-Energy Effective Field Theory below the Electroweak Scale: Operators and Matching*, *JHEP* **03** (2018) 016, [arXiv:1709.0448].

[12] T. Becher, A. Broggio, and A. Ferroglia, *Introduction to Soft-Collinear Effective Theory*, vol. 896. Springer, 2015.

[13] A. V. Manohar and M. B. Wise, *Heavy quark physics*, vol. 10. 2000.

[14] A. V. Manohar, *Effective field theories*, *Lect. Notes Phys.* **479** (1997) 311–362, [hep-ph/9606222].

[15] A. V. Manohar and M. B. Wise, *Heavy quark physics*, vol. 10. 2000.

[16] C. P. Burgess, *Introduction to Effective Field Theory*, *Ann. Rev. Nucl. Part. Sci.* **57** (2007) 329–362, [hep-th/0701053].

[17] B. Grzadkowski, M. Iskrzyński, M. Misiak, and J. Rosiek, *Dimension-six terms in the standard model lagrangian*, *Journal of High Energy Physics* **2010** (Oct, 2010).

[18] G. 't Hooft and M. J. G. Veltman, *Regularization and Renormalization of Gauge Fields*, *Nucl. Phys. B* **44** (1972) 189–213.

[19] M. Kaku, *Quantum field theory: A Modern introduction*. 1993.

[20] M. E. Peskin and D. V. Schroeder, *An Introduction to quantum field theory*. Addison-Wesley, Reading, USA, 1995.

[21] A. B. McDonald, *Nobel Lecture: The Sudbury Neutrino Observatory: Observation of flavor change for solar neutrinos*, *Rev. Mod. Phys.* **88** (2016), no. 3 030502.

[22] *Physics at the FCC-hh, a 100 TeV pp collider*, arXiv:1710.0635.

[23] **LHC New Physics Working Group** Collaboration, D. Alves, *Simplified Models for LHC New Physics Searches*, *J. Phys. G* **39** (2012) 105005, [arXiv:1105.2838].

[24] B. Henning, X. Lu, T. Melia, and H. Murayama, *2, 84, 30, 993, 560, 15456, 11962, 261485, ...: Higher dimension operators in the sm eft*, 2019.

[25] M. Bjørn and M. Trott, *Interpreting W mass measurements in the SMEFT*, *Phys. Lett. B* **762** (2016) 426–431, [arXiv:1606.0650].

[26] G. Elgaard-Clausen and M. Trott, *On expansions in neutrino effective field theory*, *JHEP* **11** (2017) 088, [arXiv:1703.0441].

[27] T. Cohen, N. Craig, X. Lu, and D. Sutherland, *Is SMEFT Enough?*, *JHEP* **03** (2021) 237, [arXiv:2008.0859].

[28] W. Buchmuller and D. Wyler, *Effective Lagrangian Analysis of New Interactions and Flavor Conservation*, *Nucl. Phys. B* **268** (1986) 621–653.

[29] B. Henning, X. Lu, T. Melia, and H. Murayama, *Hilbert series and operator bases with derivatives in effective field theories*, *Commun. Math. Phys.* **347** (2016), no. 2 363–388, [arXiv:1507.0724].

[30] E. E. Jenkins, A. V. Manohar, and M. Trott, *Renormalization Group Evolution of the Standard Model Dimension Six Operators I: Formalism and lambda Dependence*, *JHEP* **10** (2013) 087, [arXiv:1308.2627].

[31] E. E. Jenkins, A. V. Manohar, and M. Trott, *Renormalization Group Evolution of the Standard Model Dimension Six Operators II: Yukawa Dependence*, *JHEP* **01** (2014) 035, [arXiv:1310.4838].

[32] R. Alonso, E. E. Jenkins, A. V. Manohar, and M. Trott, *Renormalization Group Evolution of the Standard Model Dimension Six Operators III: Gauge Coupling Dependence and Phenomenology*, *JHEP* **04** (2014) 159, [arXiv:1312.2014].

[33] I. Brivio et al., *Truncation, validity, uncertainties*, arXiv:2201.0497.

[34] C. Hartmann, W. Shepherd, and M. Trott, *The Z decay width in the SMEFT: y_t and λ corrections at one loop*, *JHEP* **03** (2017) 060, [arXiv:1611.0987].

[35] C. Hartmann and M. Trott, *Higgs Decay to Two Photons at One Loop in the Standard Model Effective Field Theory*, *Phys. Rev. Lett.* **115** (2015), no. 19 191801, [arXiv:1507.0356].

[36] M. Grazzini, A. Ilnicka, and M. Spira, *Higgs boson production at large transverse momentum within the SMEFT: analytical results*, *Eur. Phys. J. C* **78** (2018), no. 10 808, [arXiv:1806.0883].

[37] N. Deutschmann, C. Duhr, F. Maltoni, and E. Vryonidou, *Gluon-fusion Higgs production in the Standard Model Effective Field Theory*, *JHEP* **12** (2017) 063, [arXiv:1708.0046]. [Erratum: JHEP 02, 159 (2018)].

[38] C. Zhang, *Single Top Production at Next-to-Leading Order in the Standard Model Effective Field Theory*, *Phys. Rev. Lett.* **116** (2016), no. 16 162002, [arXiv:1601.0616].

[39] C. Degrande, F. Maltoni, K. Mimasu, E. Vryonidou, and C. Zhang, *Single-top associated production with a Z or H boson at the LHC: the SMEFT interpretation*, *JHEP* **10** (2018) 005, [arXiv:1804.0777].

[40] C. Zhang and F. Maltoni, *Top-quark decay into Higgs boson and a light quark at next-to-leading order in QCD*, *Phys. Rev. D* **88** (2013) 054005, [arXiv:1305.7386].

[41] I. Brivio, Y. Jiang, and M. Trott, *The SMEFTsim package, theory and tools*, *JHEP* **12** (2017) 070, [arXiv:1709.0649].

[42] C. Degrande, G. Durieux, F. Maltoni, K. Mimasu, E. Vryonidou, and C. Zhang, *Automated one-loop computations in the standard model effective field theory*, *Phys. Rev. D* **103** (2021), no. 9 096024, [arXiv:2008.1174].

[43] T. Gleisberg, S. Hoeche, F. Krauss, M. Schonherr, S. Schumann, F. Siegert, and J. Winter, *Event generation with SHERPA 1.1*, *JHEP* **02** (2009) 007, [arXiv:0811.4622].

[44] S. Alioli, P. Nason, C. Oleari, and E. Re, *A general framework for implementing NLO calculations in shower Monte Carlo programs: the POWHEG BOX*, *JHEP* **06** (2010) 043, [arXiv:1002.2581].

[45] **SMEFiT** Collaboration, J. J. Ethier, G. Magni, F. Maltoni, L. Mantani, E. R. Nocera, J. Rojo, E. Slade, E. Vryonidou, and C. Zhang, *Combined SMEFT interpretation of Higgs, diboson, and top quark data from the LHC*, *JHEP* **11** (2021) 089, [arXiv:2105.0000].

[46] Z. Bern, J. Parra-Martinez, and E. Sawyer, *Structure of two-loop SMEFT anomalous dimensions via on-shell methods*, *JHEP* **10** (2020) 211, [arXiv:2005.1291].

[47] S. Kallweit, V. Sotnikov, and M. Wiesemann, *Triphoton production at hadron colliders in NNLO QCD*, arXiv:2010.0468.

[48] B. Mistlberger, *Higgs boson production at hadron colliders at N^3LO in QCD*, *JHEP* **05** (2018) 028, [arXiv:1802.0083].

[49] C. Duhr, F. Dulat, and B. Mistlberger, *Charged current Drell-Yan production at N^3LO*, *JHEP* **11** (2020) 143, [arXiv:2007.1331].

[50] C. Duhr, F. Dulat, and B. Mistlberger, *Drell-Yan Cross Section to Third Order in the Strong Coupling Constant*, *Phys. Rev. Lett.* **125** (2020), no. 17 172001, [arXiv:2001.0771].

[51] L. D. Landau and E. M. Lifshitz, *Mechanics, Third Edition: Volume 1* (*Course of Theoretical Physics*). Butterworth-Heinemann, 3 ed., Jan., 1976.

[52] C. N. Leung, S. Love, and S. Rao, *Low-Energy Manifestations of a New Interaction Scale: Operator Analysis*, *Z. Phys. C* **31** (1986) 433.

[53] S. Weinberg, *Baryon and Lepton Nonconserving Processes*, *Phys. Rev. Lett.* **43** (1979) 1566–1570.

[54] F. Wilczek and A. Zee, *Operator analysis of nucleon decay*, *Phys. Rev. Lett.* **43** (Nov, 1979) 1571–1573.

[55] J. de Blas, J. C. Criado, M. Perez-Victoria, and J. Santiago, *Effective description of general extensions of the Standard Model: the complete tree-level dictionary*, *JHEP* **03** (2018) 109, [arXiv:1711.1039].

[56] A. Barzinji, *Equations of Motion for the Standard Model Effective Field Theory*, . Cand.Scient. Thesis, Univ. of Copenhagen (2019).

[57] A. Helset and M. Trott, *Equations of motion, symmetry currents and EFT below the electroweak scale*, *Phys. Lett. B* **795** (2019) 606–619, [arXiv:1812.0299].

[58] R. A. Hulse and J. H. Taylor, *Discovery of a pulsar in a binary system*, *Astrophys. J. Lett.* **195** (1975) L51–L53.

[59] L. Collaboration, "Indigo."

[60] W. Hu and M. J. White, *A CMB polarization primer*, *New Astron.* **2** (1997) 323, [astro-ph/9706147].

[61] **LIGO Scientific, Virgo** Collaboration, B. P. Abbott et al., *Observation of Gravitational Waves from a Binary Black Hole Merger*, *Phys. Rev. Lett.* **116** (2016), no. 6 061102, [arXiv:1602.0383].

[62] M. Levi, *Effective Field Theories of Post-Newtonian Gravity: A comprehensive review*, *Rept. Prog. Phys.* **83** (2020), no. 7 075901, [arXiv:1807.0169].

[63] A. Buonanno and T. Damour, *Effective one-body approach to general relativistic two-body dynamics*, *Phys. Rev. D* **59** (1999) 084006, [gr-qc/9811091].

[64] A. Buonanno and T. Damour, *Transition from inspiral to plunge in binary black hole coalescences*, *Phys. Rev. D* **62** (2000) 064015, [gr-qc/0001013].

[65] T. Damour, *The General Relativistic Two Body Problem and the Effective One Body Formalism*, *Fundam. Theor. Phys.* **177** (2014) 111–145, [arXiv:1212.3169].

[66] A. Le Tiec, *The Overlap of Numerical Relativity, Perturbation Theory and Post-Newtonian Theory in the Binary Black Hole Problem*, *Int. J. Mod. Phys. D* **23** (2014), no. 10 1430022, [arXiv:1408.5505].

[67] M. Levi and J. Steinhoff, *EFTofPNG: A package for high precision computation with the Effective Field Theory of Post-Newtonian Gravity*, *Class. Quant. Grav.* **34** (2017), no. 24 244001, [arXiv:1705.0630].

[68] T. Damour, *Introductory lectures on the Effective One Body formalism*, *Int. J. Mod. Phys. A* **23** (2008) 1130–1148, [arXiv:0802.4047].

[69] W. D. Goldberger and I. Z. Rothstein, *An Effective field theory of gravity for extended objects*, *Phys. Rev. D* **73** (2006) 104029, [hep-th/0409156].

[70] W. D. Goldberger and I. Z. Rothstein, *Towers of Gravitational Theories*, *Gen. Rel. Grav.* **38** (2006) 1537–1546, [hep-th/0605238].

[71] W. D. Goldberger, *Les Houches lectures on effective field theories and gravitational radiation*, in *Les Houches Summer School - Session 86: Particle Physics and Cosmology: The Fabric of Spacetime*, 1, 2007. hep-ph/0701129.

[72] J. Blümlein, A. Maier, P. Marquard, and G. Schäfer, *The 6th post-Newtonian potential terms at $O(G_N^4)$*, *Phys. Lett. B* **816** (2021) 136260, [arXiv:2101.0863].

[73] Z. Bern, J. Parra-Martinez, R. Roiban, M. S. Ruf, C.-H. Shen, M. P. Solon, and M. Zeng, *Scattering Amplitudes and Conservative Binary Dynamics at $O(G^4)$*, *Phys. Rev. Lett.* **126** (2021), no. 17 171601, [arXiv:2101.0725].

[74] J. F. Donoghue, B. R. Holstein, B. Garbrecht, and T. Konstandin, *Quantum corrections to the Reissner-Nordstrom and Kerr-Newman metrics*, *Phys. Lett. B* **529** (2002) 132–142, [hep-th/0112237]. [Erratum: Phys.Lett.B 612, 311–312 (2005)].

[75] N. E. J. Bjerrum-Bohr, J. F. Donoghue, and B. R. Holstein, *Quantum corrections to the Schwarzschild and Kerr metrics*, *Phys. Rev. D* **68** (2003) 084005, [hep-th/0211071]. [Erratum: Phys.Rev.D 71, 069904 (2005)].

[76] J. Galusha, *Investigations into the Classical Limit of Quantum Field Theory*, . Cand.Scient. Thesis, Univ. of Copenhagen (2016).

[77] N. J. Bjerrum-Bohr, P. H. Damgaard, G. Festuccia, L. Planté, and P. Vanhove, *General Relativity from Scattering Amplitudes*, *Phys. Rev. Lett.* **121** (2018), no. 17 171601, [arXiv:1806.0492].

[78] **Planck** Collaboration, N. Aghanim et al., *Planck 2018 results. VI. Cosmological parameters*, *Astron. Astrophys.* **641** (2020) A6, [arXiv:1807.0620]. [Erratum: Astron.Astrophys. 652, C4 (2021)].

[79] N. E. Bjerrum-Bohr, *Quantum gravity, effective fields and string theory*. PhD thesis, Bohr Inst., 2004. hep-th/0410097.

[80] K. S. Stelle, *Classical Gravity with Higher Derivatives*, *Gen. Rel. Grav.* **9** (1978) 353–371.

[81] J. F. Donoghue, *Introduction to the effective field theory description of gravity*, in *Advanced School on Effective Theories*, 6, 1995. gr-qc/9512024.

[82] N. E. Bjerrum-Bohr, *Quantum gravity as an Effective Field Theory*, . Cand.Scient. Thesis, Univ. of Copenhagen (2001).

[83] L. J. Dixon, *A brief introduction to modern amplitude methods*, in *Theoretical Advanced Study Institute in Elementary Particle Physics: Particle Physics: The Higgs Boson and Beyond*, pp. 31–67, 2014. arXiv:1310.5353.

[84] H. Elvang and Y.-t. Huang, *Scattering Amplitudes*, arXiv:1308.1697.

[85] S. J. Parke and T. R. Taylor, *Amplitude for n-gluon scattering*, *Phys. Rev. Lett.* **56** (Jun, 1986) 2459–2460.

[86] M. L. Mangano, S. J. Parke, and Z. Xu, *Dual Amplitudes and Multi - Gluon Processes*, in *1st Les Rencontres de Physique de la Vallee d'Aoste: Results and Perspectives in Particle Physics*, 3, 1987.

[87] Z. Bern and D. A. Kosower, *A New Approach to One Loop Calculations in Gauge Theories*, *Phys. Rev. D* **38** (1988) 1888.

[88] R. Britto, F. Cachazo, B. Feng, and E. Witten, *Direct proof of tree-level recursion relation in Yang-Mills theory*, *Phys. Rev. Lett.* **94** (2005) 181602, [hep-th/0501052].

[89] H. Kawai, D. C. Lewellen, and S. H. H. Tye, *A Relation Between Tree Amplitudes of Closed and Open Strings*, *Nucl. Phys. B* **269** (1986) 1–23.

[90] Z. Bern, J. J. M. Carrasco, and H. Johansson, *New Relations for Gauge-Theory Amplitudes*, *Phys. Rev. D* **78** (2008) 085011, [arXiv:0805.3993].

[91] Zvi Bern, "Retrospective talk."
URL: https://indico.nbi.ku.dk/event/1321/contributions/11575/attachments/3625/5623/
amplitudes_2021_slides.pdf, 8, 2021.